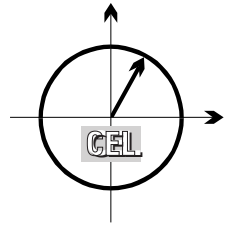


*Forschungsberichte aus dem
Institut für Nachrichtentechnik des
Karlsruher Instituts für Technologie*



Ankit Kaushik

■ Performance Analysis of Cognitive Radio Systems with Imperfect Channel Knowledge

Band 37

Copyright: Institut für Nachrichtentechnik (CEL)
Karlsruher Institut für Technologie (KIT)
2017

Druck: Frick Digitaldruck
Brühlstraße 6
86381 Krumbach

ISSN: 1433-3821

**Forschungsberichte aus dem Institut für Nachrichtentechnik
des Karlsruher Instituts für Technologie**

Herausgeber: Prof. Dr. rer. nat. Friedrich Jondral

- Band 1 Marcel Kohl
**Simulationsmodelle für die Bewertung von
Satellitenübertragungsstrecken im
20/30 GHz Bereich**
- Band 2 Christoph Delfs
**Zeit-Frequenz-Signalanalyse: Lineare und
quadratische Verfahren sowie vergleichende
Untersuchungen zur Klassifikation von Klaviertönen**
- Band 3 Gunnar Wetzker
**Maximum-Likelihood Akquisition von Direct
Sequence Spread-Spectrum Signalen**
- Band 4 Anne Wiesler
**Parametergesteuertes Software Radio
für Mobilfunksysteme**
- Band 5 Karl Lütjen
**Systeme und Verfahren für strukturelle
Musteranalysen mit Produktionsnetzen**
- Band 6 Ralf Machauer
Multicode-Detektion im UMTS
- Band 7 Gunther M. A. Sessler
**Schnell konvergierender Polynomial Expansion
Multiuser Detektor mit niedriger Komplexität**
- Band 8 Henrik Schober
**Breitbandige OFDM Funkübertragung bei
hohen Teilnehmergegeschwindigkeiten**
- Band 9 Arnd-Ragnar Rhiemeier
Modulares Software Defined Radio
- Band 10 Mustafa Mengüç Öner
**Air Interface Identification for
Software Radio Systems**

**Forschungsberichte aus dem Institut für Nachrichtentechnik
des Karlsruher Instituts für Technologie**

Herausgeber: Prof. Dr. rer. nat. Friedrich Jondral

- Band 11 Fatih Çapar
**Dynamische Spektrumverwaltung und
elektronische Echtzeitvermarktung von
Funkspektren in Hotspotnetzen**
- Band 12 Ihan Martoyo
Frequency Domain Equalization in CDMA Detection
- Band 13 Timo Weiß
OFDM-basiertes Spectrum Pooling
- Band 14 Wojciech Kuropatwiński-Kaiser
**MIMO-Demonstrator basierend
auf GSM-Komponenten**
- Band 15 Piotr Rykaczewski
**Quadratureempfänger für Software Defined Radios:
Kompensation von Gleichlauf Fehlern**
- Band 16 Michael Eisenacher
Optimierung von Ultra-Wideband-Signalen (UWB)
- Band 17 Clemens Klöck
Auction-based Medium Access Control
- Band 18 Martin Henkel
**Architektur eines DRM-Empfängers
und Basisbandalgorithmen zur Frequenzakquisition
und Kanalschätzung**
- Band 19 Stefan Edinger
**Mehrträgerverfahren mit dynamisch-adaptiver
Modulation zur unterbrechungsfreien
Datenübertragung in Störfällen**
- Band 20 Volker Blaschke
Multiband Cognitive Radio-Systeme

**Forschungsberichte aus dem Institut für Nachrichtentechnik
des Karlsruher Instituts für Technologie**

Herausgeber: Prof. Dr. rer. nat. Friedrich Jondral

- Band 21 Ulrich Berthold
**Dynamic Spectrum Access using OFDM-based
Overlay Systems**
- Band 22 Sinja Brandes
**Suppression of Mutual Interference in
OFDM-based Overlay Systems**
- Band 23 Christian Körner
**Cognitive Radio – Kanalsegmentierung und
Schätzung von Periodizitäten**
- Band 24 Tobias Renk
**Cooperative Communications: Network Design and
Incremental Relaying**
- Band 25 Dennis Burgkhardt
**Dynamische Reallokation von spektralen Ressourcen
in einem hierarchischen Auktionssystem**
- Band 26 Stefan Nagel
**Portable Waveform Development for
Software Defined Radios**
- Band 27 Hans-Ulrich Dehner
**Interferenzuntersuchungen für inkohärente
Multiband Ultra-Breitband (UWB) Übertragung**
- Band 28 Maximilian Hauske
Signalverarbeitung für optoelektronische Sensoren
- Band 29 Jens Elsner
**Interference Mitigation in
Frequency Hopping Ad Hoc Networks**
- Band 30 Georg Vallant
**Modellbasierte Entzerrung
von Analog/Digital-Wandler-Systemen**

**Forschungsberichte aus dem Institut für Nachrichtentechnik
des Karlsruher Instituts für Technologie**

Herausgeber: Prof. Dr. rer. nat. Friedrich Jondral

- Band 31 Martin Braun
**OFDM Radar Algorithms
in Mobile Communication Networks**
- Band 32 Michael Sebastian Mühlhaus
**Automatische Modulationsartenerkennung
in MIMO-Systemen**
- Band 33 Michael Schwall
**Turbo-Entzerrung: Implementierungsaspekte für
Software Defined Radios**
- Band 34 Ralph Tanbourgi
**Diversity Combining under Interference Correlation
in Wireless Networks**
- Band 35 Florian Engels
**Multidimensional Frequency Estimation with
Applications in Automotive Radar**
- Band 36 Noha El Gemayel
**Smart Passive Localization Using Time
Difference of Arrival**
- Band 37 Ankit Kaushik
**Performance Analysis of Cognitive Radio Systems
with Imperfect Channel Knowledge**

Vorwort des Herausgebers

Alle Prognosen deuten darauf hin, dass das Volumen der Datenübertragung in Mobilfunknetzen in den kommenden Jahren weiterhin dramatisch wachsen wird. Da für den Mobilfunk nur ein endlicher Frequenzumfang zur Verfügung steht, werden unterschiedliche Technologien, die einen substantiellen Beitrag zur Erhöhung des Datendurchsatzes leisten können, vorangetrieben. Dazu gehören insbesondere

- **Höhere Übertragungsbandbreiten:** Der einfachste Weg, zu höheren Funkkapazitäten zu kommen, besteht natürlich in der Zuteilung weiterer Frequenzbereiche. Solche sind aber unterhalb von 6 GHz kaum noch zu identifizieren, so dass inzwischen untersucht wird, mit welchen Mitteln höhere Frequenzen, z.B. im Bereich um 90 GHz, für die Mobilkommunikation nutzbar gemacht werden können.
- **Cognitive Radio:** Durch den Einsatz intelligenter flexibler Funkssysteme können innerhalb bestehender Mobilfunksysteme brachliegende Übertragungsressourcen genutzt werden. Das bedeutet, dass ein Primärnutzersystem innerhalb des ihm zugeteilten Frequenzbereichs unter bestimmten Bedingungen den Betrieb von Sekundärnutzersystemen zulässt.
- **Heterogene Netze:** Ein derzeit bereits genutzter Ansatz zur Kapazitätserweiterung besteht darin, Basisstationen mit niedriger Leistung und damit Pico- bzw. Femtozellen in bestehende Netze einzufügen. Andere Untersuchungen zielen auf den Einsatz der *Device-to-Device* Technologie oder von Ad-hoc Netzen ab.

- **Mehrantennentechnologien:** Die Nutzung der räumlichen Dimension durch *Multiple Input Multiple Output* Systeme zur Verbesserung der Verbindungsqualität oder zur Erhöhung der Datenrate wird in zukünftigen Netzen eine wichtige Rolle spielen. Je nachdem, welche Kanalzustandsinformation sende- und empfangsseitig verfügbar ist, kann hier an räumliches Multiplexing, räumliche Interferenzreduktion, Raumdiversity oder Kombinationen dieser Technologien gedacht werden.

Die vorliegende Dissertation untersucht den Einsatz von *Cognitive Radio* Systemen für den *Inhouse*-Betrieb. Dabei wird die Anbindung an das Mobilfunknetz über eine kognitive Kleinzellen-Basisstation gewährleistet, die auf der einen Seite den *Inhouse*-Betrieb steuert und auf der anderen Seite per Richtfunk mit der Basisstation einer Mobilfunkzelle (Makrozelle) verbunden ist. In solchen Konstellationen muss sichergestellt sein, dass die in die Makrozelle eingesetzte Kleinzelle den Betrieb innerhalb der Makrozelle nicht merklich stört. Darüber hinaus sollte natürlich auch die Makrozelle die eingesetzte Kleinzelle nicht wesentlich stören. Es geht also darum, die zwischen den beiden Zellen existierenden Querkanäle in den Griff zu bekommen, um bei gleich bleibender Übertragungsqualität in der Makrozelle den Durchsatz in der Kleinzelle zu optimieren zu können. Diese Fragestellung wird in der in den vergangenen Jahren veröffentlichten Literatur ausführlich diskutiert, wobei allerdings stets die exakte Kenntnis aller beteiligten Kanäle an der Kleinzellen-Basisstation vorausgesetzt wird. Für den praktischen Einsatz ist eine solche Voraussetzung natürlich nicht haltbar. Daher befasst sich die vorliegende Dissertation mit der Leistungsanalyse kognitiver Funkssysteme bei einer aus Schätzungen resultierenden, nicht perfekten Kanalkennntnis. Die durch die Arbeit von Ankit Kaushik geleisteten Beiträge zum Fortschritt von Wissenschaft und Technik umfassen insbesondere

- die Entwicklung und Einbeziehung von Schätzverfahren für die zwischen Primär- und Sekundärnutzern bestehenden (ungewollten) Kanäle und der Nachweis, dass deren Einsatz die Durchsätze von Primär- und Sekundärsystem praktisch kaum beeinflusst,
- die stochastische Charakterisierung dieser Kanäle.
- die Optimierung des Durchsatzes in *Cognitive Small Cells*,
- die Verifikation der im Rahmen der Arbeit entstandenen theoretischen Ergebnisse durch Simulationen und experimentelle Untersuchungen und

- den Aufbau eines Demonstrators für ein *Underlay System*¹.

Der Ausgangspunkt der Arbeiten von Ankit Kaushik findet sich im in den Jahren 2012 bis 2014 vom Bundesministerium für Bildung und Forschung (BMBF) geförderten Teilprojekt *Spektrumsmanagement und Kognitive Indoorversorgung* (SKI)² des Verbundprojekts Cognitive Mobile Radio - Intelligente Netzwerkelemente zur effizienten Ressourcennutzung in mobilen Funkzugangsnetzen (CoMoRa). Die in seiner Dissertation dokumentierten Ergebnisse gehen jedoch weit über die dort vorgenommenen Untersuchungen hinaus.

Karlsruhe, im Februar 2017
Friedrich K. Jondral

¹Ein *Underlay System* ist ein spezielles *Cognitive Radio* System.

²Förderkennzeichen: 01BU1205

Performance Analysis of Cognitive Radio Systems with Imperfect Channel Knowledge

Zur Erlangung des akademischen Grades eines

DOKTOR-INGENIEURS

von der Fakultät für

Elektrotechnik und Informationstechnik
des Karlsruher Instituts für Technologie

genehmigte

DISSERTATION

von

M.Sc. Ankit Kaushik

aus Neu Delhi, Indien

Tag der mündlichen Prüfung:

Hauptreferent:

Korreferentin:

31. Januar 2017

Prof. Dr. rer. nat. Friedrich K. Jondral

Prof. Dr. -Ing. Anja Klein

Acknowledgements

My time at Communications Engineering Lab (CEL) has been a wonderful experience. This would not have happened without the presence of some prominent personalities in my life. First and foremost, I would like to sincerely thank my supervisor Prof. Dr. rer. nat. Friedrich K. Jondral for accepting me as a Doctoral candidate. Despite my divergence to the industry, after my masters studies, he showed immense faith by giving me an opportunity to fulfill one of my goals. Besides, I admire him for his patience, guidance and providing me a suitable environment to carry out research. I would also like to thank Prof. Dr. -Ing. Anja Klein for agreeing to co-supervise my thesis.

My sincere thanks go to my colleagues at CEL, in particular, Dr. -Ing. Holger Jäkel, Dr. -Ing. Ralph Tanbourgi, Dr. -Ing. Noha El Gemayel and Dipl. -Ing Johannes Fink, who have been extremely supportive and always remained open for discussions. I would also like to thank Beate Mast and Brigitte Single for handling the administration, Angelika Olbrich for helping me out with graphics, and Reiner Linnenkohl and Peter Hertrich for providing me the necessary infrastructure. During this time period, I had an opportunity to supervise students and I must agree to the fact that students are the best teachers. I am grateful for their contributions and extensive discussions of all forms.

Outside CEL, I had an opportunity to collaborate with Dr. Shree Krishna Sharma, Prof. Symeon Chatzinotas, Prof. Björn Ottersten from University of Luxembourg. I am extremely thankful for their insightful suggestions that have been beneficial for my research. My special thanks to Dr. Sharma for

showing interest in my research, proof-reading my thesis and conducting fruitful discussions.

Last but not least, I am indebted to my parents Poonam and Rajesh, its their hard work, sacrifices and most importantly their belief that have brought me this far. In particular, my immense gratitude goes to my wife Mini for her love, support that kept me going during the stressful periods and giving me the most beautiful gift of my life, our daughter Alaiza. Honestly, I am extremely grateful to have such a life partner.

Abstract

Over the last decade, wireless communication is witnessing a tremendous growth in the data traffic due to ever-increasing number of connected devices. Certainly, in future, the state-of-the-art standards are incapable of sustaining the substantial amount of data traffic, originating from these devices. It is being visualized that a major portion of this requirement can be satisfied through an additional spectrum. Due to exclusive usage, the spectrum below 6 GHz is not able to meet this demand of additional spectrum, leading to its scarcity. To this end, Cognitive Radio (CR), along with millimeter-wave technology and visible-light communication, is envisaged as an alternative source of spectrum. The latter techniques are limited to a point-to-point communication, by which mobility is compromised. In contrast, a CR system aims at an efficient utilization of the spectrum below 6 GHz – suitable for mobile communications – by enabling a secondary access to the licensed spectrum while ensuring a sufficient protection to the licensed users (also referred as a primary system).

Despite the fact that an extensive amount of literature has been dedicated to the field of CR, its performance analysis has been dealt inadequately from a deployment perspective. Therefore, making it difficult to understand the extent of vulnerability caused to the primary system. Motivated by this fact, this thesis establishes a deployment-centric viewpoint for analyzing the performance of a CR system. Following this viewpoint, it has been identified that the involved channels' knowledge at the secondary transmitter is pivotal for the realization of cognitive techniques. However, the aspect of channel knowledge in context to CR systems, particularly its effect on the performance, has not been clearly

understood. With the purpose of curtailing this gap, this thesis proposes a successful integration of this knowledge – by carrying out channel estimation – in reference to different CR systems, namely interweave, underlay and hybrid systems. More specifically, the thesis outlines the following three aspects corresponding to the aforementioned CR systems, employing different cognitive techniques such as spectrum sensing, power control and their combination.

First, this thesis establishes an analytical framework to characterize the effects such as time allocation and variation, arising due to the incorporation of imperfect channel knowledge, that are detrimental to the performance of the CR systems. In order to facilitate hardware deployment of a CR system, received power-based estimation, a novel channel estimation technique is employed for the channels existing between the primary and the secondary systems, thus fulfilling low-complexity and versatility requirements.

Besides, this thesis follows a stochastic approach for characterizing the variations in the system. In particular, these variations cause uncertainty in the interference power received at the primary system, which may completely disrupt the operation of the CR systems. In order to maintain this uncertainty below a desired level, new interference constraints are proposed in the thesis. Moreover, the theoretical expressions, derived for the performance evaluation, are verified by means of simulations.

Second, the thesis features performance tradeoffs that determine the maximum achievable throughput of the CR systems while satisfying the interference constraint. At the system design, these tradeoffs provide insights for evaluating the performance degradation in terms of throughput caused due to an inappropriate selection of the estimation and sensing durations.

Third, using a software defined radio platform, a hardware implementation is carried out to validate the feasibility of the analysis proposed. In addition, a hardware demonstrator is deployed, which in a way presents the operation of a CR system in more practical conditions.

Zusammenfassung

Während des letzten Jahrzehnts erfährt die Drahtloskommunikation ein überaus großes Wachstum des Datenverkehrs aufgrund der seit jeher wachsenden Anzahl an angeschlossenen Funkgeräten. Es ist offensichtlich, dass die heutigen Standards zukünftig nicht mehr dazu in der Lage sein werden, das erhebliche Verkehrsaufkommen, welches von diesen Geräten erzeugt wird, zu bewältigen. Ein Großteil dieser Anforderung könnte durch die Nutzung zusätzlichen Spektrums erfüllt werden. Aufgrund der exklusiven Nutzungsrechte für das Spektrum unterhalb von 6 GHz, ist dieses nicht dazu in der Lage, der Nachfrage nach zusätzlichem Spektrum gerecht zu werden, was zu seiner Knappheit führt. Daher wird Cognitive Radio (CR) neben Millimeterwellen-Technologie und Visible Light Communications als alternative Spektrumsquelle betrachtet. Die letztgenannten Techniken eignen sich ausschließlich für Punkt-zu-Punkt-Kommunikation, was die Mobilität einschränkt. Im Gegensatz dazu ist es das Ziel eines CR Systems, eine effiziente und für Mobilfunk geeignete Nutzung des Spektrums unterhalb von 6 GHz zu ermöglichen. Dies wird dadurch erreicht, dass ein sekundärer Zugriff auf das lizenzierte Spektrum bei gleichzeitigem Schutz des Lizenznutzers, welcher auch als Primärsystem bezeichnet wird, erfolgt.

Obwohl sich eine Vielzahl an Werken in der Literatur mit dem Feld von CR beschäftigt, wurde die Analyse der Leistungsfähigkeit bislang nicht ausreichend von einem Standpunkt seitens eines Feldeinsatzes beleuchtet. Dies erschwert das Verständnis des Schadensausmaßes, welches das Primärsystem erfährt. Aus diesem Grund verfolgt diese Arbeit einen Ansatz zur Analyse

der Leistungsfähigkeit eines CR Systems mit Fokus auf den Feldeinsatz dieser Technik. Die Verfolgung dieses Ansatzes hat aufgedeckt, dass die Kenntnis der involvierten Kanäle am sekundären Sender grundlegend für die Realisierung von kognitiven Techniken ist. Jedoch wurde der Aspekt der Kanalkennntnis im Kontext von CR Systemen und insbesondere ihre Auswirkung auf die Leistungsfähigkeit noch nicht genau verstanden. Mit dem Ziel, diese Lücke zu schließen, wird in dieser Arbeit vorgeschlagen, dieses Wissen bei verschiedenen CR Systemen (Interweave, Underlay und hybriden Systemen) gewinnbringend einzusetzen, indem eine Kanalschätzung durchgeführt wird. Konkret werden in dieser Arbeit die folgenden drei Aspekte, welche mit den zuvor genannten CR Systemen korrespondieren und verschiedene kognitive Techniken einsetzen, dargelegt: Spectrum-Sensing, Power-Control und deren Kombination.

Um Effekte wie zeitliche Allokation und Schwankungen zu charakterisieren, welche aufgrund der Berücksichtigung imperfekter Kanalkennntnis entstehen, und die Leistungsfähigkeit des CR Systems beeinträchtigen, wird in dieser Arbeit zunächst ein analytischer Rahmen aufgestellt. Um den Feldeinsatz eines CR Systems seitens der Hardware zu vereinfachen, wird eine neue Technik namens Received-Power-Based-Estimation zur Schätzung der Kanäle zwischen dem Primär- und dem Sekundärsystem eingesetzt, wodurch Anforderungen hinsichtlich niedriger Komplexität sowie vielfältiger Einsetzbarkeit erfüllt werden.

Außerdem wird in dieser Arbeit ein stochastischer Ansatz zur Charakterisierung der Schwankungen im System verfolgt. Insbesondere führen diese Schwankungen zu Unsicherheit über die Interferenzleistung, welche das Primärsystem erfährt, wodurch der Betrieb des CR Systems vollständig unterbrochen werden kann. Um die Unsicherheit unter einem gewünschten Wert zu halten werden in der Arbeit neuartige Beschränkungen hinsichtlich der Interferenzleistung vorgeschlagen. Darüber hinaus werden die hergeleiteten theoretischen Ausdrücke zur Bewertung der Leistungsfähigkeit durch Simulation bestätigt.

Als zweiten zentralen Punkt zeigt diese Arbeit Performance-Tradeoffs auf, welche für den maximal erreichbaren Durchsatz der betrachteten CR Systeme bei gleichzeitiger Einhaltung der Interferenzleistungs-Beschränkung entscheidend sind. Für den Systementwurf liefern diese Zusammenhänge wertvolle Einsichten, um die Verschlechterung der Leistungsfähigkeit hinsichtlich des Durchsatzes zu bewerten, welche durch eine unangemessene Wahl der Schätz- und Sensing-Dauern hervorgerufen wird.

Zuletzt wird eine Hardware-Implementierung auf einer Software Defined Radio Plattform durchgeführt, um die Realisierbarkeit der vorgestellten Analyse zu bewerten. Zusätzlich wird ein Hardware-Vorführgerät aufgebaut, welches in einer gewissen Art und Weise den Betrieb eines CR Systems unter praxisnäheren Umständen darstellt.

Contents

- 1 Introduction 1**
 - 1.1 Background and Motivation 5
 - 1.1.1 Cognitive Small Cell: A Prominent Use-Case 6
 - 1.1.2 Performance Analysis 10
 - 1.1.3 Imperfect Channel Knowledge for CR systems 12
 - 1.2 Main Contributions 15
 - 1.3 Organization 18

- 2 Interweave System 21**
 - 2.1 Related Work 22
 - 2.2 Contributions 24
 - 2.2.1 Analytical Framework 24
 - 2.2.2 Imperfect Channel Knowledge 25
 - 2.2.3 Estimation-Sensing-Throughput Tradeoff 25
 - 2.3 System Model 26
 - 2.3.1 Interweave Scenario 26
 - 2.3.2 Signal Model 27
 - 2.3.3 Problem Description 28
 - 2.3.4 Proposed Approach 30
 - 2.3.5 Validation 34
 - 2.3.6 Assumptions 35
 - 2.4 Theoretical Analysis 36
 - 2.4.1 Deterministic Channel 36
 - 2.4.2 Random Channel 43

2.5	Numerical Results	47
2.5.1	Deterministic Channel	49
2.5.2	Random Channel	54
2.6	Summary	60
2.7	Solutions	61
2.7.1	Solution to Lemma 2	61
2.7.2	Solution to Lemma 3	61
2.7.3	Solution to Problems 1 and 2	62
3	Underlay System	65
3.1	Related Work	66
3.2	Contributions	68
3.2.1	Analytical Framework	69
3.2.2	Interference-Limited and Power-Limited Regimes	69
3.2.3	Estimation-Throughput Tradeoff	70
3.2.4	Estimation-Dominant and Channel-Dominant Regimes	70
3.3	System Model	71
3.3.1	Underlay Scenario and Medium Access	71
3.3.2	Signal Model	73
3.3.3	Problem Description	74
3.3.4	Proposed Approach	75
3.3.5	Assumptions	78
3.4	Theoretical Analysis	79
3.4.1	Deterministic Channel	79
3.4.2	Random Channel	85
3.5	Numerical Analysis	90
3.5.1	Deterministic Channel	90
3.5.2	Random Channel	95
3.6	Summary	97
3.7	Solutions	98
3.7.1	Solution to Lemma 8	98
4	Hybrid System	99
4.1	Related Work	100
4.2	Contributions	101
4.2.1	Analytical Framework	101
4.2.2	Estimation-Sensing-Throughput Tradeoff	101
4.3	System Model	102
4.3.1	Hybrid Scenario and Medium Access	102
4.3.2	Signal Model	103

4.3.3	Problem Description	104
4.4	Proposed Approach	106
4.4.1	Frame Structure	106
4.4.2	Channel Estimation	107
4.4.3	Characterization of Performance Parameters	109
4.4.4	Estimation-Sensing-Throughput Tradeoff	112
4.5	Numerical Analysis	113
4.6	Summary	120
5	Validation and Demonstration	121
5.1	System Model	122
5.1.1	Model Simplifications	122
5.1.2	Underlay Scenario and Medium Access	123
5.1.3	Signal Model	124
5.2	Theoretical Analysis	126
5.2.1	Characterization of the System Parameters	127
5.2.2	Estimation-Throughput Tradeoff	129
5.3	Hardware Validation	130
5.3.1	Experimental Setup	130
5.3.2	Determining Noise Power	134
5.3.3	Validation of System Parameters	134
5.3.4	Validation of Estimation-Throughput Tradeoff	135
5.4	Hardware Demonstration	138
5.4.1	Determining Estimation Time	139
5.4.2	Simplifications and Solutions	141
5.4.3	User Interaction and Observations	142
5.5	Summary	147
6	Conclusion	149
6.1	Summary	150
6.2	Outlook	151
	Acronyms and Abbreviation	155
	Notations and Symbols	157
	Bibliography	161
	Related Publications	173
	Supervised Theses	177

Contents

Index	179
Sponsorship	183
Biography	185

Chapter 1

Introduction

Since the invention of smart devices, the mobile traffic has been increasing tremendously over the last decade. According to the recent surveys on mobile traffic by prominent market leaders (Cisco [1] and Ericsson [2]), the existing mobile traffic is expected to increase 11-fold by 2021. The wireless community including the standardization bodies (3GPP [3]) believe that the state-of-the-art standards (fourth-Generation (4G) – LTE, WiMAX) are not capable of sustaining these ever-increasing demands in the upcoming decade. With this situation in hand, the standardization bodies are currently in the phase of conceptualizing the requirements of the fifth-Generation (5G) of mobile wireless systems. Some of these major requirements are: (i) areal capacity in bits/sec/m² must increase by a factor of 1000 compared to 4G, (ii) low latency of approximately 1 ms, and (iii) energy- and cost-efficient deployment [4, 5].

The feasibility of these requirements can be envisaged through the application of promising approaches such as maximization of the spatial degrees of freedom (using techniques like massive MIMO [6] and 3D-beamforming [7]), in-band full duplex communications [8], small cell densification [9, 10], alternatives to the already allocated spectrum – such as millimeter-Wave technology (mmW) [11], visible light communications [12] and Cognitive Radio (CR) communications – and waveform design [13, 14]. A classification of these approaches is described in Figure 1.1. In order to narrow down the perspective, in

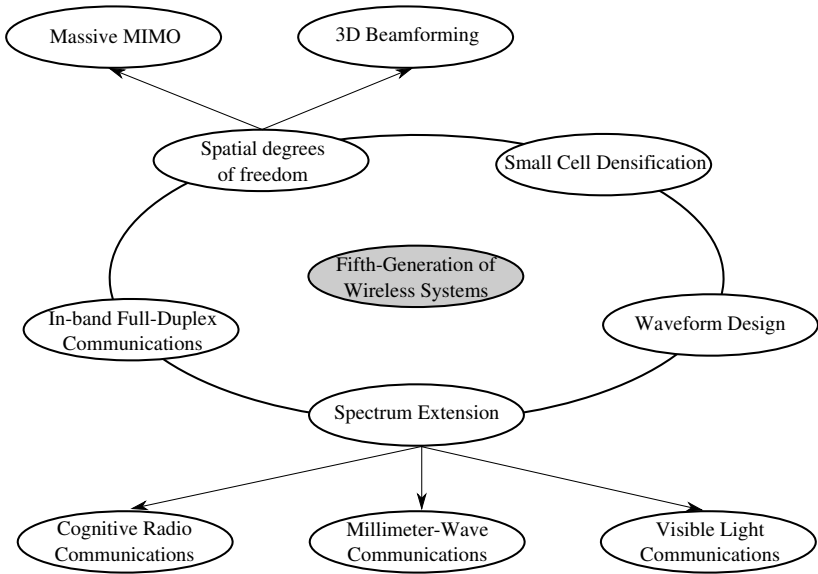


Figure 1.1: An illustration of the potential approaches considered under the 5G framework.

this thesis, a deployment scenario that lays emphasis on the small cell densification and the implementation of CR is proposed. Before proceeding further, it is essential to briefly discuss some of the prerequisites that render small cell densification and CR communication approaches, particularly their combination, a suitable candidate for a 5G network.

Small Cell Densification

In the recent past, Small Cells (SCs) have emerged as a potential solution for coverage and capacity enhancements inside a wireless network. A SC represents a low power station that ranges from 10 m to 100 m. The reduced transmit distance accomplished with the deployment of SCs enhances the link quality and aids spatial reuse [15]. As a result, small cell densification can leverage the areal capacity of a 5G network [5]. Because the capacity increases linearly with the number of SCs, it is infeasible to procure the factor of 1000 in the areal capacity with densification alone. In addition, the operation and the in-

tegration of these substantial number of SCs to the backhaul network are cost- and energy-intensive for the mobile operator. Therefore, the degree to which the densification can be achieved by a wireless network is rather limited.

Spectrum Extension

Complementing the SCs, an additional spectrum is envisioned as a power source that is capable of sustaining the desired areal capacity for 5G. In consideration to the present allocation of the spectrum below 6 GHz to different wireless services, it is difficult to procure an extension to the already available spectrum to the mobile communication. Before investigating the potential candidates for the spectrum extension, it is necessary to consider the following classification of the spectrum: (i) > 6 GHz; (ii) ≤ 6 GHz. This sort of classification allow us to focus on the feasibility characteristics and the issues thereof.

The spectrum beyond 6 GHz largely entails the mmW, which is well-known for point-to-point communications. Recently, it is envisaged as a powerful source of spectrum for 5G wireless systems. However, the mmW technology is still in its initial stage and along with complex regulatory requirements in this regime, it has to address several challenges like propagation loss, low efficiency of radio frequency components such as power amplifiers, small size of the antenna and link acquisition [11]. Therefore, in order to capture a deeper insight of its feasibility in 5G, it is essential to overcome the aforementioned challenges in the near future.

In contrast to the spectrum beyond 6 GHz, an efficient utilization of the spectrum below 6 GHz presents an alternative solution. The use of the spectrum in this regime (below 6 GHz) is fragmented and statically allocated [16, 17], leading to inefficiencies and the shortage in the availability of the spectrum for new services. A glimpse of the measurement campaign demonstrating the underutilized spectrum is presented in Figure 1.2. The measurements, acquired during the peak hours, illustrate the spectrum occupancy for the GSM 1800 MHz downlink sub-channels. The low spectrum occupancy for most of the sub-channels clearly signifies the fact that the demand for the additional spectrum can be fulfilled only by managing the utilization of the available spectrum efficiently.

In this perspective, CR is foreseen as one of the potential contenders that addresses the spectrum scarcity problem. Since its origin by Mitola *et al.* in 1999 [18], this notion has evolved at a significant pace, and consequently

1 Introduction

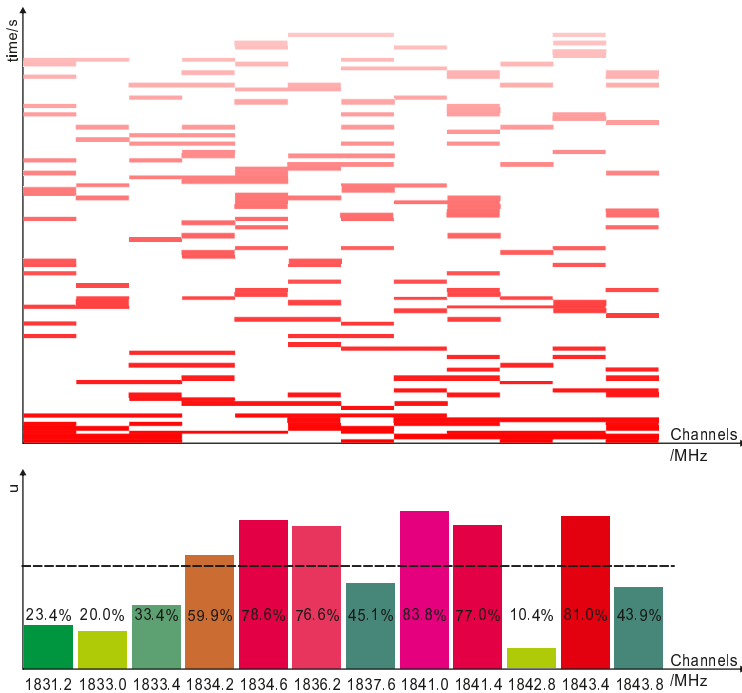


Figure 1.2: A snapshot of a hardware demonstrator that measures the spectral occupancy in GSM 1800 MHz downlink channels, whereby the black slices represent the spectrum occupancy (1 or 0) corresponding to a single measurement at a given time instant. The bar plots illustrate the spectrum occupancy (u) for each channel with a history of 500 measurements [K1].

has acquired certain maturity. Despite the existence of the theoretical analysis, from a deployment perspective, this technology is still in its preliminary phase [19]. In order to curtail the gap between the theoretical models and the practical implementations, recently, the wireless community has started to show an inclination¹ towards models and/or techniques. Hence, facilitating a hardware implementation of this concept in a way encourages the disposition of CR systems in the upcoming 5G wireless systems. Motivated by this fact,

¹As indicated by the increased promotion of hardware implementation/demonstration or the events such as spectrum challenge [K13] in conferences like IEEE DySPAN.

this thesis focuses on the performance analysis of CR systems from a deployment perspective.

In contrast to the Radio Frequency (RF) spectrum, Visible Light Communication (VLC) has started to gain extensive attention for 5G wireless communication, hence, deserves consideration in context to spectrum extension. Despite the fact that VLC offers some attractive characteristics like spatial, spectrum reuse, low energy consumption and security, it has to overcome certain challenges such as mobility and adverse effect of atmospheric conditions while operating outdoor [12].

1.1 Background and Motivation

Cognitive Radio Systems

In order to proceed further, it is essential to understand the classification of different CR systems described in the literature. An access to the licensed spectrum is an outcome of the paradigm employed by a Secondary User (SU). In this context, all CR systems that provide shared access (used interchangeably with secondary access) to the spectrum mainly fall under the following categories [20], please consider Figure 1.3 for a graphical illustration of different CR systems and their corresponding techniques considered in the thesis².

- According to Interweave System (IS) , the SUs render an interference-free access to the licensed spectrum by exploiting spectral holes in different domains such as time, frequency, space and polarization.
- Underlay System (US) enables an interference-tolerant access, according to which the SUs are allowed to use the licensed spectrum (e.g. Ultra Wide Band (UWB)) as long as they respect the interference constraints of the Primary Receivers (PRs).
- Hybrid System (HS) combines the benefits of the IS (agility to detect spectrum holes in different domains) and the US (interference-tolerant capability) so that the spectrum available for performing secondary access can be used efficiently.

²A detailed investigation of these techniques is provided in the following chapters.

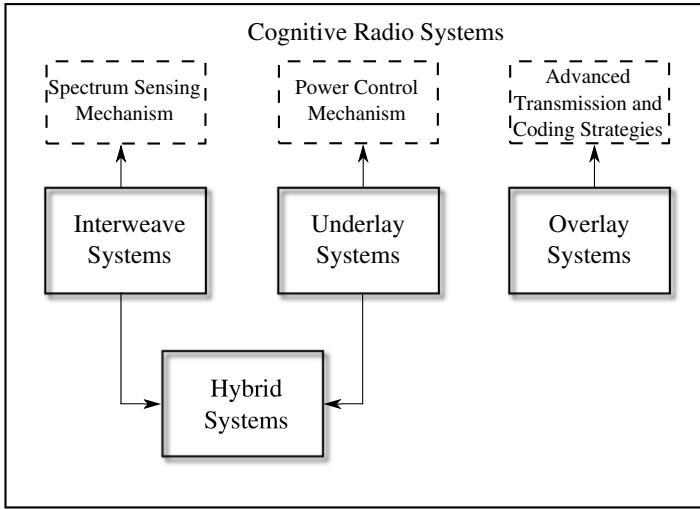


Figure 1.3: A classification of different CR systems and their corresponding techniques that allow shared access to the licensed spectrum.

- Overlay system considers advanced transmission and coding strategies, which include the participation of higher layers for enabling the spectral coexistence between two or more wireless networks.

The IS, the US and the HS are closely associated with the physical layer, hence, these systems are mostly considered not only for the theoretical analysis but for practical implementations as-well [K1, K7, K11, K13, K14], [21–23]. Underlying this fact, this thesis establishes a deployment-centric viewpoint for characterizing the performance of these CR systems. In order to illustrate a successful incorporation of the CR in a 5G network, a specific use-case (deployment scenario) is presented subsequently.

1.1.1 Cognitive Small Cell: A Prominent Use-Case

It is evident from the previous discussion that the spectrum extension via CR systems and SC densification are significant to the 5G system. Based on this, a preliminary concept of Cognitive Small Cell (CSC), a promising application that combines the benefits from the SC deployment and the efficient usage of the spectrum below 6 GHz, by realizing CR, is presented. A typical scenario

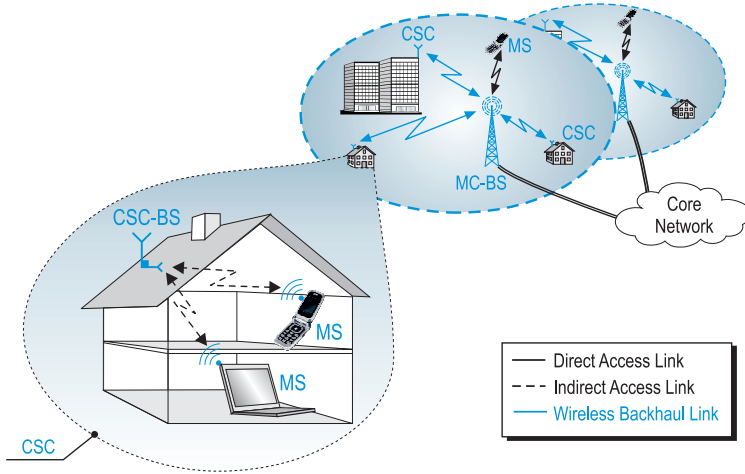


Figure 1.4: An illustration of the CSC deployment in a 5G network.

where the CSC finds its application would be the co-existence of Wi-Fi or unlicensed small cell and wireless cellular systems [24, 25]. The notion of CSC has been previously investigated by Elsayw *et al.* [26, 27] and Wildemeersch *et al.* [28], where the authors primarily emphasized on the modelling techniques³ that depict the positioning of several CSCs inside the network. Due to this, the performance analysis of the CSC has been limited mainly to network abstraction. In contrast, this thesis examines the fundamental aspects encountered while deploying a CSC, which otherwise could forbid its realization over the hardware. A comprehensive incorporation of CSC in a preliminary 5G architecture is illustrated in Figure 1.4. In order to enhance the viability of the proposed network architecture, it is reasonable to highlight some of the essential ingredients pertaining to the deployment of the CSC.

Network Elements

In order to propose a successful integration of CSC in a 5G network, the following key elements are essential: a CSC-Base Station (CSC-BS), a Macro Cell-Base Station (MC-BS) and Mobile Stations (MSs), cf. Figure 1.4. MSs

³The modelling is based on stochastic geometry, which allows a spatial averaging over multiple network geometries [29, 30].

are the devices either served by the MC-BS over a *direct access* link or the CSC-BS over an *indirect access* link. The direct access and the indirect access are the nomenclature used to distinguish a start-of-the-art (spectrum) access between the MC-BS and the MS from an access between the CSC-BS and the MS representing a CR communication, respectively. Furthermore, the MC-BS is connected to several CSC-BSs over a *wireless backhaul* link. Although the MC-BS and the MS already exist in the conventional cellular architecture, to incorporate the opportunistic access inside the CSC, it is necessary to consider a functionality upgrade.

Spectrum Access

In the proposed network architecture, the access to the spectrum is realized over the wireless backhaul, the direct access and the indirect access links, cf. Figure 1.4.

1. A wireless backhaul is a point-to-point wireless link between the CSC-BS and the MC-BS that relays the traffic generated from the CSC to the core network. With regard to the densification of the CSC in 5G network, the wireless backhaul link, in contrast to the optical fiber link, presents a cost-effective and energy-efficient alternative to the mobile operator. With limited infrastructure required for the deployment, wireless backhauling accelerates the installation process and promotes scalability of the network. For the wireless backhaul link, considering that it is utilized for a longer time duration, an exclusive spectrum represents a viable option. In this context, it is sensible to nominate a mmW band; alternatively, an exclusive band below 6 GHz can be acquired using the principles of Licensed Shared Access (LSA) [31].
2. A direct access link represents a direct access of the MS at the MC-BS over the allocated spectrum. Consequently, the spectrum access for this link is analogous to the one existing in the state-of-the-art wireless standards.
3. The CSC elements (the CSC-BS and the MS) are responsible for executing the secondary access to the licensed spectrum. The additional spectrum, acquired through the realization of CR techniques, including spectrum sensing and power control, at the CSC-BS, is used for the communication between the CSC-BS and the MS over the indirect access link.

Network Compatibility

Besides secondary access, CSC has to co-exist harmoniously with the other elements existing in the network. In this context, the network elements are embedded with additional functionality such as:

- The MS procures the control information (signalling and synchronization) over the indirect access link after connecting to the near-by CSC-BS.
- In order to accomplish a logical placement of CSCs inside the network, the CSC employs S1 and X2 interfaces over the wireless backhaul link.
- For situations where several CSC-BSs co-exist under a MC-BS, operations like seamless cross-tier and co-tier mobility constitute a challenging task for the network.

Hardware Feasibility

Along with other ingredients, it is essential to outline certain aspects that pertain to the hardware realizability of the CSC. For the CSC-BS, an antenna mount system consisting of an indoor and an outdoor antenna is proposed. Whereby, the indoor antenna exploits the walls of the building to physically separate the indoor transmissions over the indirect access link. In this way, the CSC is able to mitigate the interference to the primary system and to the neighbouring CSCs, vice-versa. Whereas, the outdoor antenna secures a narrow beam transmission to enhance the link quality for the wireless backhaul link. Besides this, it is a well-known fact that Software Defined Radio (SDR) has played an important role in the genesis of the CR [32]. Which means that the SDR can serve as a suitable platform for executing CR techniques, accomplishing rapid prototyping for the CR systems. Taking this into account, the SDR platform is utilized for realizing (or demonstrating) the CR functionality pursued by the CSC-BS over a hardware.

Indoor Deployment

From a market survey, it has been depicted that 70% of the mobile traffic is originated from indoor locations [15]. Another survey of the leading WiMAX operators revealed that 80% of their subscribers will be connected indoors [33].

In addition, a new range of wireless services, categorized as Internet of Things (IoT), will operate indoors. Following these facts, it is clear that the performance gains in terms of spectrum reuse will be far more consequential if we manage to consolidate these sources of traffic by means of SCs deployment. In order to capture the indoor originated traffic, it is sensible to consider the residential and enterprise as the main deployment scenarios for the CSC, cf. Figure 1.4. Except for a different coverage regime, the operating principles of these scenarios are analogous. Besides, in context with the CR, where the interference mitigation between the primary and the secondary systems is a significant aspect, a CR communication within walls (which attributes to an indoor deployment) provides a spatial separation between the two systems. This, however, does not indicate that CR communication is limited to indoor scenarios. As the matter of fact, the indoor deployment is opted

- to exploit the behavioral dimension of the traffic source (traffic management) and
- to mitigate the interference between the two systems

so that co-existence with the licensed users is encouraged. In this regard, an indoor scenario is considered for the deployment of the CSC, cf. Figure 1.4. Despite the interference mitigation, an effective control over the interference is essential for a successful operation of the CR systems. Therefore, the next section extensively discusses the performance of the CR systems.

1.1.2 Performance Analysis

Since the evolution of wireless systems, understanding the performance of novel algorithms/techniques related to the wireless systems has always been a challenging task. With regard to this, for a CR system, because of the involvement of two different systems, namely primary and secondary systems, this task is even more difficult. On one end, it has been engaging a large number of researchers that are eager to find solutions for the new set of problems that are emerging from an interplay between these two systems, leading them to develop theoretical models (system models). As a result, these models allow us to determine the performance limits of the CR system. However, to sustain analytical tractability, they tend to consider assumptions that in most situations are unrealistic for a hardware deployment. On the other end, due to the co-existence of the two systems sharing the same spectrum, the performance of

a CR system is critical to the regulatory bodies and the mobile operators⁴, responsible for managing the spectrum. In this regard, despite the numerous theoretical models that exist in the literature, when it comes to judging the performance of a CR system, the regulatory bodies give more preference to the hardware implementations.

These different mindsets and the lack of proper guidelines ultimately slow down the evolution of the CR in realistic scenarios. Under this situation, it is advisable to merge these mindsets and establish a deployment-centric viewpoint towards the CR systems, according to which the upcoming models and/or techniques not only associate themselves to the performance characterization but are eligible for practical implementations as-well. This viewpoint, also the main motivation behind this work, is emphasized throughout the thesis.

The co-existence between the primary and the secondary systems can be accomplished only through a detailed analysis of the performance of these systems. To address this issue, the researchers have made an intensive effort to develop system models [34–36]⁵ that characterize the performance of the CR systems. The performed analysis boils down to the fact that the CR systems are allowed to successfully co-exist with the primary system only if they respect the interference power (or interference) at the primary system caused due to an access to the licensed spectrum. In other words, imposing an interference constraint ensures a sufficient protection to the primary systems and enables the CR system to perform secondary access.

With regard to this constraint, the CR system also intends to deliver a certain Quality of Service/Quality of Experience (QoS/QoE) in the form of throughput to their corresponding Secondary Receiver (SR), defined as *Secondary throughput*. Such a QoS/QoE provisioning helps us to determine the potential applications or prominent use-cases for the CR system. For instance, the secondary throughput's knowledge over the access link enables the CR to execute a band allocation policy, based on which the CR can relinquish those channels that ineffectively contribute to the secondary throughput, and/or are responsible for causing interference at the primary system. As a result, the performance of a CR system can be jointly characterized in terms of the harmful interference received at the primary system and the throughput achieved by the secondary

⁴These operators are the ones who are willing to share their license (as primary system) or the ones who are willing to access the licensed spectrum (as secondary system).

⁵For the sake of brevity, only limited works from the literature representing the performance analysis have been cited in this chapter. The following chapters corresponding to different CR systems consider an in-depth analysis of the related work.

system. But the fact is, the derived expressions depicting the performance of the CR systems are rarely examined over the hardware. Mainly, because of the complicated deployment scenario or the computational complexity of the employed CR techniques, leaving the validity of the existing theoretical analysis questionable. Taking this issue into account, this thesis analyzes the performance of the CR systems while putting emphasis on the fact that the performed analysis can be easily validated through a hardware implementation.

1.1.3 Imperfect Channel Knowledge for CR systems

In a nutshell, a CR is an agile system that possesses the ability to adapt to the changes in the environment. From a physical layer perspective, this corresponds to the response to the changes incurred within the system or from the outside environment, which in a way leads to a performance enhancement. Inherent to the wireless systems, these changes may arise due to the variations in the signal caused by the presence of the thermal noise at the receiver and the fading in the channel. It is well-known from the text-books, related to wireless communications [37–39], that the channel fading, in particular, is critical for wireless systems. As a matter of fact, channel knowledge – in the form of Channel State Information at the Transmitter (CSIT) available through a feedback from the receivers – has rendered a substantial improvement in the performance in terms of data rate, for instance, multiplexing gains for a MIMO system [40].

In context with a CR system, the channel knowledge, unlike the conventional or state-of-the-art wireless systems, is not confined to a single transmitter-receiver link, rather it includes all the related channels that exist within as-well-as across the primary and the secondary systems, cf. Figure 1.5. At this stage, it is worth understanding the fact that channel knowledge is paramount for the hardware implementation of the CR systems, since it allows them to exercise different CR techniques, cf. Figure 1.3, and to respect the desired constraints, which are necessary for their co-existence with the primary systems. Besides, from a theoretical perspective, the channel knowledge is required for the performance characterization. Absence of this knowledge, especially of those channels that are related to the interference at the primary systems, renders the performance characterization of a CR system inadequate for the practical implementations.

Despite the existence of multitude of analytical models in the literature (ISs – [34, 41, 42], USs – [36, 43, 44], HSs – [45–48]) that consider with the performance analysis of a CR system, its performance with regard to the channel

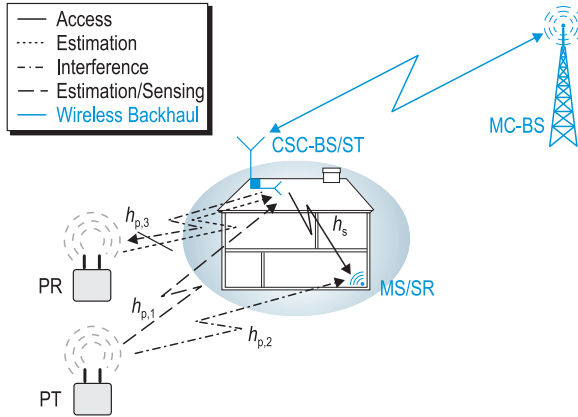


Figure 1.5: A cognitive small cell scenario demonstrating: (i) the CR systems employed at the CSC-BS, (ii) the associated network elements, which constitute Cognitive Small Cell-Base Station/Secondary Transmitter (CSC-BS/ST), Mobile Station/Secondary Receiver (MS/SR), Macro Cell-Base Station (MC-BS) and Primary Transmitter (PT), (iii) the interacting channels: sensing ($h_{p,1}$), interference ($h_{p,2}, h_{p,3}$) and access (h_s) channels.

estimation, due to the complexity of the underlying problem, has never been completely understood⁶. In order to curtail this gap, this thesis capitalizes on the estimation of the involved channels in a CR system. In this sense, the accessibility of the channel knowledge at the CSC-BS facilitates the implementation of the CR techniques at the CSC-BS, establishing a CR communication link with the MS over the acquired spectrum. More importantly, this knowledge allows us to regulate the interference at the PR below a desired level.

Certainly, an access to the channel knowledge comes at a certain cost. Firstly, the inclusion of channel estimation demands an allocation of a certain time interval by the CSC-BS. In consideration to the time allocation, a certain degradation in the performance in terms of the throughput is obvious. Secondly, the variations introduced due to the estimation process, also treated as imperfect channel knowledge, lead to an uncertainty in the interference, defined as *un-*

⁶In context to the US, certain works [49–51] have dealt with the issue of channel estimation in a CR system, however, unlike this thesis, the investigation has not been exhaustive. This augmented is extensively supported in Chapter 3 under the section “Related Work”.

*certain interference*⁷, to the primary systems. If not considered, this uncertain interference may severely degrade the performance of the CR systems. In order to approach a successful integration of channel estimation into the CR system, it is essential to consider the performance degradation arising due to the time allocation and the uncertain interference in the system model. These effects concerning the performance degradation have been completely left aside in the existing models that consider the perfect channel knowledge. This thesis takes these effects into account to establish analytical frameworks (each for the IS, the US and the HS) that allow us to understand the behaviour of the CR systems under those situations that are close to realistic scenarios.

Shifting the focus back to the deployment, it is worthy to understand that the channel estimation, facilitating shared access to the licensed spectrum, is viable only if the CR system is equipped with the knowledge about to the primary system. This implies that in order to perform channel estimation based on conventional techniques – such as training-based [52], pilot-based [53, 54], signal to noise ratio-based [55, 56] channel estimation, which already exist in the literature – a preliminary processing in the form of synchronization and demodulation of the baseband signal received from the primary system is necessary. The existence of multiple wireless standards and their complexity preclude us from deploying a dedicated circuitry corresponding to each primary system [57]. The fact is, these conventional channel estimation techniques are well-known for delivering accurate channel estimates, that is why employed in state-of-the-art wireless standards. However, in context with the CR systems, these techniques

- increase the complexity related to the channel estimation, evaluated in terms of the mathematical operations, and (or)
- demand the demodulation of the Primary User (PU) signal.

Under these circumstances, it is advisable to consider only those solutions that offer low complexity and show versatility towards different PU signals. Generally speaking, such solutions will not only ease the deployment process but also have a large acceptance among the CR community. For instance, energy-based detection (or energy detection) has been a popular choice compared to its counterparts such as matched filtering-based and cyclostationary-based detection for detecting a PU signal, required for performing spectrum sensing for the interweave systems (discussed later in Chapter 2). A direct comparison

⁷The uncertain here specifically symbolizes the variations in the interference power received at the PR that exists because of the imperfect channel knowledge.

of these techniques by simply counting their implementations for hardware demonstration has been done in [19].

On similar grounds as energy detection, in order to approach the channel estimation for the CR system, particularly for the channels that involve the primary systems, a *received power-based*⁸ channel estimation technique is proposed as a part of the analytical framework. This channel estimation technique is introduced to substitute the conventional techniques because, like energy detection, employing received power-based estimation assures the low complexity and the versatility towards unknown PU signal requirements of the CR system, and consequently facilitates its deployment. Besides, the channel within the secondary framework, treated as a conventional transmitter-receiver link, does not fall in the aforementioned category. Therefore, its knowledge is procured by employing a pilot-based channel estimation technique.

1.2 Main Contributions

At this stage, it is well-understood that the knowledge of the related channels is crucial for the application of CR techniques in the practical scenarios. In order to facilitate the hardware deployment of a CSC, a CR application, this thesis capitalizes on the successful integration of this knowledge for different CR systems, namely interweave, underlay and hybrid systems. In this context, the main contributions and the observations of this thesis (highlighted in Figure 1.6) are summarized as follows:

- *Analytical Framework*: As a major contribution, this thesis proposes an analytical framework, corresponding to the different CR systems (which are followed in Chapter 2, Chapter 3 and Chapter 4, respectively) that incorporates the estimation of the involved channels between the primary and the secondary systems, a crucial aspect that has been addressed inadequately in the literature.

Low-complex and versatile channel estimation technique - In order to satisfy the low complexity and the versatility towards unknown

⁸It is worthy to understand that the received power refers to the signal power measured after analog to digital conversion, hence, it consists of the signal and the noise power. Traditionally, received signal strength is a metric used for measuring signal quality to perform tasks such as cell association and handover [58].

PU signal requirements, which are necessary for the deployment of the CR systems, a received power-based channel estimation is included in the proposed framework. In this regard, an effort has been made to facilitate a direct incorporation of the estimated parameter (received power) to the performance characterization of the CR systems.

Impact of Incorporating Channel Estimation - In addition, a careful allocation of the time interval (referred as estimation time), for the purpose of performing channel estimation, in the medium access of the secondary system is proposed. Apart from this, this thesis considers a stochastic approach to tackle the variations in the CR system that arise due to the imperfect channel knowledge (estimation error). In contrast to the existing models that preclude channel estimation (or consider perfect channel knowledge), thereby overestimating the performance of the CR systems, this thesis captures a clear insight on the influence of the time allocation and the imperfect channel knowledge on performance of the CR system. Obviously, the imperfect channel knowledge and the time allocation have a detrimental effect on the performance of the CR system, thus leading to a *performance degradation*. This degradation is qualified through a comparison between the existing models and the estimation model (the one included as a part of the proposed framework). Particularly, the variations lead to uncertain interference, which in certain situations is deleterious to the primary system. This uncertainty in the interference is captured by means of novel constraints, introduced as a part of this framework.

In order to closely examine the relationship between the system parameters, theoretical expressions pertaining to the performance analysis of the CR system are derived. Furthermore, to understand the performance of the proposed framework in fading scenarios, especially for the interweave and the underlay systems, the analysis is extended to obtain the theoretical expressions that incur the effect of fading in the involved channels. Finally, to exclude any discrepancy in the analysis, the obtained expressions are verified by means of Monte-Carlo simulations.

- *Performance Tradeoffs* : As a major observation, it has been identified that the estimation time is closely associated with the performance of

the CR systems. On one side, it is related to the variations incurred in the system, through which the level of uncertainty in the interference can be effectively controlled, ultimately affecting the performance in terms of the secondary throughput. While on the other side, the time allocation directly influences the secondary throughput. In this thesis, this kind of dual dependency of the secondary throughput on the estimation time has been investigated in the form of performance tradeoffs, namely *estimation-sensing-throughput* tradeoff for the IS and the HS, and *estimation-throughput* tradeoff for the US.

Suitable estimation and sensing durations - These tradeoffs present a useful tool for visualizing the response of a CR system to different choices of the estimation time so that the performance degradation introduced due to the channel estimation can be precisely regulated. In other words, a system designer can utilize these tradeoffs to preclude situations under which the performance degradation becomes intolerable. Conversely, from a theoretical perspective, these tradeoffs can be used to determine a suitable estimation time that yields the maximum achievable secondary throughput while obeying the interference constraints.

- *Hardware deployment*: In contrast to the theoretical analysis, this thesis lays emphasis on the portability of the analytical framework on a hardware platform. To a great extent, this not only validates the accuracy of the assumptions made while deriving the theoretical expressions but also justifies the applicability of the proposed framework in realistic scenarios.

Empirical Validation - With the implementation of the received power-based estimation technique, this thesis adds further justification to the claims such as the low complexity and the versatility to unknown PU signals, presented while developing the analytical framework. Considering these facts, a software defined radio platform is deployed for obtaining the measurements, required for the validation process. In order to complement the validation, the theoretical expressions, which include the probability density functions (characterizing the variations in the estimated parameters) and the

performance tradeoff, are compared with their empirical counterparts.

Hardware Demonstration - Besides validation, this thesis presents a demonstrator that certifies the necessity of channels' knowledge for the performance characterization as-well-as for the operation of a CR system over the hardware. In this regard, following the guidelines of an US a demonstrator is deployed.

As a part of the deployment process, in order to illustrate a successful deployment of the CR systems, this thesis identifies some key issues, that are usually left aside while performing the theoretical analysis, and proposes the corresponding simplifications/solutions.

1.3 Organization

The rest of the chapters in this thesis are organized as follows:

Chapter 2 develops an analytical framework that incorporates the estimation of the involved channels in accordance with the interweave scenario. In this context, the indoor deployment scenario is transformed into an interweave scenario, whereby a spectrum sensing mechanism is employed at the CSC-BS enabling a secondary access to the licensed spectrum. Section 2.4 derives the theoretical expressions to capture the effect of imperfect channel knowledge on the performance of an IS. Further, Section 2.5 establishes an estimation-sensing-throughput tradeoff that depicts the suitable estimation and the suitable sensing time intervals at which the maximum secondary throughput is achieved by an IS.

Following a similar methodology as Chapter 2, Chapter 3 develops an analytical framework that incorporates the estimation of the involved channels in accordance to the underlay scenario. To implement the underlay technique within the CSC, the deployment scenario is modified such that a power control mechanism is employed at the CSC-BS so that interference remains within the desired tolerance limits at the PR. As a part of the proposed framework, Section 3.4 derives the theoretical expressions for the power control and the secondary throughput, capturing the effect of imperfect channel knowledge and

characterizing the performance of an US. In the end, the performance is jointly characterized in terms of estimation-throughput tradeoff that determines the achievable secondary throughput for an US.

Although the interweave and the underlay system, discussed in Chapter 2 and Chapter 3, propose effective ways of performing secondary access, these systems do not represent the best techniques of utilizing the licensed spectrum efficiently. In this regard, to promote the efficient usage of the licensed spectrum by the secondary users, the underlay and the interweave techniques are combined to realize a hybrid scenario. Motivated by this fact, Chapter 4 develops an analytical framework that incorporates the estimation of involved channels with respect to the hybrid scenario. In this context, the indoor scenario is modified such that the CSC-BS employs spectrum sensing as-well-as power control mechanism to perform secondary access. The theoretical expressions derived in this chapter incorporate the effect of imperfect channel knowledge, depicting the performance of the HS. Analog to Chapter 2, an estimation-sensing-throughput tradeoff that yields the achievable secondary throughput for an HS is characterized in this chapter.

In order to reveal the ground truth regarding the analysis proposed in previous chapters, Chapter 5 identifies some of the essential aspects that facilitate the deployment of the proposed framework. In this regard, a hardware is deployed that implements the channel estimation, realizes the interference constraints, validates the performance analysis and demonstrates the principle working of the US.

Finally, Chapter 6 summarizes the thesis and presents some extensions of performed analysis for future investigations.

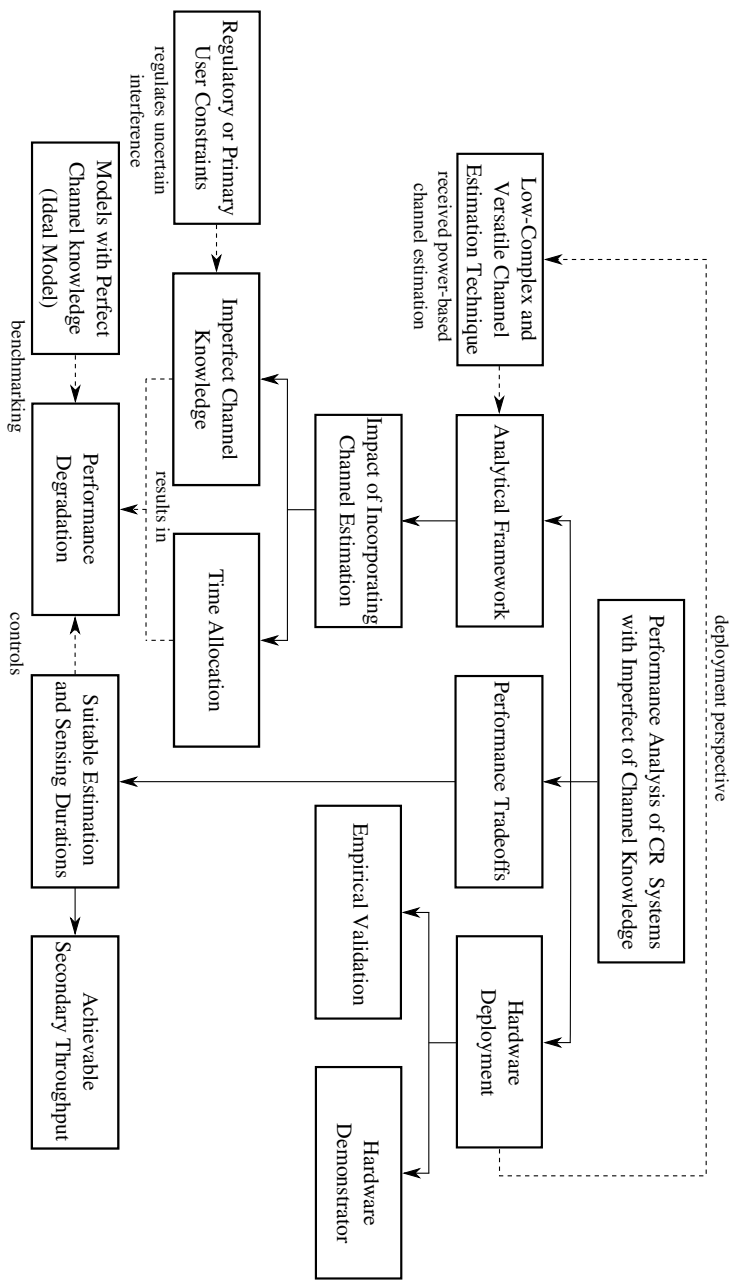


Figure 1.6: An illustration of the interconnection between the major contributions and the key observations.

Chapter 2

Interweave System

Secondary access to the licensed spectrum is viable only if the interference is avoided at the primary system. Among the different paradigms conceptualized in the literature, ISs have been extensively investigated. In order to enable interference-free access to the licensed spectrum, IS employs spectrum sensing at the Secondary Transmitter (ST). Spectrum sensing (or only sensing) is necessary for detecting the presence or the absence of a PU signal. In this way, sensing assists the IS in protecting the PRs against harmful interference. A sensing mechanism at the ST can be accomplished by listening to the signal transmitted by the PT. The existing models (termed as baseline models), investigated in the literature [34,41,42], characterize the performance of IS in terms of a sensing-throughput tradeoff. However, this characterization assumes the perfect knowledge of the involved channels at the ST, which is unavailable in practice. Motivated by this fact, this chapter, which is based on [K2–K4], proposes a novel approach to incorporate channel estimation corresponding to the IS in the system model, and consequently investigates the impact of imperfect channel knowledge on the performance of the IS.

More particularly, the variations induced in the detection probability affect the detector's performance at the ST. Since the detector installed at the ST is largely responsible for regulating the interference, uncertainty in its performance may result in severe interference at the PRs. In order to capture this uncertainty, an

average constraint and an outage constraint¹ on the detection probability are proposed. The analysis, performed in this chapter, reveals that an appropriate choice of the estimation time and the sensing time intervals² can effectively control the performance degradation. Thus, depicting the achievable secondary throughput of the IS.

2.1 Related Work

For detecting a PU signal, several techniques such as energy-based detection (or energy detection), matched filtering-based, cyclostationary-based and feature-based detection exist [59, 60]. Because of its versatility towards unknown PU signals and its low computational complexity, energy detection has been extensively investigated in the literature [61–65]. In this technique, the decision is accomplished by comparing the power received at the ST to a decision threshold. In reality, the ST encounters variations in the received power due to the existence of thermal noise at the receiver and fading in the channel. Subsequently, these variations lead to sensing errors described as misdetection and false alarm, which limit the performance of the IS. In order to determine the performance of a detector, it is essential to obtain the expressions of detection probability and false alarm probability.

In particular, detection probability is critical for IS because it protects the PR from the interference induced by the ST. As a result, the IS has to ensure that they operate above a target detection probability [66]. Therefore, the characterization of the detection probability becomes absolutely necessary for the performance analysis of the IS. In this context, Urkowitz [61] introduced a probabilistic framework for characterizing the sensing errors, however, the characterization accounts only for the noise in the system.

To encounter the variation caused by channel fading, a frame structure has been introduced in [34], assuming that the channel remains constant over the frame duration (corresponds to a quasi-static block fading). Upon exceeding the frame duration, the system may observe a different realization of the channel. Based on this frame structure, the performance of the IS has been investigated in terms of a deterministic (corresponding to a non-random behaviour)

¹The outage constraint is an essential metric employed for designing communication systems, which ensures that the outage occurs no more than a certain percentage of time.

²Throughout the thesis, the estimation time interval and sensing time interval are used interchangeably with estimation time and sensing time, respectively.

channel [34, 41, 42] and a random channel [62–64]. In the thesis, the deterministic channel symbolizes that the performance of the CR system is analyzed for a specific frame, i.e., for a particular realization of the channel. Whereas the random channel represents that the performance is evaluated over multiple frames, i.e., the CR system observes multiple realizations of the channel. For the latter case, a fading model is employed to capture the random behaviour of the channel.

Besides the detection probability, false alarm probability has a large influence on the throughput achieved by the secondary system. Recently, the performance characterization of CR systems in terms of a sensing-throughput trade-off has received significant attention [34, 42, 67, 68]. According to Liang *et al.* [34], the ST assures a reliable detection of a PU signal by retaining the detection probability above a desired level with an objective of maximizing the throughput at the SR. In this way, the sensing-throughput tradeoff depicts a suitable sensing time interval that achieves a maximum secondary throughput. To characterize the detection probability and the secondary throughput, the system requires the knowledge of interacting channels, namely, a *sensing* channel, an *access* channel and an *interference* channel, refer to Figure 2.1³. The baseline models, investigated in the literature, assume the knowledge of these channels to be available at the ST. However, in practice, this knowledge is not available and, thus, it needs to be estimated by the secondary system. As a result, the existing solutions for the IS are considered inadequate from a practical viewpoint.

As a matter of fact, the sensing and the interference channels related to the CR system (refer to Figure 2.1) represent the channels between two different (primary and secondary) systems. In this context, it becomes challenging to select the estimation methods in such a way that low complexity and versatility (towards different PU signals) requirements are satisfied. These issues, discussed later in Section 2.3.4, render the existing estimation techniques [52–56] unsuitable for hardware implementations. To tackle the issue related to the channel estimation, a received power-based estimation at the ST and at the SR for the sensing and the interference channels is employed, respectively. Considering the fact that the access channel corresponds to the link between the ST and the SR, conventional channel estimation techniques such as pilot-based channel estimation at the ST is employed.

³As the interference to the PR is controlled by a regulatory constraint over the detection probability, in this view, the interaction with the PR is excluded in the considered scenario [34].

Inherent to the estimation process, the variations due to the channel estimation translate to the variations in the performance parameters, namely detection probability and secondary throughput. In particular, the variations induced in the detection probability cause uncertain interference at the PR, which may severely degrade the performance of a CR system. The detrimental effect due to the time allocation for the channel estimation and the uncertain interference due to imperfect channel knowledge have not been considered in [34,42,67,68] or studied partially in [55,69]. In this context, the performance characterization of an IS with imperfect channel knowledge remains an open problem. Motivated by this fact, this chapter focuses on the performance characterization of the IS in terms of sensing-throughput tradeoff taking these aforementioned aspects into account.

2.2 Contributions

The major contributions of this chapter can be summarized as follows:

2.2.1 Analytical Framework

In contrast to the existing models that assume perfect knowledge of the channels, the main goal of this chapter is to derive an analytical framework that constitutes the estimation of: (i) sensing channel at the ST, (ii) access channel and (iii) interference channel at the SR. As illustrated later in Figure 2.2, under this framework, a novel integration of the channel estimation in the secondary system's frame structure is proposed. According to which the samples considered for channel estimation (of the sensing channel) are accounted also for the sensing such that the time resources within the frame are utilized efficiently. Furthermore, the estimation techniques are selected in such a way that the hardware complexity and the versatility towards unknown PU signals requirements (as considered while employing an energy based detection) are not compromised. In this context, a received power-based estimation for the sensing and the interference channels is proposed. Based on proposed framework, this chapter characterizes the performance of the IS by considering the performance degradation due to:

- the variations caused by imperfect channel knowledge and
- the inclusion of time allocated for performing channel estimation.

The proposed analytical framework is further complemented by considering a random behaviour of the interacting channels (or channel fading). Based on the derived expressions, the performance of the IS that employs channel estimation is evaluated, where the interacting channels are subjected to Nakagami- m fading.

2.2.2 Imperfect Channel Knowledge

In order to capture the variations induced due to imperfect channel knowledge, the cumulative distribution functions (cdfs) of performance parameters such as detection probability and achievable secondary throughput are characterized. More importantly, the cdf of the detection probability is utilized to incorporate two PU constraints, namely, an average constraint and an outage constraint on the detection probability. In this way, the proposed approach is able to control the amount of uncertainty in the interference caused at the PR due to the imperfect channel knowledge.

2.2.3 Estimation-Sensing-Throughput Tradeoff

Subject to the average and the outage constraints, the expressions of the sensing-throughput tradeoff that capture the aforementioned variations and evaluate the performance loss (in terms of the achievable secondary throughput) are established. In particular, two different optimization approaches for countering the variations in the IS and determining suitable estimation and suitable sensing time intervals, which attain a maximum secondary throughput, are proposed. Finally, a fundamental tradeoff between estimation time, sensing time and achievable secondary throughput is depicted. This tradeoff is exploited to determine suitable estimation and suitable sensing time intervals that depict the maximum achievable performance of the IS. Besides, the estimation-sensing-throughput tradeoff is adapted to the scenarios with channel fading, thus determining the achievable secondary throughput subject to the random behaviour of the channels.

2.3 System Model

2.3.1 Interweave Scenario

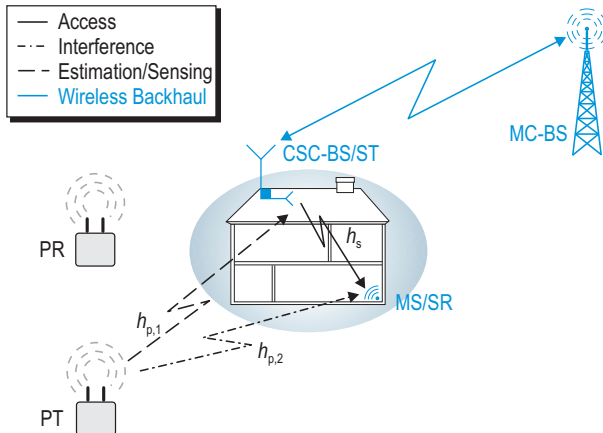


Figure 2.1: A cognitive small cell scenario demonstrating: (i) the interweave paradigm, (ii) the associated network elements, which constitute cognitive small cell-base station/secondary transmitter (CSC-BS/ST), mobile station/secondary receiver (MS/SR), macro cell-base station (MC-BS) and primary transmitter (PT), (iii) the interacting channels: sensing ($h_{p,1}$), access (h_s) and interference ($h_{p,2}$).

To consider the applicability of IS, the CSC, a CR application illustrated in the previous chapter, is transformed into an interweave scenario. Considering the fact that the IS is employed at the CSC-BS, the CSC-BS and the MS represent the ST and the SR, respectively. A hardware prototype of the CSC-BS operating as IS was presented in [K1]. For simplification, a PU constraint based on false alarm probability was considered in [K1]. With the purpose of improving system's reliability, the analysis is extended to employ a PU constraint on the detection probability.

Complementing the analysis depicted in [34], a slotted medium access for the IS is considered, where the time axis is segmented into frames of length T , according to which the ST employs periodic sensing. Hence, each frame consists of a sensing slot τ_{sen} and the remaining duration $T - \tau_{\text{sen}}$ is utilized for data transmission. For small T relative to the PUs' expected ON/OFF period,

the requirement of the ST to be in alignment to PUs' medium access can be relaxed [70–72].

2.3.2 Signal Model

Subject to the underlying hypothesis that illustrates the presence (\mathcal{H}_1) or the absence (\mathcal{H}_0) of a PU signal, the discrete and complex signal received at the ST is given by

$$y_{\text{ST}}[n] = \begin{cases} h_{\text{p},1} \cdot x_{\text{PT}}[n] + w_{\text{ST}}[n] & : \mathcal{H}_1 \\ w_{\text{ST}}[n] & : \mathcal{H}_0 \end{cases}, \quad (2.1)$$

where $x_{\text{PT}}[n]$ corresponds to a discrete and complex sample transmitted by the PT, $|h_{\text{p},1}|^2$ represents the power gain of the sensing channel for a given frame and $w_{\text{ST}}[n]$ is circularly symmetric Additive White Gaussian Noise (AWGN) $\mathcal{CN}(0, \sigma_w^2)$ at the ST.

According to [34], the signal $x_{\text{PT}}[n]$ transmitted by the PUs can be modeled as: (i) a phase shift keying modulated signal, or (ii) a Gaussian signal. The signals that are prone to high inter-symbol interference or entail precoding, for instance Orthogonal Frequency Division Multiplexing (OFDM) signal with linear precoding, can be modeled as Gaussian signals. In this chapter and the Chapter 4 (dedicated to the HS), the analysis is focused on the latter case, i.e., the primary and the secondary systems employ OFDM to carry out their transmission. In contrast, Chapter 3 associated with the US, considers the former case for the analysis. As a result, the mean and the variance for the signal and the noise are determined as $\mathbb{E}[x_{\text{PT}}[n]] = 0$, $\mathbb{E}[w_{\text{ST}}[n]] = 0$, $\mathbb{E}[|x_{\text{PT}}[n]|^2] = \sigma_s^2 (= P_{\text{Tx,PT}})$ and $\mathbb{E}[|w_{\text{ST}}[n]|^2] = \sigma_w^2$. The channel $h_{\text{p},1}$ is considered to be independent of $x_{\text{PT}}[n]$ and $w_{\text{ST}}[n]$. Thus, $y_{\text{ST}}[n]$ is also an independent and identically distributed (i.i.d.) random process.

Similar to (2.1), during data transmission, the discrete and complex received signal at the SR conditioned on the detection probability (P_d) and the false alarm probability (P_{fa}) is given by

$$y_{\text{SR}}[n] = \begin{cases} h_s \cdot x_{\text{ST}}[n] + h_{\text{p},2} \cdot x_{\text{PT}}[n] + w_{\text{SR}}[n] & : 1 - P_d \\ h_s \cdot x_{\text{ST}}[n] + w_{\text{SR}}[n] & : 1 - P_{\text{fa}} \end{cases}, \quad (2.2)$$

where $x_{\text{ST}}[n]$ corresponds to discrete and complex sample transmitted by the ST and $w_{\text{SR}}[n]$ is the AWGN at the SR with $\mathcal{CN}(0, \sigma_w^2)$ ⁴. Further, $|h_s|^2$ and $|h_{p,2}|^2$ represent the power gains for the access and the interference channels, refer to Figure 2.1.

2.3.3 Problem Description

In accordance with the conventional frame structure, the ST performs sensing for a duration of τ_{sen} . The test statistics $\mathbf{T}(\mathbf{y})$ at the ST is evaluated as

$$\mathbf{T}(\mathbf{y}) = \frac{1}{\tau_{\text{sen}} f_s} \sum_{n=1}^{\tau_{\text{sen}} f_s} |y_{\text{ST}}[n]|^2 \underset{\mathcal{H}_0}{\overset{\mathcal{H}_1}{\geq}} \mu, \quad (2.3)$$

where μ is the decision threshold, f_s represents the sampling frequency and \mathbf{y} is a vector with $\tau_{\text{sen}} f_s$ samples. $\mathbf{T}(\mathbf{y})$ represents a random variable, whereby the characterization of the cdf depends on the underlying hypothesis. With regard to the Gaussian signal model, which corresponds to the OFDM signal transmitted by the PU, $\mathbf{T}(\mathbf{y})$ follows a central chi-squared⁵ (\mathcal{X}^2) distribution for both hypotheses \mathcal{H}_0 and \mathcal{H}_1 [73].

As a result, the detection probability (P_d) and the false alarm probability (P_{fa}) corresponding to (2.3) are determined as [74]

$$P_d = \Gamma \left(\frac{\tau_{\text{sen}} f_s}{2}, \frac{\tau_{\text{sen}} f_s \mu}{2P_{\text{Rx,ST},h_{p,1}}} \right), \quad (2.4)$$

$$P_{\text{fa}} = \Gamma \left(\frac{\tau_{\text{sen}} f_s}{2}, \frac{\tau_{\text{sen}} f_s \mu}{2\sigma_w^2} \right), \quad (2.5)$$

where $P_{\text{Rx,ST},h_{p,1}}$ is the power received over the sensing channel and $\Gamma(\cdot, \cdot)$ represents a regularized upper-incomplete Gamma function [75].

⁴In practice, the noise power at different network nodes (the ST, the SR and the PR) have different values. The fact is, only the signal to noise ratios received at these nodes are affected due to these different values, which are already included in the performance analysis. For the brevity of the exposition, in the thesis, the noise powers at these nodes are expressed using a single notation (σ_w^2).

⁵It is worthy to mention here that, by avoiding the Gaussian approximation that exists due to the application of central limit theorem, thereby limiting the applicability of the considered analysis to only large sample sizes. In the thesis, an effort has been made to derive the theoretical expressions so that the performance analysis is valid for all sample sizes.

Following the characterization of P_{fa} and P_d , Liang *et al.* [34] established a tradeoff between the sensing time and the secondary throughput (R_s) subject to a target detection probability (\bar{P}_d). This tradeoff is represented as

$$\begin{aligned} R_s(\tilde{\tau}_{\text{sen}}) &= \max_{\tau_{\text{sen}}} R_s(\tau_{\text{sen}}) \\ &= \frac{T - \tau_{\text{sen}}}{T} \left[C_0(1 - P_{fa})\mathbb{P}(\mathcal{H}_0) + C_1(1 - P_d)\mathbb{P}(\mathcal{H}_1) \right], \end{aligned} \quad (2.6)$$

$$\text{s.t. } P_d \geq \bar{P}_d, \quad (2.7)$$

$$\text{where } C_0 = \log_2 \left(1 + |h_s|^2 \frac{P_{\text{Tx,ST}}}{\sigma_w^2} \right) = \log_2(1 + \gamma_s), \quad (2.8)$$

$$\begin{aligned} C_1 &= \log_2 \left(1 + \frac{|h_s|^2 P_{\text{Tx,ST}}}{|h_{p,2}|^2 P_{\text{Tx,PT}} + \sigma_w^2} \right) \\ &= \log_2 \left(1 + \frac{|h_s|^2 P_{\text{Tx,ST}}}{P_{\text{Rx,SR}}} \right) = \log_2 \left(1 + \frac{\gamma_s}{\gamma_{p,2} + 1} \right), \end{aligned} \quad (2.9)$$

where $\mathbb{P}(\mathcal{H}_0)$ and $\mathbb{P}(\mathcal{H}_1)$ are the occurrence probabilities for the respective hypothesis, whereas $\gamma_{p,1}$ and γ_s represent the signal to noise ratio for the links PT-ST and ST-SR, respectively, and $\gamma_{p,2}$ corresponds to interference (from the PT) to noise ratio for the link PT-SR. Moreover, $P_{\text{Tx,PT}}$ and $P_{\text{Tx,ST}}$ represent the transmit power at the PT and the ST, whereas $P_{\text{Rx,SR}}$ corresponds to the received power (which includes the interference power from the PT and the noise power) at the SR. In addition, C_0 and C_1 represent the data rate⁶ without and with the interference from the PT.

In other words, using (2.6), the ST determines a suitable sensing time $\tau_{\text{sen}} = \tilde{\tau}_{\text{sen}}$, such that the secondary throughput is maximized subject to a target detection probability, refer to (2.7). From the deployment perspective, the tradeoff depicted above has the following fundamental issues:

- Without the knowledge of the received power $P_{\text{Rx,ST},h_{p,1}}$ over the sensing channel, it is not feasible to characterize P_d , refer to (2.4). This renders the characterization of the secondary throughput (2.6) impossible and the constraint defined in (2.7) inappropriate.
- Moreover, the knowledge of the interference and the access channels is

⁶Please note, the following terms the data rate C_0 , C_1 and the throughput R_s have been introduced to make a clear distinction between the instantaneous data rate and its average value over the frame duration. Also, the use of the term ‘‘capacity’’ is avoided for representing C_0 and C_1 , since it implies the optimization of the mutual information over the cognitive channel.

required at the ST, refer to (2.8) and (2.9) for characterizing the throughput in terms of C_0 and C_1 at the SR.

Taking these issues into account, it is not feasible to employ the performance analysis depicted by this model (referred as ideal model, hereafter) for hardware implementation. In the subsequent section, an analytical framework (also referred as estimation model) that addresses the aforementioned issues – including the estimation of the sensing and the access channels at the ST and the interference at the SR – is proposed. Based on the proposed approach, the performance of the IS in terms of the sensing-throughput tradeoff is investigated.

2.3.4 Proposed Approach

In order to overcome the difficulties discussed in Section 2.3.3, the following strategy is proposed.

1. As a first step, the estimation of the involved channels is considered. In order to characterize the detection probability, a received power-based estimation at the ST for the sensing channel is employed. This is done to ensure that the detection probability remains above a desired level. Further, a pilot-based estimation and a received power-based estimation for the access channel and the interference channel are employed at the ST and the SR, respectively, to characterize the secondary throughput.
2. Next, the variations due to channel estimation in the estimated parameters, namely, received power (for the sensing and the interference channels) and the power gain (for the access channel) are characterized in terms of their cdfs.
3. In order to investigate the performance of the IS subject to the channel estimation, these variations in the performance parameters, which include the detection probability and the secondary throughput, are characterized in terms of their cdfs.
4. Finally, the derived cdfs are utilized to obtain the expressions of sensing-throughput tradeoff. Hence, based on these expressions, the impact of imperfect channel knowledge on the performance of the ISs is qualified, and subsequently the achievable secondary throughput at a suitable sensing time is determined.

Considering the channel estimation, it is well-known that systems with transmitter information (which includes the filter parameters, pilot symbols, modulation type and time-frequency synchronization) at the receiver acquire the channel knowledge by listening to the pilot data sent by the ST [53, 54, 76, 77]. Other systems, where the receiver possesses either no access to this information or is limited by hardware complexity, procure channel knowledge indirectly by estimating a different parameter that entails the channel knowledge, for instance, received signal power [K2] or received signal to noise ratio [55, 56]. Recently, estimation techniques such as pilot-based estimation [50, 51] and received power-based estimation [K8] have been applied to obtain channel knowledge for the CR systems. However, the performance analysis has been limited to the underlay systems, where the emphasis has been given on modeling the interference at the PR.

Since the pilot-based estimation requires the knowledge of the PU signal at the secondary system, the versatility (in terms of PU signals) of the secondary system is compromised. On the other side, for the estimation of the received signal to noise ratio, Eigenvalue (which involves matrix operations) based approach [56] or iterative approaches such as expectation-maximization have been proposed [55]. Due to the complicated mathematical operations or the complexity of the iterative algorithms, such approaches tend to increase the hardware complexity of the ISs. In order to resolve these issues, a received power-based estimation for the sensing and the interference channels, and a pilot-based estimation for the access channel is employed. Similar to the energy based detection, since the received power-based estimation involves simple operations on the obtained samples such as magnitude squared followed by summation, the proposed estimation provides a reasonable tradeoff between complexity and versatility.

However, with the inclusion of this channel estimation, the system suffers a performance loss in terms of: (i) temporal resources (time allocation) used and (ii) variations in the aforementioned performance parameters. A preliminary analysis of this performance loss was carried out in [K2], where it was revealed that in low signal to noise ratio regime, imperfect knowledge of received power corresponds to a large variation in the detection probability, causing a severe degradation in the performance. However, this performance degradation was determined by means of lower and upper bounds. In this chapter, a more exact analysis is considered, whereby the variations in detection probability are captured by characterizing its cdf, and subsequently apply new probabilistic constraints on the detection probability, which allow the IS to operate at low signal to noise ratio regime.

Frame Structure

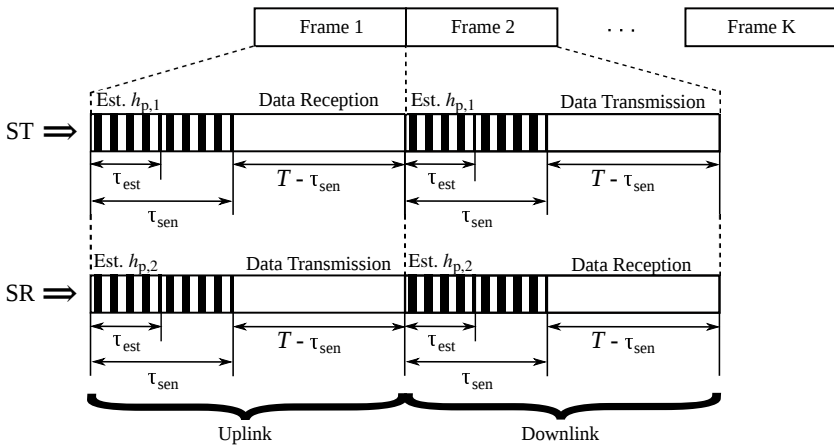


Figure 2.2: Frame structure of the IS illustrating the time allocation of the channel estimation, sensing and data transmission from the perspective of the ST and the SR.

In order to include channel estimation, a frame structure that constitutes estimation τ_{est} , sensing τ_{sen} and data transmission $T - \tau_{\text{sen}}$ is proposed, where τ_{est} and τ_{sen} correspond to time intervals and $0 < \tau_{\text{est}} \leq \tau_{\text{sen}} < T$, refer to Figure 2.2. Since the estimated values of the interacting channels are required for determining the suitable sensing time (the duration of the sensing phase), the sequence depicted in Figure 2.2 is reasonable for the hardware deployment, whereby estimation is followed by sensing. Particularly for the sensing channel, it is worthy to note that the samples used for estimation can be combined with the samples acquired for sensing⁷ such that the time resources within the frame duration can be utilized efficiently, as shown in the frame structure in Figure 2.2. Considering the fact that the number of pilot symbols is relatively small in comparison to the samples used for performing received power-based channel estimation, the time allocation of the pilot symbols does not affect the overall performance of the ISs. Hence, no time resources are allocated for the estimation of the access channel in the frame structure⁸. In the following paragraphs, the estimation of the involved channels is considered.

⁷Therefore, the sensing phase incorporates the estimation phase, see Figure 2.2.

⁸Please note that this argument is also applicable to the frame structures concerning the US and the HS, which will appear in the following two chapters.

Estimation of sensing channel ($h_{p,1}$)

Following the previous discussions, the ST acquires the knowledge of $|h_{p,1}|^2$ (included in $P_{\text{Rx,ST},h_{p,1}}$, cf. (2.4)) to characterize P_d , and to further evaluate the detector's performance. This knowledge is acquired by estimating the power received at the ST over the sensing channel.

Under \mathcal{H}_1 , the received power-based estimated during the estimation phase at the ST is given as [61]

$$\hat{P}_{\text{Rx,ST},h_{p,1}} = \frac{1}{\tau_{\text{est}}f_s} \sum_{n=1}^{\tau_{\text{est}}f_s} |y_{\text{ST}}[n]|^2. \quad (2.10)$$

$\hat{P}_{\text{Rx,ST},h_{p,1}}$ determined in (2.10) using $\tau_{\text{est}}f_s$ samples follows a central chi-squared distribution \mathcal{X}^2 [73]. f_s and τ_{est} are such that the number of samples $\tau_{\text{est}}f_s$ is an integer⁹. The cdf of $\hat{P}_{\text{Rx,ST},h_{p,1}}$ is given by

$$F_{\hat{P}_{\text{Rx,ST},h_{p,1}}}(x) = 1 - \Gamma\left(\frac{\tau_{\text{est}}f_s}{2}, \frac{\tau_{\text{est}}f_s x}{2P_{\text{Rx,ST},h_{p,1}}}\right). \quad (2.11)$$

Estimation of access channel (h_s)

The signal received from the SR undergoes matched filtering and demodulation at the ST, hence, it is reasonable to employ pilot-based estimation for h_s . Unlike received power-based estimation, pilot-based estimation renders a direct estimation of the channel. Now, to accomplish pilot-based estimation, the ST aligns itself to the pilot symbols transmitted by the SR.

Under \mathcal{H}_0 , the discrete and complex pilot symbol at the output of the demodulator is given by [54]

$$p[n] = \sqrt{E_s}h_s + w_{\text{ST}}[n], \quad (2.12)$$

where E_s denotes the pilot energy. Without loss of generality, the pilot symbols are considered to be +1. The maximum likelihood estimate, representing a sample average of N_s pilot symbols, is given by [53]

$$\hat{h}_s = h_s + \frac{\sum_{n=1}^{N_s} w_{\text{ST}}[n]}{N_s}, \quad (2.13)$$

⁹Please note that this assumption is considered throughout the thesis.

where ϵ denotes the estimation error. The estimate \hat{h}_s is unbiased, efficient and achieves a Cramér-Rao bound with equality, with variance $\mathbb{E} \left[|h_s - \hat{h}_s|^2 \right] = \sigma_w^2 / N_s$ [54].

Consequently, \hat{h}_s conditioned on h_s follows a circularly symmetric Gaussian distribution.

$$\hat{h}_s | h_s \sim \mathcal{CN} \left(h_s, \frac{\sigma_w^2}{N_s} \right). \quad (2.14)$$

As a result, the power gain $|\hat{h}_s|^2$ follows a non-central chi-squared (\mathcal{X}'^2) distribution with 2 degrees of freedom and non-centrality parameter $\lambda_s = \frac{N_s |h_s|^2}{\sigma_w^2}$.

Estimation of interference channel ($h_{p,2}$)

The knowledge of $|h_{p,2}|^2$ is required to characterize the interference from the PT. Analog to the sensing channel, the SR performs received power-based estimation by listening to the signal transmitted by the PT.

Under \mathcal{H}_1 , in the estimation phase (which implies ST is not transmitting, please consider Figure 2.2), the discrete and complex signal received at the SR is given as

$$y_{\text{SR}}[n] = h_{p,2} \cdot x_{\text{PT}}[n] + w_{\text{SR}}[n]. \quad (2.15)$$

As a result, the estimated power at the SR, from the signal transmitted by the PT, is given by

$$\hat{P}_{\text{Rx,SR}} = \frac{1}{\tau_{\text{est}} f_s} \sum_{n=1}^{\tau_{\text{est}} f_s} |y_{\text{SR}}[n]|^2, \quad (2.16)$$

where $\hat{P}_{\text{Rx,SR}}$ follows a \mathcal{X}^2 distribution.

2.3.5 Validation

At this stage, it is clear that the estimates $\hat{P}_{\text{Rx,ST},h_{p,1}}$, $|\hat{h}_s|^2$ and $\hat{P}_{\text{Rx,SR}}$ exhibit the knowledge corresponding to the involved channels, however, it is essential to validate them, mainly $\hat{P}_{\text{Rx,ST},h_{p,1}}$ and $\hat{P}_{\text{Rx,SR}}$. In this context, it is necessary

to ensure the presence of the PU signal (\mathcal{H}_1) for that particular frame. In this direction, Chavali *et al.* [55] recently proposed a detection followed by the estimation of the signal to noise ratio, while [69] implemented a blind technique for estimating the signal power of non-coherent PU signals.

In this thesis, a different methodology is proposed, according to which a coarse detection¹⁰ on the estimates ($\hat{P}_{\text{Rx,ST},h_{p,1}}, \hat{P}_{\text{Rx,SR}}$) at the end of the estimation phase τ_{est} is applied. Through an appropriate selection of the time interval τ_{est} (for instance, $\tau_{\text{est}} \in [1, 10]\text{ms}$) during the system design, the reliability of the coarse detection can be ensured. With the existence of a separate control channel such as cognitive pilot channel, the reliability of the coarse detection can be further enhanced by exchanging the detection results between the ST and the SR.

The estimation and the coarse detection processes in the proposed method are equivalent in terms of their mathematical operations, which consist of magnitude squared and summation. In this regard, the validity of the channel estimates with certain reliability and without comprising the complexity of the estimators, employed by the secondary system, is considered. Moreover, by performing a joint estimation and (coarse) detection, an efficient way of utilizing the time resources within the frame duration is proposed. The ST considers these estimates to determine a suitable sensing time based on the sensing-throughput tradeoff such that the desired detector's performance is ensured. At the end of the detection phase, a fine detection¹¹ of the PU signals is carried out, thereby improving the performance of the detector.

2.3.6 Assumptions

To simplify the analysis and sustain analytical tractability for the proposed approach, several assumptions, considered in the thesis, are summarized as follows:

- All transmitted signals are subjected to distance dependent path loss and small scale fading gain. With no loss of generality, it is considered that the channel gains include distance dependent path loss and small scale

¹⁰For the coarse detection, an energy detection is employed whose threshold can be determined by means of a constant false alarm rate.

¹¹In accordance with the proposed frame structure in Figure 2.2, fine detection represents the main detection, which also includes the samples acquired during the estimation phase.

gain. Moreover, the coherence time for the channel gain is considered to be greater than the frame duration¹².

- Perfect knowledge of the noise power is assumed in the system, however, the uncertainty in noise power can be captured as a bounded interval [74]. Inserting this interval in the derived expressions, refer to Section 2.4, the performance of the IS can be expressed in terms of the upper and the lower bounds.

For analytical tractability, the following approximation is considered.

Approximation 1 For all degrees of freedom, \mathcal{X}'^2 distribution can be approximated by a Gamma distribution [78]. The parameters of the Gamma distribution are obtained by matching the first two central moments to those of \mathcal{X}'^2 .

2.4 Theoretical Analysis

2.4.1 Deterministic Channel

At first, the performance of the proposed framework in context to the deterministic channel is evaluated. It is evident that the variation due to the imperfect channel knowledge translates to the variations in the performance parameters

$$\hat{P}_d = \Gamma \left(\frac{\tau_{\text{sen}} f_s}{2}, \frac{\tau_{\text{sen}} f_s \mu}{2 \hat{P}_{\text{Rx,ST},h_{p,1}}} \right), \quad (2.17)$$

$$\hat{C}_0 = \log_2 \left(1 + |\hat{h}_s|^2 \frac{P_{\text{Tx,ST}}}{\sigma_w^2} \right) \quad (2.18)$$

and

$$\hat{C}_1 = \log_2 \left(1 + \frac{|\hat{h}_s|^2 P_{\text{Tx,ST}}}{\hat{P}_{\text{Rx,SR}}} \right), \quad (2.19)$$

which are fundamental to sensing-throughput tradeoff. It is worth noticing the fact (2.17), (2.18) and (2.19) are determined using the estimated parameters,

¹²In scenarios, where the coherence time exceeds the frame duration, the proposed characterization depicts a lower performance bound.

which include $\hat{P}_{\text{Rx,ST},h_{p,1}}$, $|\hat{h}_s|^2$ and $\hat{P}_{\text{Rx,SR}}$, determined in previous section. Below, the variations in these performance parameters are characterized in terms of their cdfs $F_{\hat{P}_d}(\cdot)$, $F_{\hat{C}_0}(\cdot)$ and $F_{\hat{C}_1}(\cdot)$.

Lemma 1 The cdf of \hat{P}_d is characterized as

$$F_{\hat{P}_d}(x) = 1 - \Gamma\left(\frac{\tau_{\text{est}}f_s}{2}, \frac{\tau_{\text{est}}\tau_{\text{sen}}f_s^2\mu}{4P_{\text{Rx,ST},h_{p,1}}\Gamma^{-1}\left(x, \frac{\tau_{\text{sen}}f_s}{2}\right)}\right), \quad (2.20)$$

where $\Gamma^{-1}(\cdot, \cdot)$ is the inverse of the regularized upper-incomplete Gamma function [75].

Solution: The cdf of \hat{P}_d is defined as

$$F_{\hat{P}_d}(x) = \mathbb{P}(\hat{P}_d \leq x). \quad (2.21)$$

Using (2.17)

$$= \mathbb{P}\left(\Gamma\left(\frac{\tau_{\text{sen}}f_s}{2}, \frac{\tau_{\text{sen}}f_s\mu}{2\hat{P}_{\text{Rx,ST},h_{p,1}}}\right) \leq x\right), \quad (2.22)$$

$$= 1 - \mathbb{P}\left(\hat{P}_{\text{Rx,ST},h_{p,1}} \geq \frac{\mu\tau_{\text{sen}}f_s}{2\Gamma^{-1}\left(x, \frac{\tau_{\text{sen}}f_s}{2}\right)}\right). \quad (2.23)$$

Replacing the cdf of $\hat{P}_{\text{Rx,ST},h_{p,1}}$ in (2.23), an expression of $F_{\hat{P}_d}(\cdot)$ is obtained.

Lemma 2 The cdf of \hat{C}_0 is defined as

$$F_{\hat{C}_0}(x) = \int_0^x f_{\hat{C}_0}(t)dt, \quad (2.24)$$

where

$$f_{\hat{C}_0}(x) = 2^x \ln 2 \frac{(2^x - 1)^{a_s - 1}}{\Gamma(a_s)b_s^{a_s}} \exp\left(-\frac{2^x - 1}{b_s}\right), \quad (2.25)$$

and, a_s and b_s are defined in (2.46).

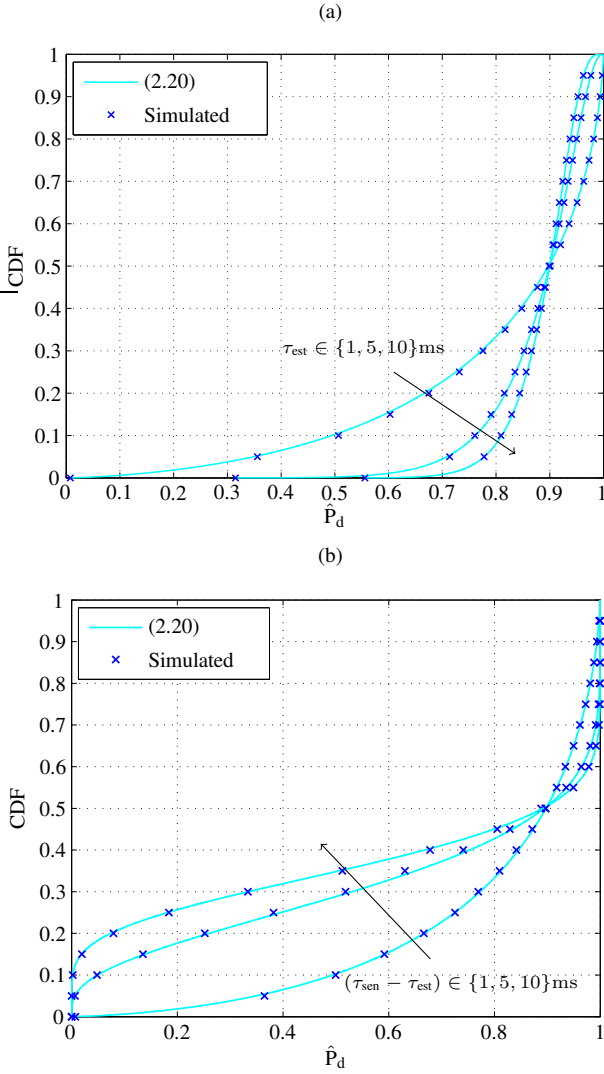


Figure 2.3: The cdf of \hat{P}_d for different τ_{est} and τ_{sen} . (a) $\tau_{\text{est}} \in \{1, 5, 10\}$ ms and $(\tau_{\text{sen}} - \tau_{\text{est}}) = 1$ ms, (b) $\tau_{\text{est}} = 1$ ms and $(\tau_{\text{sen}} - \tau_{\text{est}}) \in \{1, 5, 10\}$ ms.

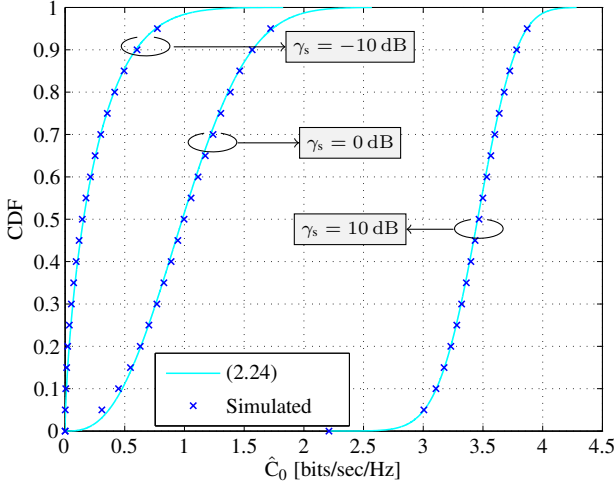


Figure 2.4: The cdf of \hat{C}_0 for different values of $\gamma_s \in \{-10, 0, 10\}$ dB.

Solution: See Section 2.7.1

Lemma 3 The cdf of \hat{C}_1 is given by

$$F_{\hat{C}_1}(x) = \int_0^x f_{\hat{C}_1}(t) dt, \quad (2.26)$$

where

$$f_{\hat{C}_1}(x) = 2^x \ln 2 \frac{(2^x - 1)^{a_s - 1} \Gamma(a_s + a_p)}{\Gamma(a_s) \Gamma(a_p) b_s^{a_s} b_p^{a_p}} \left(\frac{1}{b_p} + \frac{2^x - 1}{b_s} \right)^{(a_s + a_p)}, \quad (2.27)$$

where a_s and b_s are defined in (2.46), whereas a_p and b_p are defined in (2.49).

Solution: See Section 2.7.2

In consideration to Approximation 1, which is applied to approximate the cdf of $|\hat{h}_s|^2$ in (2.45), the theoretical expressions of the cdfs $F_{\hat{P}_d}(\cdot)$, $F_{\hat{C}_0}(\cdot)$ and $F_{\hat{C}_1}(\cdot)$ – depicted in Lemma 1, Lemma 2 and Lemma 3 – are validated by means of simulations in Figure 2.3, Figure 2.4 and Figure 2.5, respectively, with different choices of system parameters, including $\tau_{\text{est}} \in \{1, 5, 10\}$ ms,

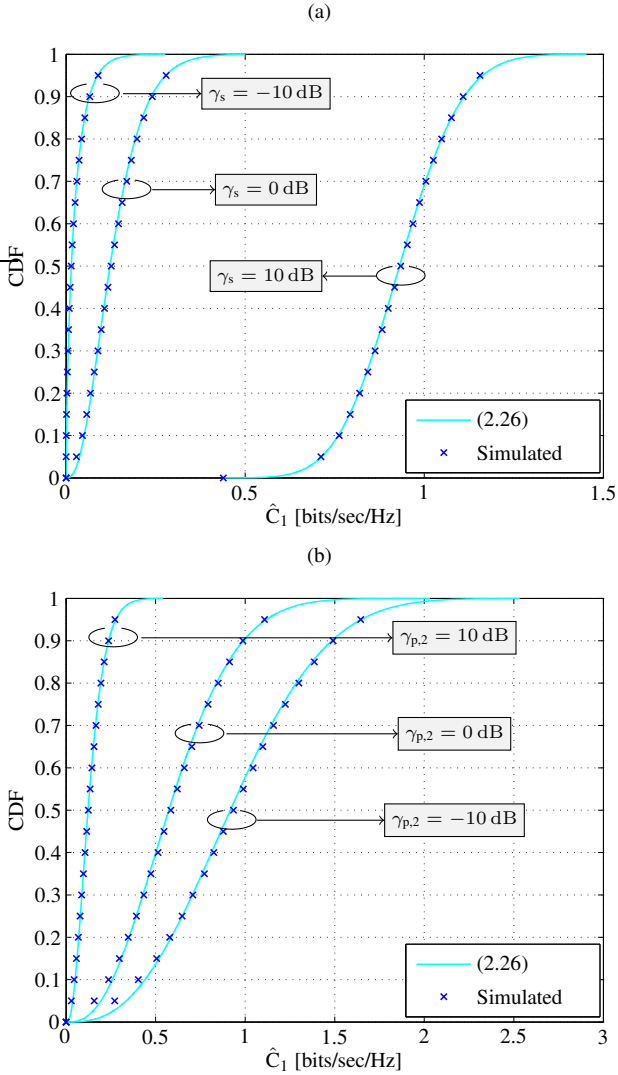


Figure 2.5: The cdf of \hat{C}_1 for different γ_s and $\gamma_{p,2}$. (a) $\gamma_s \in \{-10, 0, 10\}$ dB and $\gamma_{p,2} = 10$ dB, (b) $\gamma_s = 0$ dB and $\gamma_{p,2} \in \{-10, 0, 10\}$ dB.

$(\tau_{\text{sen}} - \tau_{\text{est}}) = \{1, 5, 10\}$ ms, $\gamma_s \in \{-10, 0, 10\}$ dB and $\gamma_{p,2} \in \{-10, 0, 10\}$ dB.

Next, a sensing-throughput tradeoff for the estimation model is established that includes the estimation time and incorporates the variations in the performance parameter. Most importantly, to restrain the harmful effect of the uncertain interference at the PR due to the variations in the detection probability, two new PU constraints at the PR, namely an Average Constraint (AC) and an Outage Constraint (OC) on the detection probability are proposed. Based on these constraints, the sensing-throughput tradeoff for the IS is characterized.

Problem 1 The achievable expected secondary throughput subject to an average constraint on \hat{P}_d that employs channel estimation corresponding to the deterministic behavior of the interacting channels, is given by

$$\begin{aligned} R_s(\tilde{\tau}_{\text{est}}, \tilde{\tau}_{\text{sen}}) &= \max_{\tau_{\text{est}}, \tau_{\text{sen}}} \mathbb{E}_{\hat{P}_d, \hat{C}_0, \hat{C}_1} [R_s(\tau_{\text{est}}, \tau_{\text{sen}})] \\ &= \frac{T - \tau_{\text{sen}}}{T} \left[\mathbb{E}_{\hat{C}_0} [\hat{C}_0] (1 - P_{\text{fa}}) \mathbb{P}(\mathcal{H}_0) + \right. \\ &\quad \left. \mathbb{E}_{\hat{C}_1} [\hat{C}_1] (1 - \mathbb{E}_{\hat{P}_d} [\hat{P}_d]) \mathbb{P}(\mathcal{H}_1) \right], \end{aligned} \quad (2.28)$$

$$\text{s.t. } \mathbb{E}_{\hat{P}_d} [\hat{P}_d] \geq \bar{P}_d, \quad (2.29)$$

$$\text{s.t. } 0 < \tau_{\text{est}} \leq \tau_{\text{sen}} \leq T,$$

where $\mathbb{E}_{\hat{P}_d} [\cdot]$ represents the expectation with respect to \hat{P}_d , $\mathbb{E}_{\hat{P}_d, \hat{C}_0, \hat{C}_1} [\cdot]$ denotes the expectation with respect to \hat{P}_d , \hat{C}_0 and \hat{C}_1 . Unlike (2.7), \bar{P}_d in (2.28) represents the constraint on expected detection probability.

Solution: See Section 2.7.3. For simplification, the proof of Problem 1 is included in the proof of Problem 2.

Problem 2 The achievable expected secondary throughput subject to an outage constraint on \hat{P}_d that employs channel estimation corresponding to the deterministic behavior of the interacting channels, is given by

$$\begin{aligned} R_s(\tilde{\tau}_{\text{est}}, \tilde{\tau}_{\text{sen}}) &= \max_{\tau_{\text{est}}, \tau_{\text{sen}}} \mathbb{E}_{\hat{P}_d, \hat{C}_0, \hat{C}_1} [R_s(\tau_{\text{est}}, \tau_{\text{sen}})] \\ &= \frac{T - \tau_{\text{sen}}}{T} \left[\mathbb{E}_{\hat{C}_0} [\hat{C}_0] (1 - P_{\text{fa}}) \mathbb{P}(\mathcal{H}_0) + \right. \end{aligned}$$

$$\mathbb{E}_{\hat{C}_1} \left[\hat{C}_1 \right] (1 - \mathbb{E}_{\hat{P}_d} \left[\hat{P}_d \right]) \mathbb{P}(\mathcal{H}_1) \Big], \quad (2.30)$$

$$\text{s.t. } \mathbb{P}(\hat{P}_d \leq \bar{P}_d) \leq \rho_d, \quad (2.31)$$

$$\text{s.t. } 0 < \tau_{\text{est}} \leq \tau_{\text{sen}} \leq T,$$

where ρ_d represents the outage constraint.

Solution: See Section 2.7.3.

Remark 1 In contrast to the ideal model, the sensing-throughput tradeoff investigated by the estimation model (refer to Problems 1 and 2) incorporates the imperfect channel knowledge. In this context, the performance characterization considered by the proposed framework is closer to the realistic situations. Herein, based on the estimation model, a fundamental relation between estimation time (that regulates the variation in the detection probability according to the PU constraint), sensing time (that represents the detector performance) and achievable throughput is established. This relationship is characterized as estimation-sensing-throughput tradeoff. Based on this tradeoff, a suitable estimation time $\tau_{\text{est}} = \tilde{\tau}_{\text{est}}$ and a suitable sensing time $\tau_{\text{sen}} = \tilde{\tau}_{\text{sen}}$ that attains a maximum achievable throughput $R_s(\tilde{\tau}_{\text{est}}, \tilde{\tau}_{\text{sen}})$ for the IS is determined.

Corollary 1 Problems 1 and 2 consider the optimization of the expected secondary throughput to incorporate the effect of variations due to the channel estimation, and subsequently determine the suitable sensing and the suitable estimation time. Here, an alternative approach to the optimization problem that captures the effect of imperfect channel knowledge is investigated. According to which, the suitable sensing time for a certain value of estimation time, subject to the average constraint, is determined as

$$\tilde{\tau}_{\text{sen}} = \underset{\tau_{\text{sen}}}{\text{argmax}} R_s(\tau_{\text{est}}, \tau_{\text{sen}}) \quad (2.32)$$

$$= \frac{T - \tau_{\text{sen}}}{T} \left[\hat{C}_0(1 - P_{\text{fa}}) \mathbb{P}(\mathcal{H}_0) + \hat{C}_1(1 - \hat{P}_d) \mathbb{P}(\mathcal{H}_1) \right],$$

$$\text{s.t. } \mathbb{E}_{\hat{P}_d} \left[\hat{P}_d \right] \geq \bar{P}_d,$$

$$\text{s.t. } 0 < \tau_{\text{est}} \leq \tau_{\text{sen}} \leq T.$$

Similarly, the suitable sensing time for a certain value of estimation time, subject to the outage constraint, is determined as

$$\tilde{\tau}_{\text{sen}} = \underset{\tau_{\text{sen}}}{\text{argmax}} R_s(\tau_{\text{est}}, \tau_{\text{sen}}) \quad (2.33)$$

$$\begin{aligned}
 &= \frac{T - \tau_{\text{sen}}}{T} \left[\hat{C}_0(1 - P_{\text{fa}})\mathbb{P}(\mathcal{H}_0) + \hat{C}_1(1 - \hat{P}_d)\mathbb{P}(\mathcal{H}_1) \right], \\
 \text{s.t. } &\mathbb{P}(\hat{P}_d \leq \bar{P}_d) \leq \rho_d, \\
 \text{s.t. } &0 < \tau_{\text{est}} \leq \tau_{\text{sen}} \leq T.
 \end{aligned}$$

In contrast to (2.28) and (2.30), the suitable sensing time evaluated in (2.32) and (2.33) entails the variations due to the channel estimation from the performance parameters $(\hat{P}_d, \hat{C}_0, \hat{C}_1)$. Hence, the expected secondary throughput subject to the average and the outage constraints that captures the variations in the suitable sensing time and the performance parameters, is determined as

$$\mathbb{E}_{\hat{P}_d, \hat{C}_0, \hat{C}_1, \tilde{\tau}_{\text{sen}}} [R_s(\tau_{\text{est}}, \tilde{\tau}_{\text{sen}})], \quad (2.34)$$

where $\mathbb{E}_{\hat{P}_d, \hat{C}_0, \hat{C}_1, \tilde{\tau}_{\text{sen}}} [\cdot]$ corresponds to an expectation over $\hat{P}_d, \hat{C}_0, \hat{C}_1, \tilde{\tau}_{\text{sen}}$.

In reference to Remark 1, the expected secondary throughput, defined in (2.34), is further optimized over the estimation time to yield the achievable expected secondary throughput

$$R_s(\tilde{\tau}_{\text{est}}, \tilde{\tau}_{\text{sen}}) = \max_{\tau_{\text{est}}} \mathbb{E}_{\hat{P}_d, \hat{C}_0, \hat{C}_1, \tilde{\tau}_{\text{sen}}} [R_s(\tau_{\text{est}}, \tilde{\tau}_{\text{sen}})]. \quad (2.35)$$

In this way, an estimation-sensing-throughput tradeoff for the alternative approach is established that determines the suitable estimation and the suitable sensing time intervals.

Remark 2 Complementing the analysis in [34], it is complicated to obtain a closed-form expression of $\tilde{\tau}_{\text{sen}}$, thereby rendering the analytical tractability of its cdf difficult. In this view, the performance of the alternative approach is captured by means of simulations.

2.4.2 Random Channel

In this section, the proposition is to extend the performance analysis of the proposed framework, where the interacting channels encounter quasi-static block fading. From a system perspective, it corresponds to slow and flat fading channel. In this view, the channel gains $h_{p,1}$, $h_{p,2}$ and h_s are characterized according to Nakagami- m fading model. As a consequence, the power gains $|h_{p,1}|^2$,

$|h_{p,2}|^2$ and $|h_s|^2$ follow a Gamma distribution [38], whose corresponding cdfs are defined as

$$F_{|h_{p,1}|^2}(x) = 1 - \Gamma\left(m_{p,1}, \frac{m_{p,1}x}{|\bar{h}_{p,1}|^2}\right), \quad (2.36)$$

$$F_{|h_{p,2}|^2}(x) = 1 - \Gamma\left(m_{p,2}, \frac{m_{p,2}x}{|\bar{h}_{p,2}|^2}\right), \quad (2.37)$$

$$F_{|h_s|^2}(x) = 1 - \Gamma\left(m_s, \frac{m_s x}{|\bar{h}_s|^2}\right), \quad (2.38)$$

where $m_{p,1}$, $m_{p,2}$ and m_s represent the Nakagami- m parameter, whereas $|\bar{h}_{p,1}|^2$, $|\bar{h}_{p,2}|^2$ and $|\bar{h}_s|^2$ are the expected values for the channels $|h_{p,1}|^2$, $|h_{p,2}|^2$ and $|h_s|^2$, respectively. In contrast to the deterministic channel where the power gains were treated as deterministic variables, $|h_{p,1}|^2$, $|h_{p,2}|^2$ and $|h_s|^2$ represent the random variables.

It is a well-known fact that Nakagami- m fading model is considered as a generalized fading model. In this context, it facilitates in understanding the performance behaviour of CR systems under fading conditions (severe and mild fading).

Perfect Channel Knowledge

First a scenario (also represented as the ideal model for the random channels) that precludes channel estimation is considered, in other words, the ST assumes perfect knowledge of the interacting channels. In this context, the ST encounters variations caused due to the channel fading only. These variations translate to the variations in the detection probability, more specifically those variations that do not meet the desired detection probability (\bar{P}_d), results in uncertain interference¹³ at the PR. To deal with this issue, an outage constraint is employed over P_d [67], given as

$$\mathbb{P}(P_d \leq \bar{P}_d) \leq \rho_d, \quad (2.39)$$

where ρ_d represents the outage constraint. Using (2.39), the ST is able to regulate the uncertain interference at the PR. As a result, a decision threshold (μ) on $P_{R_x, ST, h_{p,1}}$ is obtained such that it satisfies the constraint defined (2.39) for a certain value of τ_{sen} .

¹³Please note, in the context with perfect channel knowledge, the uncertainty is due to the variations in the channel gain, and is characterized as channel fading.

Besides the interference at the PR, the throughput at the SR is given by

$$R_s(\tau_{\text{sen}}) = \frac{T - \tau_{\text{sen}}}{T} \mathbb{E}_{|h_s|^2 | h_{p,2}|^2} \left[\overbrace{\mathbb{P}(\mathcal{H}_0)(1 - P_{\text{fa}}) \log_2 \left(1 + \frac{|h_s|^2 P_{\text{Tx,ST}}}{\sigma_w^2} \right)}^{C_0} + \overbrace{\mathbb{P}(\mathcal{H}_1)(1 - P_d) \log_2 \left(1 + \frac{|h_s|^2 P_{\text{Tx,ST}}}{|h_{p,2}|^2 P_{\text{Tx,PT}} + \sigma_w^2} \right)}^{C_1} \right]. \quad (2.40)$$

Since the detection probability and the secondary throughput are related through the sensing time, this relationship is exploited to determine a sensing-throughput tradeoff for the case with the perfect channel estimation.

Problem 3 The achievable expected secondary throughput subject to an outage constraint on P_d at the PR that considers the perfect channel estimation and the random behaviour of the interacting channels, is given by

$$\begin{aligned} R_s(\tilde{\tau}_{\text{sen}}) &= \max_{\tau_{\text{sen}}} \mathbb{E}_{P_d, |h_s|^2, |h_{p,2}|^2} [R_s(\tau_{\text{sen}})], & (2.41) \\ &\text{s.t. (2.39),} \\ &\text{s.t. } 0 < \tau_{\text{sen}} \leq T. \end{aligned}$$

Remark 3 It is worth noticing the fact that the authors in [67] applied channel fading only to the sensing channel, however, according to Problem 3, here, a more practical approach is considered, whereby the channel fading is also employed for the access and the interference channels. The perfect channel knowledge scenario is employed to benchmark the performance of those IS that employs channel estimation (discussed later in Section 2.4.2). In this view, the parameters such as threshold (which is used for evaluating P_d and P_{fa}) and the expected secondary throughput are evaluated numerically. Despite the knowledge of the fading model, similar to the ideal model depicted for the deterministic channel, the characterization in (2.41) and (2.39) assumes the perfect knowledge¹⁴ of the power gains for the corresponding channels. In view of this, the proposed framework is further extended to investigate the effect of the random channel (channel fading) on the performance of the ISs that incorporates estimation of the involved channels.

¹⁴For the channel fading case, this knowledge signifies the perfect knowledge of the different realizations of the corresponding channel.

Imperfect Channel Knowledge

Here, the estimation of the interacting channels in context to the channel fading is considered. To incorporate channel estimation, the similar frame structure, depicted in Figure 2.2, is employed. In contrast to the deterministic channel, here the IS incorporates variations in the performance parameters (\hat{P}_d and R_s) due to the channel estimation and the channel fading.

It is worth mentioning that the characterization of the estimated parameters $\hat{P}_{\text{RX,ST},h_{p,1}}$ and $\hat{P}_{\text{RX,SR}}$ for the sensing and the interference channel, and $|\hat{h}_s|^2$ for the access channel, in terms of their cdfs, has been performed in Section 2.3.4. In addition, the characterization of the performance parameters \hat{P}_d , \hat{C}_0 and \hat{C}_1 , in terms of their cdfs $F_{\hat{P}_d}(\cdot)$, $F_{\hat{C}_0}(\cdot)$ and $F_{\hat{C}_1}(\cdot)$, has been performed in Lemma 1, Lemma 2 and Lemma 3 of Section 2.4.1.

In order to regulate the uncertainty in detection probability, an outage constraint that jointly captures the variations due to channel estimation and channel fading, which result in uncertain interference at the PR, is defined as

$$\underbrace{\mathbb{E}_{|h_{p,1}|^2} \left[\overbrace{\mathbb{P}(\hat{P}_d \leq \bar{P}_d)}^{\text{Channel Estimation}} \right]}_{\text{Channel fading}} \leq \rho_d, \quad (2.42)$$

where $\mathbb{E}_{|h_{p,1}|^2} [\cdot]$ represents the expectation over the sensing channel. The variations due to the channel estimation only ($\mathbb{P}(\hat{P}_d \leq \bar{P}_d)$) are characterized in terms of cdf in (2.20). It is worth noticing that $\mathbb{E}_{|h_{p,1}|^2} [\cdot]$ in (2.42) acts on $\hat{P}_{\text{RX,ST},h_{p,1}}$, included in the characterization of \hat{P}_d , as $\hat{P}_{\text{RX,ST},h_{p,1}}$ incorporates the variations due to fading in the sensing channel $|h_{p,1}|^2$.

Next, the expression of the secondary throughput for the random channel is characterized as

$$\begin{aligned} R_s(\tau_{\text{est}}, \tau_{\text{sen}}) &= \mathbb{E}_{\hat{P}_d, \hat{C}_0, \hat{C}_1, |h_{p,1}|^2, |h_s|^2, |h_{p,2}|^2} \left[\frac{T - \tau_{\text{sen}}}{T} \times \right. \\ &\quad \left. \left(\mathbb{P}(\mathcal{H}_0)(1 - \mathbf{P}_{\text{fa}})\hat{C}_0 + \mathbb{P}(\mathcal{H}_1)(1 - \hat{P}_d)\hat{C}_1 \right) \right] \quad (2.43) \\ &= \frac{T - \tau_{\text{sen}}}{T} \left[\mathbb{P}(\mathcal{H}_0)(1 - \mathbf{P}_{\text{fa}})\mathbb{E}_{\hat{C}_1, |h_s|^2} [\hat{C}_1] + \right. \\ &\quad \left. \mathbb{P}(\mathcal{H}_1)\mathbb{E}_{\hat{P}_d, |h_{p,1}|^2} [\hat{P}_d] \mathbb{E}_{\hat{C}_1, |h_s|^2, |h_{p,2}|^2} [\hat{C}_1] \right], \end{aligned}$$

where $\mathbb{E}_{\hat{P}_d, \hat{C}_0, \hat{C}_1, |h_{p,1}|^2, |h_s|^2, |h_{p,2}|^2} [\cdot]$ corresponds to an expectation over the estimated parameters $(\hat{P}_d, \hat{C}_0, \hat{C}_1)$ and the channel fading $(|h_{p,1}|^2, |h_s|^2, |h_{p,2}|^2)$. Please note that the randomness due to channel fading is included in the system parameters \hat{P}_d, \hat{C}_0 and \hat{C}_1 , refer to (2.40).

Problem 4 The achievable expected secondary throughput subject to an outage constraint on P_d at the PR that considers the imperfect channel estimation and the random behaviour of the interacting channels, is given by

$$\begin{aligned} R_s(\tilde{\tau}_{\text{est}}, \tilde{\tau}_{\text{sen}}) &= \max_{\tau_{\text{est}}, \tau_{\text{sen}}} \mathbb{E}_{\hat{P}_d, \hat{C}_0, \hat{C}_1, |h_{p,1}|^2, |h_s|^2, |h_{p,2}|^2} [R_s(\tau_{\text{est}}, \tau_{\text{sen}})], \\ \text{s.t. (2.42),} & \\ \text{s.t. } 0 < \tau_{\text{est}} \leq \tau_{\text{sen}} \leq T. & \end{aligned} \quad (2.44)$$

Solution: In order to solve the constrained optimization problem, the following approach is considered. First the underlying constraint (2.42) is exploited to determine the decision threshold μ . Since it is complicated to obtain a closed form expression of μ , in this regard, its value is obtained numerically.

Using μ to determine \hat{P}_d and P_{fa} and evaluating an expectation over $\hat{P}_d, \hat{C}_0, \hat{C}_1, |h_{p,1}|^2, |h_s|^2, |h_{p,2}|^2$, the expected throughput as a function of estimation and sensing time is determined. Finally, this function is used to determine the suitable estimation time ($\tilde{\tau}_{\text{est}}$) and suitable sensing time ($\tilde{\tau}_{\text{sen}}$).

Remark 4 Similar to the deterministic channel, the expression $R_s(\tau_{\text{est}}, \tau_{\text{sen}})$ derived by the estimation model (referred as the proposed approach) establishes a fundamental relation between estimation time, sensing time and achievable secondary throughput, characterized as estimation-sensing-throughput tradeoff for the random channel that incorporates channel estimation. Based on this tradeoff, a suitable estimation $\tau_{\text{est}} = \tilde{\tau}_{\text{est}}$ and a sensing time $\tau_{\text{sen}} = \tilde{\tau}_{\text{sen}}$ that attains a maximum achievable throughput $R_s(\tilde{\tau}_{\text{est}}, \tilde{\tau}_{\text{sen}})$ for the IS is determined.

2.5 Numerical Results

Here, the performance of the IS based on the proposed approach is investigated. In this regard: (i) the simulations are performed to validate the expressions obtained, (ii) the performance degradation incurred due to the channel estimation

Table 2.1: Parameters for Numerical Analysis

Parameter	Value
f_s	1 MHz
$ h_{p,1} ^2$ (or $ \bar{h}_{p,1} ^2$)	-100 dB
$ h_{p,2} ^2$ (or $ \bar{h}_{p,2} ^2$)	-100 dB
$ h_s ^2$ (or $ \bar{h}_s ^2$)	-80 dB
T	100 ms
\bar{P}_d	0.9
ρ_d	0.05
σ_w^2	-100 dBm
$\gamma_{p,1}$	-10 dB
$\gamma_{p,2}$	-10 dB
γ_s	10 dB
$\sigma_s^2 = P_{Tx,PT}$	-10 dBm
$P_{Tx,ST}$	-10 dBm
$\mathbb{P}(\mathcal{H}_1) = 1 - \mathbb{P}(\mathcal{H}_0)$	0.2
τ_{est}	5 ms
N_s	10

is analyzed. In this regard, the ideal model is considered to benchmark, and to evaluate the performance loss, (iii) the mathematical justification to the considered approximations is established. Although the expressions derived in this chapter depicting the performance analysis are general and applicable to all CR systems, the parameters are selected in such a way that they closely relate to the deployment scenario described in Figure 2.1. Unless stated explicitly, the choice of the parameters given in Table 2.1 is considered for the analysis.

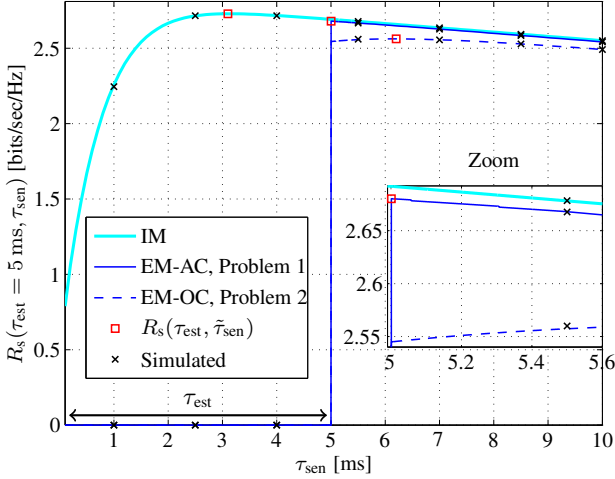


Figure 2.6: Sensing-throughput tradeoff for the Ideal Model (IM) and Estimation Model (EM), $\gamma_{p,1} = -10$ dB, $\tau_{\text{est}} = 5$ ms and $\rho_d = 0.05$.

2.5.1 Deterministic Channel

At first, the performance of the IS in terms of sensing-throughput tradeoff corresponding to the Ideal Model (IM) and Estimation Model (EM) for a fixed $\tau_{\text{est}} = 5$ ms is analyzed, refer to Figure 2.6. In contrast to constraint on P_d for the ideal model, the average constraint (EM-AC) and the outage constraint (EM-OC) for the proposed estimation model are employed. With the inclusion of received power-based estimation in the frame structure, the ST achieves no throughput at the SR for the interval τ_{est} . For the given cases, namely, IM, EM-AC and EM-OC, a suitable sensing time that results in a maximum secondary throughput $R_s(\tau_{\text{est}} = 5 \text{ ms}, \tilde{\tau}_{\text{sen}})$ is determined. Apart from that, a performance degradation is depicted in terms of the achievable throughput, refer to Figure 2.6. For $\rho_d = 0.05$, it is observed that the outage constraint is more sensitive to the performance loss in comparison to the average constraint. It is clear that the analysis, illustrated in Figure 2.6, is obtained for a certain choice of system parameters, particularly $\gamma_{p,1} = -10$ dB, $\tau_{\text{est}} = 5$ ms and $\rho_d = 0.05$. To acquire more insights, the effect of these variations on the performance parameters is considered, subsequently.

Hereafter, the theoretical expressions are considered for the analysis, in ad-

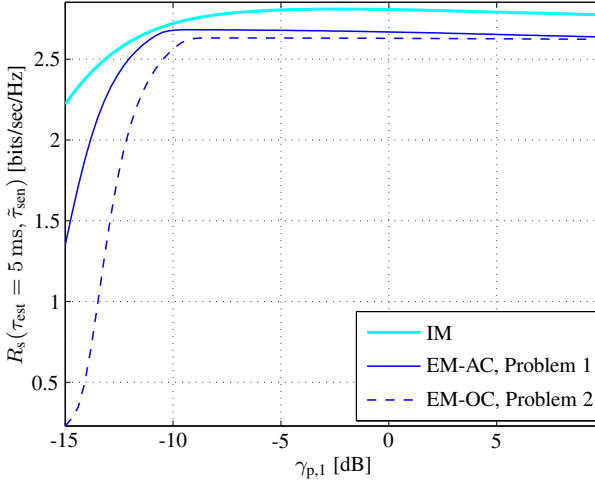


Figure 2.7: Secondary throughput versus $\gamma_{p,1}$ with $\tau_{\text{est}} = 5$ ms for the deterministic channel.

dition, the IS is operated at the suitable sensing time. Next, the variation in the achievable throughput $R_s(\tau_{\text{est}}, \tilde{\tau}_{\text{sen}})$ against the received signal to noise ratio $\gamma_{p,1}$ at the ST with $\tau_{\text{est}} = 5$ ms is considered, refer to Figure 2.7. For $\gamma_{p,1} < -10$ dB, the estimation model incurs a significant performance loss. This clearly reveals that the ideal model overestimates the performance of the IS. From the previous discussion, it is concluded that the inclusion of the average and the outage constraints (depicted by the proposed framework) precisely tackles the uncertainty in the interference at the PR, arising due to channel estimation, without considerably degrading the performance of the IS.

Upon maximizing the secondary throughput, it is interesting to analyze the variation of the secondary throughput with the estimation time. Corresponding to the estimation model, Figure 2.8 illustrates a tradeoff among the estimation time, the sensing time and the secondary throughput, refer to Remark 1. From Figure 2.8, it can be noticed that the function $R_s(\tau_{\text{est}}, \tau_{\text{sen}})$ is well-behaved in the region $0 < \tau_{\text{est}} \leq \tau_{\text{sen}} \leq T$ and consists of a global maximum, yielding the achievable secondary throughput.

This tradeoff depicted by the proposed framework, further presented in Figure 2.9, can be explained from the fact that low values of the estimation time result in large variations in \hat{P}_d . To counteract and satisfy the average and the

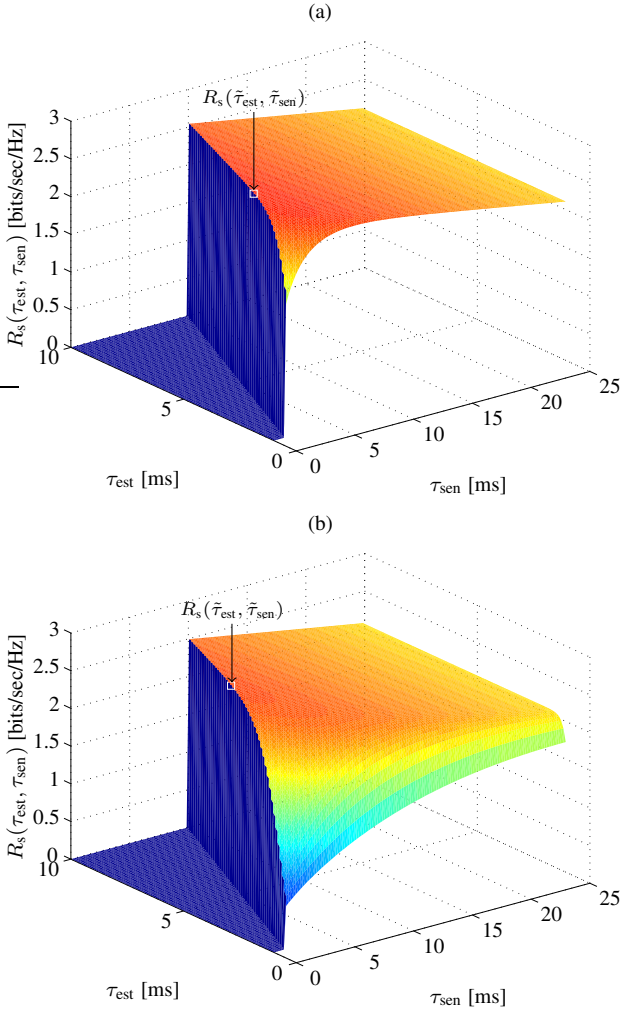


Figure 2.8: Estimation-sensing-throughput tradeoff for the estimation model for (a) average constraint and (b) outage constraint with $\rho_d = 0.05$.

outage constraints, the corresponding thresholds shift to a lower value. This causes an increase in P_{fa} , thereby increasing the sensing-throughput curvature. As a result, the suitable sensing time is obtained at a higher value. However,

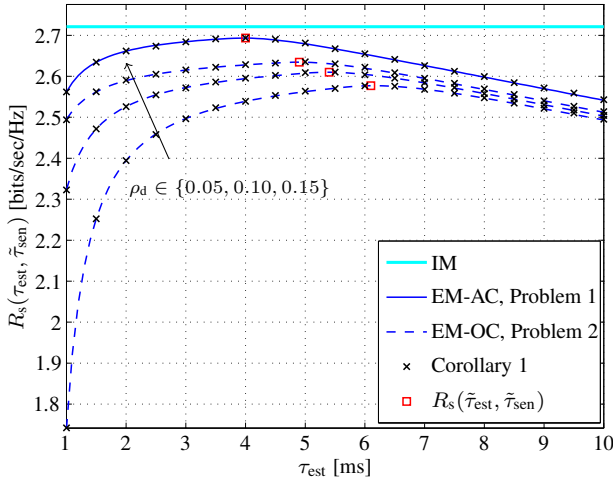


Figure 2.9: Estimation-sensing-throughput tradeoff for the average and the outage constraints with $\gamma_{p,1} = -10$ dB, where the secondary throughput is maximized over the sensing time, $R_s(\tau_{\text{est}}, \tilde{\tau}_{\text{sen}})$.

beyond a certain value ($\tilde{\tau}_{\text{est}}$), a further increase in the estimation time slightly contributes to the performance improvement and largely consumes the time resources. As a consequence to the estimation-sensing-throughput tradeoff, the suitable estimation time that yields an achievable throughput $R_s(\tilde{\tau}_{\text{est}}, \tilde{\tau}_{\text{sen}})$ is determined.

Besides that, the variation in the secondary throughput for different values of the outage constraint is illustrated, refer to Figure 2.9. It is observed that for the selected choice of ρ_d , the outage constraint is severe as compared to the average constraint, hence, results in a lower secondary throughput or achieves a greater performance degradation. Thus, depending on the nature of the policy (aggressive or conservative) followed by the regulatory bodies towards the interference at the primary system, it is possible to define ρ_d accordingly during the system design. Moreover, it is observed that the alternative approach proposed in Corollary 1 does not present any noticeable performance difference depicted in terms of the achievable throughput corresponding to the one characterized in Problems 1 and 2.

To procure further insights, the variations of expected \hat{P}_d and P_{fa} with the estimation time are studied. From Figure 2.10, it is observed that the expected \hat{P}_d

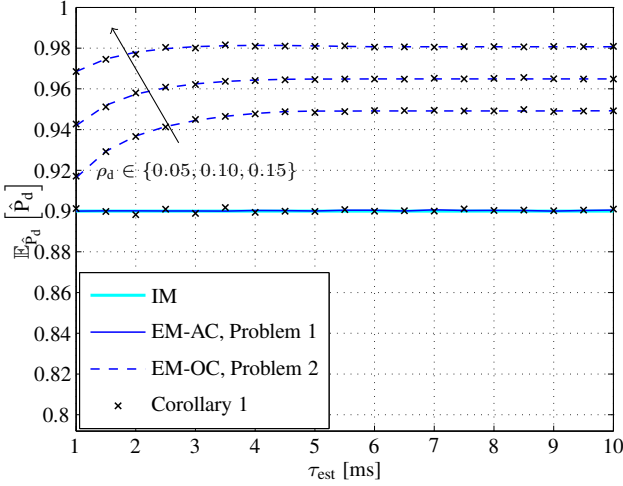


Figure 2.10: Variation of $\mathbb{E}_{\hat{P}_d} [\hat{P}_d]$ versus the τ_{est} , where the secondary throughput is maximized over the sensing time, $R_s(\tau_{\text{est}}, \tilde{\tau}_{\text{sen}})$.

corresponding to the outage constraint is strictly above the desired level \bar{P}_d for all values of the estimation time. However, for lower values of the estimation time, this margin reduces. This is based on the fact that lower estimation time shifts the probability mass of P_d to a lower value, refer to Figure 2.3a.

According to Figure 2.11, the system notices a considerable improvement in P_{fa} at small values of τ_{est} , which saturates for a certain period and falls drastically beyond a certain value. To understand this, it is important to study the dynamics between the estimation and the sensing time. Low τ_{est} increases the variations in the detection probability, these variations are compensated by an increase in the suitable sensing time, and vice versa. The performance improves until a maximum ($\tilde{\tau}_{\text{est}}, \tilde{\tau}_{\text{sen}}$) is reached, beyond this, the time resources (allocated in terms of the sensing and the estimation time) contribute more in improving the detector's performance (in terms of P_{fa} as P_d is already constrained) and less in reducing the variations due to the channel estimation.

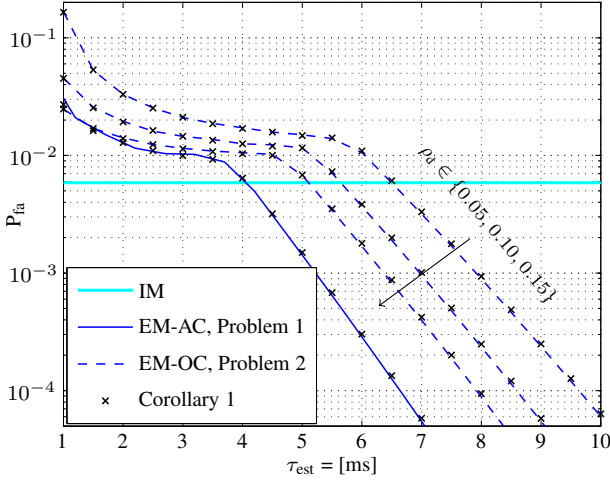


Figure 2.11: Variation of P_{fa} versus the τ_{est} , where the secondary throughput is maximized over the sensing time, $R_s(\tau_{est}, \tilde{\tau}_{sen})$.

2.5.2 Random Channel

In contrast to the deterministic scenario, the choice of the system parameters is slightly modified, $\gamma_{p,1} = 0$ dB, $\gamma_{p,2} = 0$ dB, $\gamma_s = 10$ dB, $\sigma_s^2 = P_{Tx,PT} = 0$ dBm, $P_{Tx,ST} = -10$ dBm, $\mathbb{P}(\mathcal{H}_1) = 1 - \mathbb{P}(\mathcal{H}_0) = 0.2$, $\tau_{est} = 1$ ms. This is done to illustrate the effectiveness of the proposed approach for the random channel. In addition, the performance of the IS under the following fading scenarios is evaluated: (i) severe fading $m = 1$ (Rayleigh fading¹⁵) and (ii) mild fading $m = 1.5$. For simplification of the analysis, it is assumed that m is same for all the involved channels.

First, the sensing-throughput tradeoff for a certain value of estimation time $\tau_{est} = 1$ ms is studied, corresponding to the IM and the EM that represent the perfect and the imperfect channel estimation, respectively, refer to Figure 2.12. Again like the deterministic channel, it is observed that with the inclusion of τ_{est} in the frame structure, the EM procure no throughput at the SR for the time interval τ_{est} . Furthermore, it is noticed that the suitable sensing time increases

¹⁵Please note that the objective here is to consider the impact of severity in fading on the performance of the IS with regard to the channel estimation. The value $m = 1$, which corresponds to Rayleigh fading, is an obvious representative of a severe fading scenario.

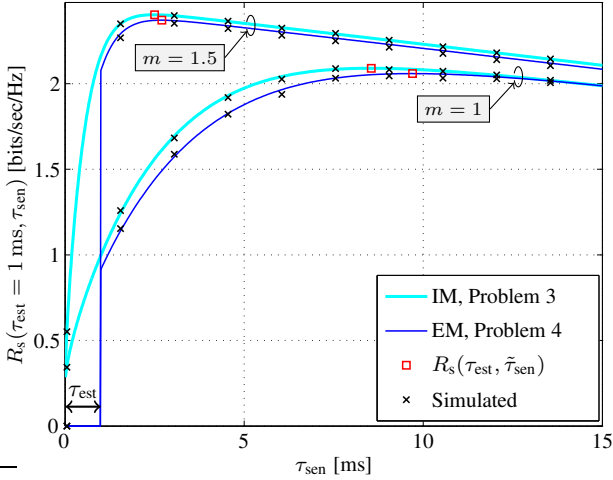


Figure 2.12: Sensing-throughput tradeoff for the ideal model (IM) and estimation model (EM), $\gamma_{p,1} = 0$ dB, $\tau_{\text{est}} = 1$ ms and $\rho_d = 0.05$.

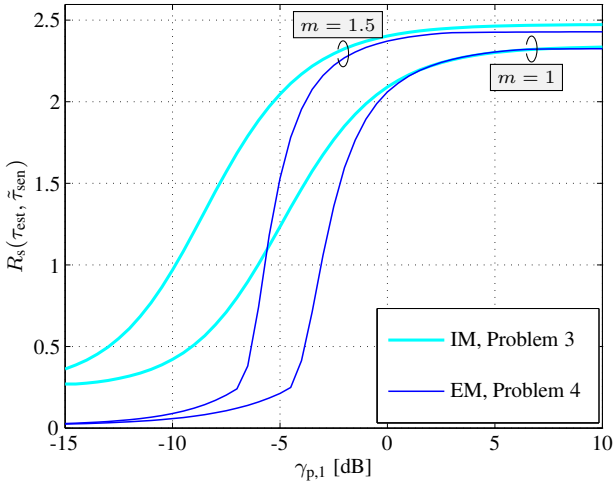


Figure 2.13: Secondary throughput versus $\gamma_{p,1}$ with $\tau_{\text{est}} = 1$ ms for the random channel.

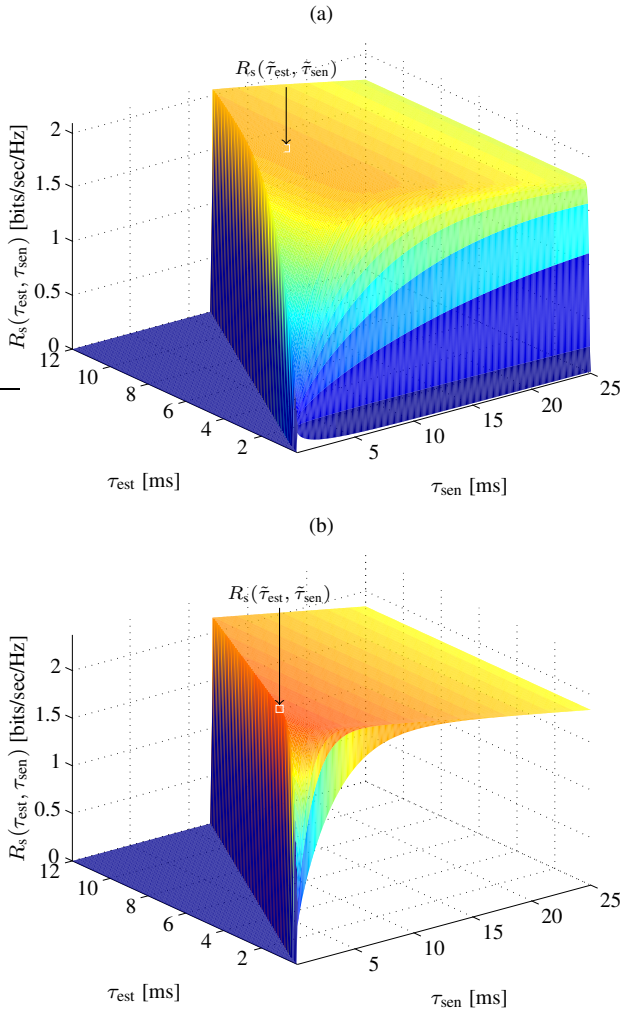


Figure 2.14: Estimation-sensing-throughput tradeoff for the estimation model for different fading scenarios (a) $m = 1$ (b) $m = 1.5$.

with severity in the fading. To further understand the effect of the channel fading on the performance of the IS, the variation of other parameters on the performance of the IS are considered.

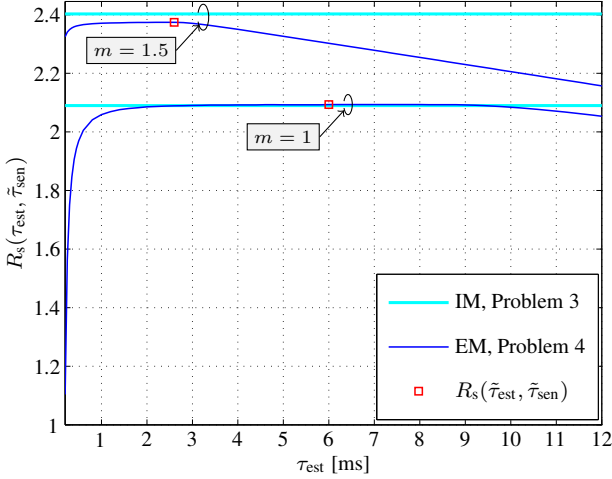


Figure 2.15: Estimation-sensing-throughput tradeoff subject to the random channel with $\gamma_{p,1} = 0$ dB, where the throughput is maximized over the sensing time, $R_s(\tau_{\text{est}}, \tilde{\tau}_{\text{sen}})$.

After maximizing the secondary throughput for a certain estimation time, the variation of $R_s(\tau_{\text{est}}, \tilde{\tau}_{\text{sen}})$ along the received signal to noise ratio for the different choice of the aforementioned fading scenarios is analyzed. From Figure 2.13, it is evident that the performance degrades severely below $\gamma_{p,1} = 0$ dB. More specifically, the performance degradation decreases with the severity in the fading.

Complementing the analysis for the deterministic channel depicted in Figure 2.8, Figure 2.14 presents the variation of the secondary throughput along the estimation and the sensing time. In contrast to the deterministic channel, Figure 2.14 jointly incorporates the variations due to channel estimation and channel fading. It is clearly noticed that the mild fading scenarios are sensitive to the performance degradation around the suitable estimation and the suitable sensing time.

Next, the variation of $R_s(\tau_{\text{est}}, \tilde{\tau}_{\text{sen}})$ along the estimation time is examined, refer to Figure 2.15. It is noticed that $R_s(\tau_{\text{est}}, \tilde{\tau}_{\text{sen}})$ increases for low values of τ_{est} and then decreases beyond $\tilde{\tau}_{\text{est}}$. This can be explained as follows, low τ_{est} increases the variations in \hat{P}_d , shifting the threshold to lower values, which subsequently increases P_{fa} , hence, degrading the achievable secondary throughput. Beyond

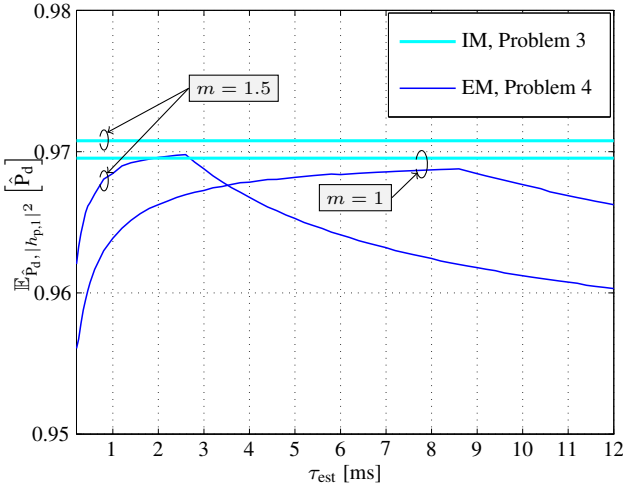


Figure 2.16: Expected detection probability versus estimation time.

$\tilde{\tau}_{\text{est}}$, the variations are largely dominated by the channel fading, therefore, the IS observes no improvement in the performance through an increase in τ_{est} . It is again depicted that the mild fading scenarios are more sensitive to the performance degradation in terms of the achievable secondary throughput.

Figure 2.16 presents the variation of expected detection probability against τ_{est} . It is indicated that the EM compensates for the variations due to the channel estimation and the channel fading to satisfy the outage constraint. Subsequently, Figure 2.17 illustrates the performance in terms of the false alarm probability. The random channel case encounters a similar behaviour as depicted by the deterministic channel, where P_{fa} severely reduces beyond a certain τ_{est} . Beyond this value of τ_{est} , since $1 - P_{\text{fa}} \approx 1$, the reduction in P_{fa} does not influence the performance of the IS in terms of the secondary throughput.

Lastly, the performance degradation in terms of the achievable secondary throughput $R_s(\tilde{\tau}_{\text{est}}, \tau_{\text{sen}})$ versus the Nakagami- m parameter (that accounts for severity in the fading) is investigated, refer to Figure 2.18. For both scenarios, i.e., perfect (IM) and imperfect channel estimation (EM), the performance decreases with the severity in fading. In addition, by comparing the IM and the EM, it can be concluded that for situations where the variations in the system are largely dominated by the channel estimation (or conversely, where the interacting channels observe mild fading), the EM notices a greater performance

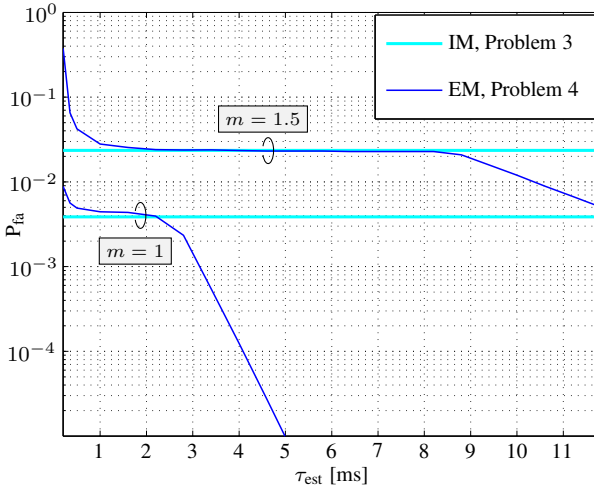


Figure 2.17: False alarm probability versus estimation time.

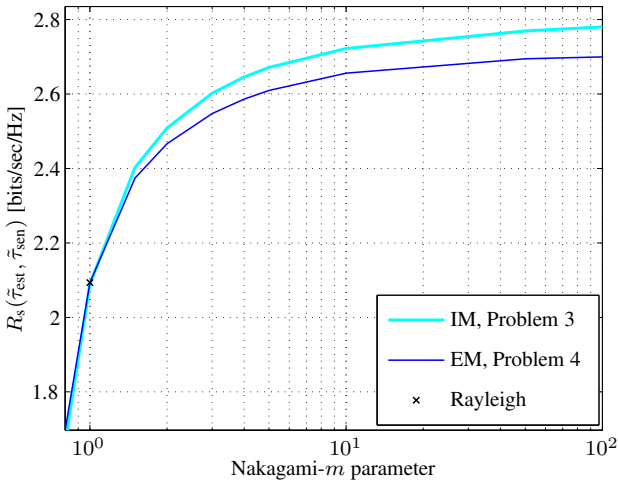


Figure 2.18: Variation of the achievable throughput $R(\tilde{\tau}_{est}, \tilde{\tau}_{sen})$ with Nakagami- m parameter for $\gamma_{p,1} = 0$ dB.

degradation.

2.6 Summary

In this chapter, the performance of cognitive radio as an interweave system is investigated from a deployment perspective. It has been argued that the knowledge of the interacting channels is a key aspect that enables the performance characterization of the interweave system. In this regard, a novel framework that facilitates channel estimation and captures the effect of channel estimation in the system model has been proposed. As a major outcome of the analysis, it has been justified that the existing model, illustrating an ideal scenario, disregards the effects such as time allocation and imperfect channel knowledge encountered by the IS due to the inclusion of channel estimation. In this context, the existing model overestimates the performance of the interweave system, and hence, is less suitable for deployment.

Moreover, it has been clearly identified that the variations induced in the system, specially in the detection probability, cause uncertain interference. Unless controlled, this uncertain interference may severely degrade the performance of the primary system. To overcome this situation, average and outage constraints as primary user constraints have been employed. As a consequence, for the proposed estimation model, novel expressions for the sensing-throughput tradeoff based on the mentioned constraints have been established. More importantly, by analyzing the estimation-sensing-throughput tradeoff, the suitable estimation time and the suitable sensing time that maximize the secondary throughput have been determined.

In addition to this, the performance of the interweave systems that incorporate imperfect knowledge of the involved channels, where these channels are subject to Nakagami- m fading, is characterized. In this context, an outage constraint that jointly captures the variations in the IS due to channel estimation and channel fading has been employed. Subject to this constraint, a sensing-estimation-throughput tradeoff has been characterized that incorporates channel estimation and channel fading, yielding a maximum secondary throughput at a suitable estimation time and a sensing time. Finally through numerical analysis, it has been concluded that the suitable choice of the estimation time is essential for controlling the performance degradation in terms of the achievable secondary throughput, particularly for scenarios that encounter less severe (mild) fading.

2.7 Solutions

2.7.1 Solution to Lemma 2

Solution: Following the probability density function (pdf) of \hat{h}_s in (2.14), the pdf of $|\hat{h}_s|^2$ is given by $\mathcal{X}'^2(\lambda_s, 2)$, where 2 represents the degrees of freedom and $\lambda_s = \frac{N_s |\hat{h}_s|^2}{\sigma_w^2}$ is the non-centrality parameter.

Applying Approximation 1 to approximate $\mathcal{X}'^2(\lambda_s, 2)$ with Gamma distribution $\Gamma(a_s, b_s)$ [78]. The pdf of $|\hat{h}_s|^2$ is characterized as

$$f_{|\hat{h}_s|^2}(x) \approx \frac{1}{\Gamma(a_s)} \frac{x^{a_s-1}}{b_s^{a_s}} \exp\left(-\frac{x}{b_s}\right), \quad (2.45)$$

where

$$a_s = \frac{(2 + \lambda_s)^2}{(4 + 4\lambda_s)} \text{ and } b_s = \sigma_w^2 \frac{(4 + 4\lambda_s)}{(2 + \lambda_s)} \quad (2.46)$$

where the parameters a_s and b_s in (2.46) are determined by comparing the first two central moments of the two distributions.

Following (2.45), the pdf of $\frac{|\hat{h}_s|^2 P_{\text{Tx,ST}}}{\sigma_w^2}$ is given by

$$f_{\frac{|\hat{h}_s|^2 P_{\text{Tx,ST}}}{\sigma_w^2}}(x) = \frac{P_{\text{Tx,ST}}}{\sigma_w^2} \frac{1}{\Gamma(a_s) \left(\frac{b_s P_{\text{Tx,ST}}}{\sigma_w^2}\right)^{a_s}} x^{a_s-1} \exp\left(-\frac{x \sigma_w^2}{b_s P_{\text{Tx,ST}}}\right). \quad (2.47)$$

Finally, using (2.47) and substituting $\frac{|\hat{h}_s|^2 P_{\text{Tx,ST}}}{\sigma_w^2}$ in the expression of \hat{C}_0 , defined in (2.18), yields (2.25).

2.7.2 Solution to Lemma 3

Solution: For simplification, $\left(\frac{|\hat{h}_s|^2 P_{\text{Tx,ST}}}{\hat{P}_{\text{Rx,SR}}}\right)$ in (2.9) is dealt as individual terms $E_1 = \left(\frac{|\hat{h}_s|^2 P_{\text{Tx,ST}}}{\sigma_w^2}\right)$ and $E_2 = \left(\frac{\hat{P}_{\text{Rx,SR}}}{\sigma_w^2}\right)$, where $\hat{C}_1 = \log_2\left(1 + \frac{E_1}{E_2}\right)$, refer to (2.19). The pdf of the expression E_1 is determined in (2.47).

2 Interweave System

Following the characterization $\hat{P}_{\text{Rx,SR}}$ (χ^2 distribution), the pdf of E_2 is determined as

$$f_{\frac{\hat{P}_{\text{Rx,SR}}}{\sigma_w^2}}(x) = \frac{1}{\Gamma(a_p)} \frac{x^{a_p-1}}{b_p^{a_p}} \exp\left(-\frac{x}{b_p}\right), \quad (2.48)$$

$$\text{where } a_p = \frac{\tau_{\text{sen}} f_s}{2} \text{ and } b_p = \frac{2P_{\text{Rx,SR}}}{\sigma_w^2 \tau_{\text{sen}} f_s}. \quad (2.49)$$

Using the characterizations of pdfs $f_{\frac{|\hat{h}_s|^2 P_{\text{Tx,ST}}}{\sigma_w^2}}(\cdot)$ and $f_{\frac{\hat{P}_{\text{Rx,SR}}}{\sigma_w^2}}(\cdot)$, Mellin transform [79] is applied to determine the pdf of $\frac{E_1}{E_2}$ as

$$f_{\frac{|\hat{h}_s|^2 P_{\text{Tx,ST}}}{\sigma_w^2} / \frac{\hat{P}_{\text{Rx,SR}}}{\sigma_w^2}}(x) = \frac{x^{a_s-1} \Gamma(a_s + a_p)}{\Gamma(a_s) \Gamma(a_p) b_s^{a_s} b_p^{a_p}} \left(\frac{1}{b_p} + \frac{x}{b_s} \right)^{-(a_s+a_p)}. \quad (2.50)$$

Finally, substituting the expression $\frac{E_1}{E_2}$ in \hat{C}_1 yields (2.27).

2.7.3 Solution to Problems 1 and 2

Solution: In order to solve the constrained optimization problems illustrated in Problem 1 and Problem 2, the following approach is considered. As a first step, the underlying constraint is employed to determine μ as a function of the τ_{sen} and τ_{est} .

For the average constraint, the expression $\mathbb{E}_{\hat{p}_d} [\hat{P}_d]$ in (2.29) did not lead to a closed form expression, consequently, no analytical expression of μ is obtained. In this context, μ for the average constraint is procured numerically from (2.29).

Next, μ based on the outage constraint is determined. This is accomplished by combining the expression of $F_{\hat{p}_d}$ in (2.20) with the outage constraint (2.31)

$$P(\hat{P}_d \leq \bar{P}_d) = F_{\hat{p}_d}(\bar{P}_d) \leq \rho_d. \quad (2.51)$$

Rearranging (2.51) gives

$$\mu \geq \frac{4P_{\text{Rx,ST},h_{p,1}} \Gamma^{-1}\left(1 - \rho_d, \frac{\tau_{\text{est}} f_s}{2}\right) \Gamma^{-1}\left(\bar{P}_d, \frac{\tau_{\text{sen}} f_s}{2}\right)}{\tau_{\text{est}} \tau_{\text{sen}} (f_s)^2}. \quad (2.52)$$

Clearly, the random variables \hat{P}_d , and \hat{C}_0 and \hat{C}_1 are functions of the independent random variables $\hat{P}_{Rx,ST,h_{p,1}}$, and $|\hat{h}_s|^2$ and $\hat{P}_{Rx,SR}$, respectively. In this context, the independence property on \hat{P}_d , \hat{C}_0 and \hat{C}_1 is applied to obtain

$$\mathbb{E}_{\hat{P}_d, \hat{C}_0, \hat{C}_1} \left[\hat{C}_0(1 - P_{fa}) + \hat{C}_1(1 - \hat{P}_d) \right] = \mathbb{E}_{\hat{C}_0} \left[\hat{C}_0 \right] (1 - P_{fa}) + \quad (2.53)$$

$$\mathbb{E}_{\hat{C}_1} \left[\hat{C}_1 \right] \mathbb{E}_{\hat{P}_d} \left[(1 - \hat{P}_d) \right] \quad (2.54)$$

in (2.28) and (2.30). Upon replacing the respective thresholds in \hat{P}_d and P_{fa} and evaluating the expectation over \hat{P}_d , \hat{C}_0 and \hat{C}_1 using the cdfs characterized in Lemma 1, Lemma 2 and Lemma 3, the expected throughput as a function of estimation time and sensing time is determined.

Underlay System

This chapter (based on [K5]) studies the performance of cognitive USs that employ power control mechanism at the CSC-BS (or ST) from a deployment perspective. From the previous chapter, it is understood that the interweave systems employ spectrum sensing to detect the presence of PU signals while avoiding harmful interference at the primary system. In contrast to this, an US exploits the interference tolerance capability of the primary systems that allows the SUs to transmit even in the presence of the PUs. In order to accomplish secondary access to the licensed spectrum, the US employs techniques such as power control to maintain the interference received at the PR below a specified level defined as Interference Threshold (IT) [43]. In this regard, this chapter focuses on performance characterization of the US that employs power control at the ST. It is important to understand that the power control mechanism can be executed at the ST only if the knowledge of the channel between the ST and the PR is present at the ST. Despite this fact, the existing models termed as the baseline models considered for performance analysis of the US either assume the knowledge of involved channels at the ST or retrieve this information by means of a band manager or a feedback channel from the PR. However, it is challenging to realize such solutions in practice.

Motivated by this fact, a novel approach that incorporates estimation of the involved channels at the ST is proposed, and subsequently characterizes the performance of the US in terms of interference power received at the PR and

throughput at the SR. Moreover, an outage constraint is applied to capture the impact of the variations induced in the US due to imperfect channel knowledge, particularly on the uncertain interference. Besides this, in reference to the constraint on transmit power at the ST, the operation of the US is classified in terms of an interference-limited regime and a power-limited regime.

Subsequently, the performance analysis of the proposed approach is extended to investigate the influence of channel fading. In this regard, the expressions of the uncertain interference and the secondary throughput are characterized for the case where the involved channels encounter Nakagami- m fading. Finally, this chapter investigates a fundamental tradeoff between the estimation time and the secondary throughput that allows us to effectively control the performance degradation incurred due to the imperfect channel knowledge.

3.1 Related Work

In order to enable shared access to the licensed spectrum, it is essential to characterize the performance of a CR system in reference of the primary system and the secondary system. With regard to the primary system, the performance of a US is characterized in terms of interference received at the PR. This interference arises due to concurrent data transmission over the same channel by the secondary system. Recently, power control at the ST has emerged as an effective way of regulating the interference induced by the ST. However, the power control primarily requires the knowledge of the *primary interference* channel between the ST and the PR at the ST. The preliminary investigations [36, 43, 44, 80, 81], considered for the performance evaluation of the US, assume this knowledge to be perfectly known at the ST. Such situations rarely exist in practical implementations. In order to address this, the performance analysis based on imperfect channel knowledge has been dealt extensively in [49–51, 59, 82–88].

It is worth noticing that the majority of these works [49, 51, 82] in reference to the imperfect channel knowledge consider that the channel knowledge at the ST is obtained from a band manager¹, an approach proposed in [89]. Whereas [50, 84] rely on the presence of a feedback link from the PR to the ST [90]. The fact is, the feasibility of the band manager or the feedback link across two completely different systems is unrealistic from a practical standpoint. In

¹An entity that mediates between the primary and the secondary systems.

addition, due to latency, the channel knowledge obtained while implementing these approaches may be outdated, as considered in [50, 51, 82, 84]. Besides, for the existence of the feedback link, the demodulation of the secondary user signals at the PR and a resource (time) allocation, explicitly for communicating the channel knowledge, impose an additional overhead for the primary system. These issues render the hardware implementation of the US in reference to the aforementioned approaches challenging. In contrast to these approaches, a novel strategy is proposed in this chapter, according to which the channel estimation is employed directly at the secondary transmitter. Thus, by avoiding the realization of the band manager or the feedback link and the issues related to it, the key aspects that facilitate the hardware deployment of the US are highlighted.

Along with the performance of the primary system, the achievable data rate at the SR for the link between the ST and the SR contributes significantly to the overall performance of the US [36, 49, 50, 82, 84–86]. In order to characterize the data rate, the ST (along with the primary interference channel, which is associated with power control mechanism) requires the knowledge of *access* channel between the ST and the SR, and *secondary interference* channel between the PT and the SR. Despite this fact, the performance characterization of the US's data rate in reference to the estimation of the access and the secondary interference channels has not been considered in [49–51, 82, 84, 85] or only marginally in [83, 86, 87].

From a deployment perspective, it is worthy to understand that the interference channels are representative of the channels that exist between different (primary and secondary) systems. This implies that in order to carry out channel estimation based on the conventional techniques such as pilot-based channel estimation, which is mainly employed in the previous works, a preliminary processing (which include synchronization and demodulation) of the primary user signal is necessary. In this regard, in order to facilitate hardware deployment, it is necessary to select the estimation techniques such that complexity and versatility (to the unknown primary user signals) requirements are satisfied. In this chapter, similar to Chapter 2, this critical problem is addressed by employing a received power-based estimation at the ST and the SR for the interference channels. In contrast to the interweave scenario considered in the previous chapter, here, an underlay scenario is investigated. To certify the significance of the received power-based channel estimation for the hardware implementation, a successful deployment of the received power-based channel estimation at the ST (however, limited to only primary interference channel) on a hardware platform in context to the US, is presented later in Chapter 5.

It is worthy to note that [49–51, 82–88] consider that the PR employs pilot-based channel estimation for the channel PR-ST, which is possible only if the PR is willing: (i) to allocate resources, (ii) to assign a dedicated circuitry for demodulating the secondary user signals and (iii) to establish a feedback link to the ST. Such aspects challenge the hardware implementation of the US. In contrast, for the received power-based estimation proposed, a certain time needs to be allocated by the secondary user for channel estimation, affecting the secondary throughput. Since the aspect concerning the time allocation for the channel estimation has not been taken into account in any of the previous investigations related to the cognitive US [49–51, 82–88], the performance of the US in terms of the secondary throughput is overestimated. Moreover, the imperfect channel knowledge leads to an uncertainty in the interference, which in certain cases may exceed the IT. Under such conditions, the conventional constraint imposed in [36, 43, 44, 81] is strictly violated. As a result, this uncertain interference originated from imperfect channel knowledge (of the primary interference channel) may seriously degrade the performance of the primary systems. In order to tackle this issue, an outage constraint (also referred as interference constraint) that regulates the uncertain interference caused at the PR is proposed.

Besides, through the analysis (depicted later in Section 3.4) it is revealed that the uncertain interference is associated with the estimation time and the controlled power. In order to quantify this relationship, the controlled power is expressed as a function of the estimation time such that the outage constraint is fulfilled. In this context, the estimation time is indirectly associated with the secondary throughput through the controlled power, depicting the influence of the imperfect channel knowledge. On the other side, the time allocation directly affects the secondary throughput. In this chapter, this relationship between the estimation time and the secondary throughput is examined while constraining the uncertain interference below a desired level. It is important to note that although the previous studies have considered channel estimation, an extensive investigation on the influence of imperfect channel knowledge depicted in terms of the time allocation and the uncertain interference in the considered underlay scenario is still underdeveloped.

3.2 Contributions

The main contributions of this chapter are summarized as follows:

3.2.1 Analytical Framework

The main contribution of this chapter is to derive an analytical framework for underlay CR systems that employ a power control mechanism and incorporate the estimation of the following interacting channels: (i) primary interference channel between the ST and the PR, (ii) secondary interference channel between the PT and the SR, and (iii) access channel between the ST and the SR. In contrast to existing works that demand the presence of a band manager or a feedback link in order to retrieve channel estimates, channel estimation at the secondary system is proposed. In order to facilitate the deployment of the US, a received power-based channel estimation is proposed, specially for the interference channels so that low complexity and versatility requirements to estimate primary user signals is accomplished. Clearly, the channel estimation is detrimental (in terms of the time allocation and the uncertain interference) to the performance of the US, leading to its degradation. By comparing its performance with the ideal scenario (which corresponds to the systems with perfect channel knowledge), the performance degradation caused due to imperfect channel knowledge is studied.

Besides, these variations due to the imperfect channel knowledge in the performance parameters, which include the interference at the PR and the secondary throughput at the SR, are characterized in terms of their cdfs pertaining to the deterministic (not random) and the random behavior (channel fading) of the interacting channels. Particularly, these variations lead to uncertainty in the interference that may seriously disrupt the operation of the primary system. To regulate this uncertain interference below a tolerable limit, an outage constraint is employed over the uncertain interference. In addition to this, the variations in the secondary throughput are captured in terms of its expected value.

3.2.2 Interference-Limited and Power-Limited Regimes

The power control at the ST depends on the received signal (from the PR) to noise ratio at the ST of the link between the PR and the ST, which characterizes the quality of the primary interference channel. In this chapter, the controlled power is characterized in terms of the estimation time and the signal to noise ratio such that the outage constraint is satisfied. In practice, the controlled power is limited by the maximum transmit power. Due to this limitation, good channel conditions (which corresponds to a low signal to noise power) do not

translate into performance gains for the US. This behavior of the USs is analyzed in terms of the performance bound, which is illustrated as a relation between the received signal to noise ratio and the estimation time. As depicted later in Figure 3.3, based on this performance bound, the operation of the US is classified as the interference-limited and the power-limited regimes.

3.2.3 Estimation-Throughput Tradeoff

Besides, a successful incorporation of the time allocated for the channel estimation in the secondary system's frame structure is proposed. The time resources dedicated to the channel estimation cause a linear decrease in the secondary throughput. Therefore, a low estimation time increases the secondary throughput, since less time is allocated for the channel estimation. On the other side, its low value increases the uncertain interference, thus requiring a severe power control that ultimately reduces the secondary throughput. The association of the estimation time in reference to the time allocation and the controlled power is studied to derive a fundamental tradeoff between the estimation time and the secondary throughput such that the uncertain interference is kept below a desired level. The analysis of this tradeoff in reference to the realistic underlay scenarios that takes imperfect channel estimation into account is a significant aspect investigated in this chapter. Finally, this tradeoff is employed to derive a suitable estimation time that achieves a maximum secondary throughput for the US. In other words, the considered tradeoff signifies the fact that the performance degradation in terms of the secondary throughput can be effectively controlled only if the estimation time is selected appropriately.

3.2.4 Estimation-Dominant and Channel-Dominant Regimes

For the random channel, the variations in the interference arising due to channel estimation and channel fading are classified as an estimation-dominant regime and a channel-dominant regime, respectively. Based on this analysis, it is revealed that a suitable selection of estimation time can achieve a performance gain (in terms of the secondary throughput) closer to the one predicted by the existing models that consider perfect channel knowledge of the interacting channels.

3.3 System Model

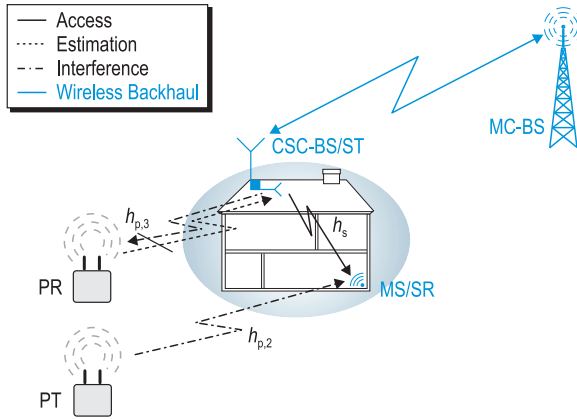


Figure 3.1: A cognitive small cell scenario demonstrating: (i) the underlay paradigm, (ii) the associated network elements, which constitute Cognitive Small Cell-Base Station/Secondary Transmitter (CSC-BS/ST), Mobile Station/Secondary Receiver (MS/SR), Macro Cell-Base Station (MC-BS) and Primary Transmitter (PT), (iii) the interacting channels: primary interference channel ($h_{p,3}$), secondary interference channel ($h_{p,2}$) and access channel (h_s).

3.3.1 Underlay Scenario and Medium Access

Considering the fact that the power control is employed at the CSC-BS, the CSC-BS and the MS represent the ST and the SR, respectively. In order to acquire channel knowledge concerning the primary interference channel, the ST listens to the transmissions from the PR, refer to Figure 3.1. In this work, those primary systems where the PR² performs transmissions interchangeably over time (time division duplexing TDD and half-duplex frequency division duplexing FDD) or frequency (full-duplex FDD) with the PT are considered. These transmissions can occur over the same band (TDD) or over separate bands (half-duplex and full-duplex FDD).

²Clearly, it is ambiguous to consider transmissions from a PR, different terms such as primary radio or simply primary user can be used instead. Since the main focus is to characterize the interference at the PR, it is sensible to use the nomenclature PR.

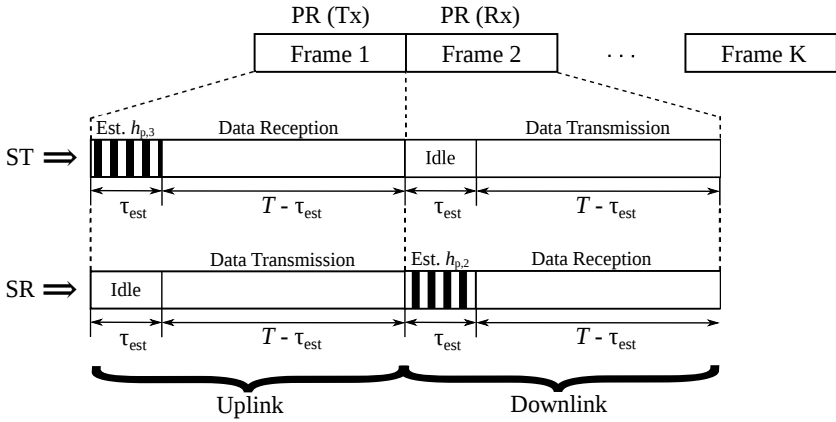


Figure 3.2: Frame structure of the USs illustrating the time allocation for channel estimation and data transmission from the perspective of a ST and a SR. PR (Tx)/PR (Rx) presents the transmission/reception of the primary signal from the PR/PT to the PT/PR.

In cellular networks, these duplexing modes are effectively deployed in LTE standard [91]. The ST follows these duplexing modes to exploit channel reciprocity principle and determine the interference received at the PR. Based on this knowledge, the ST controls its power for transmitting signals over the access channel such that it satisfies the interference constraint by operating at the IT. Particularly, for half-duplex and full duplex FDD, it is assumed that the coherence bandwidth is large as compared to frequency separation between the estimation channel and the band of interest.

A slotted medium access for the US is considered, where the time axis is segmented into frames. As depicted in Figure 3.2, the frame duration T is chosen in such a way that the frames are aligned to the PUs' transmissions, i.e., the uplink and the downlink transmissions for the primary and the secondary systems occur simultaneously. In this regard, a perfect frame synchronization is assumed between the two systems. In order to incorporate channel estimation, a periodic channel estimation³ is proposed, according to which the US uses a time interval $\tau_{est} (< T)$ to perform channel estimation followed by data transmission $T - \tau_{est}$, see Figure 3.2. Besides, to consider variations due to channel fading, it is assumed that the interacting channels remain constant at least over

³This frame structure is similar to the periodic sensing followed by the interweave systems [34].

two frame durations ($2T$). Based on this assumption, every alternating transmission frame observes a different received power, consider Figure 3.2. Since the channel knowledge is essential to employ power control so that the PRs are sufficiently protected from the uncertain interference, it is reasonable to carry out estimation for τ_{est} time interval followed by data transmission with power control in the remaining time $T - \tau_{\text{est}}$ for each frame.

In accordance with the half duplexing modes, the ST and the SR implement received power-based estimation to acquire the knowledge of the primary and the secondary interference channel over consecutive frames, as illustrated in Figure 3.2. For the case, where primary system follows full-duplex FDD, the proposed frame structure can be adapted such that the estimation of the primary and the secondary interference channels occurs in a single frame. Besides this, the access channel estimation is performed by listening to the pilot symbols transmitted by the SR depicted as a pilot-based estimation. At first, the proposed frame structure in context to the deterministic behavior of the interacting channels (deterministic channel) is considered, i.e., the performance is analyzed for a certain channel gain. Then, the performance analysis of the proposed framework is extended by considering channel fading (random channel).

3.3.2 Signal Model

In the uplink, during the estimation phase, the discrete and complex signal received at the ST, transmitted by the PR, is given by

$$y_{\text{ST}}[n] = h_{\text{p},3} \cdot x_{\text{PR}}[n] + w_{\text{ST}}[n], \quad (3.1)$$

where $x_{\text{PR}}[n]$ corresponds to a discrete and complex sample transmitted by the PR with constant transmit power $P_{\text{Tx,PR}}$. It is assumed that $P_{\text{Tx,PR}}$ is known at the ST (an assumption discussed later in Section 3.3.5). $|h_{\text{p},3}|^2$ represents the power gain for the primary interference channel and $w_{\text{ST}}[n]$ is circularly symmetric AWGN at the ST with $\mathcal{CN}(0, \sigma_w^2)$.

In the downlink, during data transmission phase, the interference (received from the ST) plus noise signal at the PR is given by

$$y_{\text{PR}}[n] = h_{\text{p},3} \cdot x_{\text{ST,cont}}[n] + w_{\text{PR}}[n], \quad (3.2)$$

and on the other side, the received signal at the SR follows

$$y_{\text{SR}}[n] = h_{\text{s}} \cdot x_{\text{ST,cont}}[n] + h_{\text{p},2} \cdot x_{\text{PT}}[n] + w_{\text{SR}}[n], \quad (3.3)$$

where $x_{\text{ST,cont}}[n]$ corresponds to a discrete and complex sample transmitted by the ST with controlled power $P_{\text{Tx,ST,cont}}$, whereas $x_{\text{PT}}[n]$ is the transmit signal at the PT with transmit power $P_{\text{Tx,PT}}$.

In reference to the proposed framework, the knowledge of the PT's transmit power is not necessary at the secondary system. Hence, its ignorance at the SR does not affect the analysis concerning the secondary interference. Further, $|h_s|^2$ and $|h_{p,2}|^2$ represent the power gain for the access channel and the secondary interference channel, respectively. $w_{\text{PR}}[n]$ and $w_{\text{SR}}[n]$ are AWGN at the PR and at the SR, respectively, with $\mathcal{CN}(0, \sigma_w^2)$.

3.3.3 Problem Description

According to the existing investigations (also referred as ideal model), an ST of an US is required to control its transmit power in such a way that the interference received $P_{\text{Rx,PR}}$ at the PR is below IT (θ_1) [43]

$$P_{\text{Rx,PR}} = |h_{p,3}|^2 P_{\text{Tx,ST,cont}} \leq \theta_1. \quad (3.4)$$

After determining the controlled power at the ST using (3.4), the data rate at the SR over the access channel is defined as

$$C_3 = \log_2 \left(1 + \frac{|h_s|^2 P_{\text{Tx,ST,cont}}}{|h_{p,2}|^2 P_{\text{Tx,PT}} + \sigma_w^2} \right). \quad (3.5)$$

From the deployment perspective, the ideal model depicted in (3.4) and (3.5) has following issues:

- Without the knowledge of the primary interference channel $|h_{p,3}|^2$, it is impossible to employ the power control, based on (3.4).
- Furthermore, along with $P_{\text{Tx,ST,cont}}$, the knowledge of the access channel $|h_s|^2$ and the secondary interference channel $|h_{p,2}|^2$ is required to determine C_3 , according to (3.5).

The ideal model considers perfect knowledge of the aforementioned channels at the ST, which is not available in practice. In this regard, it is necessary to incorporate channel estimation in the system model. The imperfect channel knowledge, however, translates to the variations in the performance parameters, $P_{\text{Rx,PR}}$ and C_3 . Particularly, a variation in $P_{\text{Rx,PR}}$ that exceeds θ_1 causes the violation of the interference constraint illustrated in (3.4). Unless captured,

this uncertain interference may seriously degrade the performance of the US. Because the ideal model assumes the perfect knowledge of the involved channels, it is incapable of depicting the degradation in the performance due to the time resources allocated for the channel estimation and the imperfect channel knowledge.

3.3.4 Proposed Approach

In order to facilitate channel estimation for the US, it is essential to take the aforementioned issues into account. To accomplish this, the following strategy is proposed in this chapter.

- At first, the estimation of the involved channels is considered. In this regard, a received power-based estimation for the interference channels and a pilot-based estimation for the access channel is employed.
- To capture the effect of the imperfect channel knowledge, the variations in the estimated parameters (namely, received power for the interference channels and power gain for the access channels) are characterized in terms of their cdfs.
- The aforementioned variations are translated to the performance parameters such as the interference at the PR and the secondary throughput. These variations in the performance parameters are further characterized in terms of their cdfs. More specifically, using the characterization of the uncertain interference, a novel power control mechanism is proposed that regulates the uncertain interference at the PR.
- Finally, using the derived expressions, a relationship between the estimation time and the expected secondary throughput for the USs is analyzed. The proposed framework (also referred as estimation model) is further extended to analyze the impact of channel fading on the performance of the system.

It is also worth stating that, since the signal model in Chapter 2 (OFDM transmission) differs from the one (constant power transmission) studied in this chapter, new mathematical expressions for the performance parameters are derived. In the following paragraphs, the estimation of the power gains of the primary interference channel $|\hat{h}_{p,3}|^2$, the access channel $|\hat{h}_s|^2$ and the secondary interference channel $|\hat{h}_{p,2}|^2$ is considered.

Estimation of primary interference channel

Considering

$$P_{\text{Rx,ST},h_{p,3}} = |h_{p,3}|^2 P_{\text{Tx,PR}} + \sigma_w^2, \quad (3.6)$$

and the knowledge of PR's transmit power $P_{\text{Tx,PR}}$ (an assumption discussed in Section 3.3.5), the ST employs received power-based estimation to obtain the knowledge of $|h_{p,3}|^2$. To accomplish channel estimation, in reference to (3.1), the ST listens to the transmissions from the PR and acquires the knowledge of $|h_{p,3}|^2$ indirectly by estimating the power received in the uplink as $\hat{P}_{\text{Rx,ST},h_{p,3}} = \frac{1}{\tau_{\text{est}} f_s} \sum_{n=1}^{\tau_{\text{est}} f_s} |y_{\text{ST}}[n]|^2$, where f_s being the sampling frequency and τ_{est} represents the estimation time interval. The estimated received power $\hat{P}_{\text{Rx,ST},h_{p,3}}$ is utilized to determine the controlled power $P_{\text{Tx,ST,cont}}$ at which the data transmission over the downlink is carried out, Figure 3.2.

For a certain value of $|h_{p,3}|^2$, the received power at the ST estimated using $\tau_{\text{est}} f_s$ samples, refer to (3.6), follows a non-central chi-squared distribution $F_{\hat{P}_{\text{Rx,ST},h_{p,3}}} \sim \mathcal{X}'^2(\lambda_{p,3}, \tau_{\text{est}} f_s)$ with non-centrality parameter $\lambda_{p,3} = \tau_{\text{est}} f_s |h_{p,3}|^2 \times P_{\text{Tx,PR}} / \sigma_w^2 = \tau_{\text{est}} f_s \gamma_{p,3}$ [73], where $\gamma_{p,3}$ is defined as the ratio of the received signal power (from the PR) to noise at the ST and $\tau_{\text{est}} f_s$ corresponds to the degrees of freedom. In order to sustain analytical tractability in the analysis, the Approximation 1 presented in Chapter 2 is considered.

Lemma 4 The cdf of $\hat{P}_{\text{Rx,ST},h_{p,3}}$ is characterized as

$$F_{\hat{P}_{\text{Rx,ST},h_{p,3}}}(x) \approx 1 - \Gamma\left(a_{p,1}, \frac{x}{b_{p,1}}\right), \quad (3.7)$$

$$\text{where } a_{p,1} = \frac{\tau_{\text{est}} f_s (1 + \gamma_{p,3})^2}{2 + 4\gamma_{p,3}} \text{ and } b_{p,1} = \frac{\sigma_w^2 (2 + 4\gamma_{p,3})}{\tau_{\text{est}} f_s (1 + \gamma_{p,3})}, \quad (3.8)$$

and $\Gamma(\cdot, \cdot)$ represents the regularized upper-incomplete Gamma function [78].

Solution: Applying Approximation 1 from Chapter 2 to $\mathcal{X}'^2(\lambda_{p,3}, \tau_{\text{est}} f_s)$ yields (3.7).

Estimation of access channel

Analog to Chapter 2, in the uplink, the pilot signal transmitted by the SR undergoes matched filtering and demodulation at the ST, hence, a pilot-based estimation is employed at the ST to acquire the knowledge of the access channel.

In this regard, \hat{h}_s conditioned on h_s follows a circularly symmetric Gaussian distribution

$$\hat{h}_s|h_s \sim \mathcal{CN}\left(h_s, \frac{\sigma_w^2}{N_s}\right). \quad (3.9)$$

Consequently, for a certain value $|h_s|^2$, the estimated power gain $|\hat{h}_s|^2$ follows a non-central chi-squared $\mathcal{X}'^2(\lambda_s, 2)$ distribution with 2 degrees of freedom and non-centrality parameter $\lambda_s = \frac{N_s|h_s|^2}{\sigma_w^2}$.

Lemma 5 The cdf of $|\hat{h}_s|^2$ is characterized as

$$F_{|\hat{h}_s|^2}(x) \approx 1 - \Gamma\left(a_s, \frac{x}{b_s}\right), \quad (3.10)$$

$$\text{where } a_s = \frac{(2 + \lambda_s)^2}{4 + 4\lambda_s} \text{ and } b_s = \frac{\sigma_w^2(4 + 4\lambda_s)}{(2 + \lambda_s)}. \quad (3.11)$$

Solution: Applying Approximation 1 from Chapter 2 to $\mathcal{X}'^2(\lambda_s, 2)$ yields (3.10).

Estimation of secondary interference channel

In the downlink, the SR estimates the interference power received from the PT. The power estimated over the signal $h_{p,2} \cdot x_{PT}[n] + w_{SR}[n]$ corresponds to the interference plus noise power ($P_{RX,SR} = |h_{p,2}|^2 \cdot P_{TX,PT} + \sigma_w^2$, where $P_{RX,SR}$ represents the true value, consider (3.5)).

The estimated received power at the SR is determined as

$$\hat{P}_{RX,SR} = \frac{1}{\tau_{est}f_s} \sum_{n=1}^{\tau_{est}f_s} |h_{p,2} \cdot x_{PT}[n] + w_{SR}[n]|^2. \quad (3.12)$$

To characterize the secondary throughput, $\hat{P}_{RX,SR}$ is made available to the ST over a low rate feedback channel. Similar to $\hat{P}_{RX,ST,h_{p,3}}$, for a certain value of $|h_{p,2}|^2$, $\hat{P}_{RX,SR}$ follows a non-central chi-squared distribution $\mathcal{X}'^2(\lambda_{p,2}, \tau_{est}f_s)$ with $\tau_{est}f_s$ degrees of freedom and non-centrality parameter

$$\lambda_{p,2} = \frac{\tau_{est}f_s|h_{p,2}|^2P_{TX,PT}}{\sigma_w^2}. \quad (3.13)$$

Lemma 6 The cdf of $\hat{P}_{\text{Rx,SR}}$ is characterized as

$$F_{\hat{P}_{\text{Rx,SR}}}(x) \approx 1 - \Gamma\left(a_{p,2}, \frac{x}{b_{p,2}}\right), \quad (3.14)$$

$$\text{where } a_{p,2} = \frac{(\tau_{\text{est}}f_s + \lambda_{p,2})^2}{2\tau_{\text{est}}f_s + 4\lambda_{p,2}} \text{ and } b_{p,2} = \frac{\sigma_w^2(2\tau_{\text{est}}f_s + 4\lambda_{p,2})}{(\tau_{\text{est}}f_s + \lambda_{p,2})}. \quad (3.15)$$

Solution: Applying Approximation 1 from Chapter 2 to $\mathcal{X}'^2(\lambda_{p,2}, \tau_{\text{est}}f_s)$ yields (3.14).

3.3.5 Assumptions

In accordance to the received power-based estimation for the channel $|h_{p,3}|^2$ in (3.6), it is noticed that the knowledge of $P_{\text{Tx,PR}}$ at the ST is essential for the characterization of the controlled power (considered later in Lemma 7). However, this knowledge can be retrieved by considering the specifications of different wireless standards such as GSM, EDGE and LTE, etc. [41]. It is well-known that certain standards (considered as primary systems) follow adaptive modulation and coding, which can consequently change $P_{\text{Tx,PR}}$. Under this situation, the ST can employ more complex techniques such as pilot assisted techniques in order to determine $P_{\text{Tx,PR}}$ for the given frame.

It is important to note that the scenario described in this chapter considers a single PT and a single PR. However, in practice, it is possible that the ST and the SR accumulate significant interference (defined as aggregate interference) from other PRs and PTs (co-channel interference due to frequency reuse) in the network [27], [K12] over the primary interference channel and the secondary interference channel, respectively. For the secondary interference channel, the only difference is that the SR now estimates the aggregate interference. Due to this, the expression of $\hat{P}_{\text{Rx,SR}}$ in the secondary throughput remains unchanged. On the other side, by estimating the aggregate interference on the primary interference channel, the ST overestimates $\hat{P}_{\text{Rx,ST},h_{p,3}}$ and exercises a greater power control. Even for such a case, the outage constraint on the primary interference channel to the desired PR is satisfied, which consequently reduces the secondary throughput.

3.4 Theoretical Analysis

3.4.1 Deterministic Channel

In this section, the performance of the US is investigated for a specific frame. In this sense, the involved channels are considered to be deterministic (not random). First, an outage probability constraint (ρ_{cont}) on the uncertain interference is employed to capture the variations in the $P_{\text{Rx,PR}}$ incurred due to channel estimation, defined as

$$\mathbb{P} \left(P_{\text{Rx,PR}} = |\hat{h}_{p,3}|^2 P_{\text{Tx,ST,cont}} \geq \theta_1 \right) \leq \rho_{\text{cont}}. \quad (3.16)$$

Substituting $|\hat{h}_{p,3}|^2$ from (3.6) yields

$$\mathbb{P} \left(\left(\frac{\hat{P}_{\text{Rx,ST},h_{p,3}} - \sigma_w^2}{P_{\text{Tx,PR}}} \right) P_{\text{Tx,ST,cont}} \geq \theta_1 \right) \leq \rho_{\text{cont}}. \quad (3.17)$$

Besides the outage constraint, $P_{\text{Tx,ST,cont}}$ is limited by a maximum allowable transmit power $P_{\text{Tx,ST}}$. To capture this aspect, the transmit power constraint at the ST is defined as

$$P_{\text{Tx,ST,cont}} \leq P_{\text{Tx,ST}}. \quad (3.18)$$

It is considered that the same power is allocated to all the symbols transmitted within a frame by the ST. In this regard, the transmit power constraint on symbol basis and frame basis is equivalent. As a consequence, the constraint depicted in (3.18) is applicable to both the scenarios. Based on the constraints in (3.17) and (3.18), an expression of the controlled power for the proposed framework is determined, subsequently.

Lemma 7 Subject to the outage constraint on the uncertain interference and the transmit power constraint at the ST, the controlled power at the ST is given by

$$P_{\text{Tx,ST,cont}} = \begin{cases} \frac{\theta_1 P_{\text{Tx,PR}}}{(b_{p,1} \Gamma^{-1}(\rho_{\text{cont}}, a_{p,1}) - \sigma_w^2)}, & \text{for } P_{\text{Tx,ST,cont}} < P_{\text{Tx,ST}}, \\ P_{\text{Tx,ST}}, & \text{for } P_{\text{Tx,ST,cont}} \geq P_{\text{Tx,ST}}, \end{cases} \quad (3.19)$$

where $a_{p,1}$ and $b_{p,1}$ are defined in (3.8).

3 Underlay System

Solution: Substituting the cdf $F_{\hat{P}_{\text{Rx,ST},h_{p,3}}}(x)$, defined in (3.7), in (3.17) and combining with (3.18) yields (3.19).

Clearly, the performance (in terms of the secondary throughput) of the US improves over the access channel with $P_{\text{Tx,ST,cont}}$, but $P_{\text{Tx,ST,cont}}$ increases for the values of $|h_{p,3}|^2$, which correspond to the lower values of $\gamma_{p,3}$ ⁴. However, in practice, the wireless systems are limited by the transmit power $P_{\text{Tx,ST}}$, which bounds the performance of the US. In order to understand the effect of the power limitation on the US, a performance bound is characterized in terms of the estimation time.

Corollary 2 Subject to the outage constraint on the uncertain interference and the transmit power constraint at the ST, the performance bound ($\gamma_{p,3}^*$) of the US is defined as

$$\Gamma \left(\frac{\tau_{\text{est}} f_s (1 + \gamma_{p,3}^*)^2}{2 + 4\gamma_{p,3}^*}, \frac{\tau_{\text{est}} f_s (1 + \gamma_{p,3}^*)}{\sigma_w^2 (2 + 4\gamma_{p,3}^*)} \left(\frac{\theta_1 P_{\text{Tx,PR}}}{P_{\text{Tx,ST}}} + \sigma_w^2 \right) \right) = \rho_{\text{cont}}. \quad (3.20)$$

Solution: Substituting $P_{\text{Tx,ST,cont}}$ with $P_{\text{Tx,ST}}$ in (3.17) and reformulating gives

$$\mathbb{P} \left(\hat{P}_{\text{Rx,ST},h_{p,3}} \geq \frac{\theta_1 P_{\text{Tx,PR}}}{P_{\text{Tx,ST}}} + \sigma_w^2 \right) \leq \rho_{\text{cont}}. \quad (3.21)$$

Using (3.7) in Lemma 4 gives

$$\Gamma \left(\frac{\tau_{\text{est}} f_s (1 + \gamma_{p,3})^2}{2 + 4\gamma_{p,3}}, \frac{\tau_{\text{est}} f_s (1 + \gamma_{p,3})}{\sigma_w^2 (2 + 4\gamma_{p,3})} \left(\frac{\theta_1 P_{\text{Tx,PR}}}{P_{\text{Tx,ST}}} + \sigma_w^2 \right) \right) \leq \rho_{\text{cont}}. \quad (3.22)$$

Substituting $\gamma_{p,3}$ with $\gamma_{p,3}^*$ and replacing the expression in (3.22) with equality yields (3.20).

Remark 5 Figure 3.3 analyzes the variations of $\gamma_{p,3}^*$ with τ_{est} . Using the expression $\gamma_{p,3}^*$ obtained in Corollary 2, the operation of the US into the following regimes is classified: (i) interference-limited regime and (ii) power-limited regime. Inside the interference-limited regime $\gamma_{p,3} > \gamma_{p,3}^*$, due to good quality of the channel ST-PR (unfavorable to the US), the system is limited due to the exceeding level of the uncertain interference, which can be regulated

⁴Signal to noise ratio is mostly used as a design parameter for characterizing the performance of a wireless system.

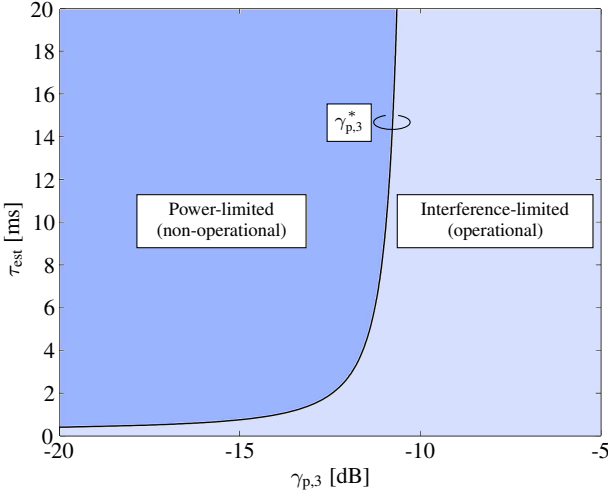


Figure 3.3: An illustration of the performance bound ($\gamma_{p,3}^*$) for the US depicted in terms of estimation time (τ_{est}), where $\gamma_{p,3}$ represents the ratio of the received signal power (from the PR) to noise at the ST. It further classifies the operation of the US as the interference-limited and the power-limited regimes.

effectively by employing power control at the US to satisfy the given outage constraint (ρ_{cont}).

At $\gamma_{p,3} = \gamma_{p,3}^*$, the ST operates at the maximum allowable power $P_{\text{Tx,ST,cont}} = P_{\text{Tx,ST}}$ while respecting the tolerance limits defined for the uncertain interference. From a different perspective, the situation $\gamma_{p,3} = \gamma_{p,3}^*$ also represents those USs that are unable to carry out power control. With regard to the outage constraint and the lack of the power control, for a given choice of $\gamma_{p,3}^*$, such systems can operate only at a specific value of τ_{est} .

On the other side, the region $\gamma_{p,3} \leq \gamma_{p,3}^*$, which depicts a weak link quality between the ST and the PR, is beneficial to the secondary user. However, due to the transmit power constraint, the USs can operate at or below $P_{\text{Tx,ST}}$. As a result, these favorable conditions do not translate into a performance gain. Therefore, this regime is characterized as a power-limited regime. Besides, it is interesting to observe that for low values of the estimation time, $\gamma_{p,3}^* \rightarrow -\infty$. This signifies that low τ_{est} increases the level of uncertainty in the interference. In order to regulate this increased level of uncertainty, US has to be proactive

3 Underlay System

in terms of power control to be able to satisfy the outage constraint.

It is also observed that as $\tau_{\text{est}} \rightarrow \infty$, $\gamma_{p,3}^*$ converges asymptotically to a certain value. This signifies the fact that, beyond a certain value, the time resources allocated for the channel estimation do not account for any significant improvement in the terms of the uncertain interference or indirectly in terms of the controlled power. As a result, the performance of the US in the form of controlled power gets saturated, thus limiting the performance of the US in terms of the secondary throughput.

Next, the variations in the secondary throughput are captured in terms of its expected value. To accomplish this, the cdf of the estimated data rate, given by

$$\hat{C}_3 = \log_2 \left(1 + \frac{|\hat{h}_s|^2 P_{\text{Tx,ST,cont}}}{\hat{P}_{\text{Rx,SR}}} \right) \quad (3.23)$$

is evaluated over the access channel at the ST. It is worth noticing the fact that unlike C_3 , defined in (3.5), \hat{C}_3 entails the random behavior due to the estimation of $|\hat{h}_s|^2$ and $\hat{P}_{\text{Rx,SR}}$.

Lemma 8 The cdf of data rate \hat{C}_3 is given by

$$F_{\hat{C}_3}(x) = \int_0^x f_{\hat{C}_3}(t) dt, \quad (3.24)$$

where the $f_{\hat{C}_3}(x)$ pdf is given by

$$f_{\hat{C}_3}(x) = 2^x \ln 2 \frac{(2^x - 1)^{a_s - 1} \Gamma(a_s + a_{p,2})}{\Gamma(a_s) \Gamma(a_{p,2}) (b_s P_{\text{Tx,ST,cont}})^{a_s} b_{p,2}^{a_{p,2}}} \left(\frac{1}{b_{p,2}} + \frac{2^x - 1}{b_s P_{\text{Tx,ST,cont}}} \right). \quad (3.25)$$

Solution: See Appendix 3.7.1.

In consideration to the Approximation 1, which is applied to obtain the cdfs' of $\hat{P}_{\text{Rx,ST},h_{p,3}}$, $|\hat{h}_s|^2$ and $\hat{P}_{\text{Rx,SR}}$ (the estimated parameters included in the characterization of \hat{C}_3), the theoretical expression of the cdf depicted in (3.24) is validated by means of simulations in Figure 3.4 with different choices of system parameters, including signal to noise ratio over the primary interference

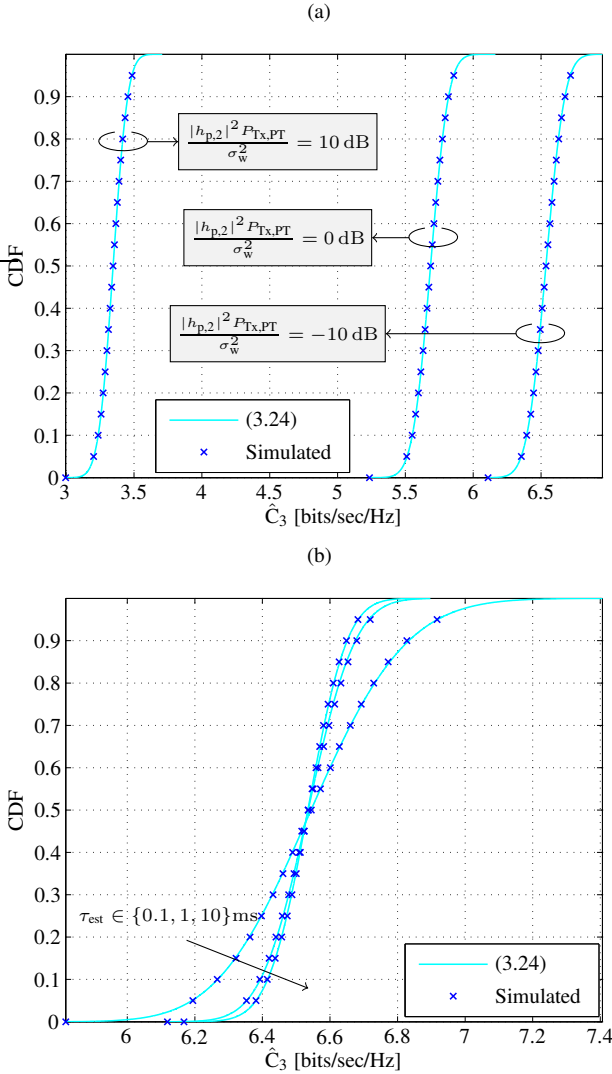


Figure 3.4: CDF of \hat{C}_3 for different $|h_{p,2}|^2 P_{\text{Tx,PT}}/\sigma_w^2$ and τ_{est} . (a) $|h_{p,2}|^2 P_{\text{Tx,PT}}/\sigma_w^2 \in \{-10, 0, 10\}$ dB and $\tau_{\text{est}} = 1$ ms, (b) $\tau_{\text{est}} \in \{0.1, 1, 10\}$ ms and $|h_{p,2}|^2 P_{\text{Tx,PT}}/\sigma_w^2 = 0$ dB.

3 Underlay System

channel at the ST $\gamma_{p,3} = 10$ dB, controlled power $P_{\text{Tx,ST,cont}} = 0$ dBm, interference to noise ratio at the SR over the secondary interference channel $\frac{|h_{p,2}|^2 P_{\text{Tx,PT}}}{\sigma_w^2} \in \{-10, 0, 10\}$ dB and estimation time $\tau_{\text{est}} \in \{0.1, 1, 10\}$ ms.

Besides the outage constraint on the uncertain interference, the expected secondary throughput over the access channel at the SR is defined as

$$R_s(\tau_{\text{est}}) = \frac{T - \tau_{\text{est}}}{T} \mathbb{E}_{\hat{\mathbf{C}}_3} [\hat{\mathbf{C}}_3], \quad (3.26)$$

where $\mathbb{E}_{\hat{\mathbf{C}}_3} [\cdot]$ corresponds to an expectation over $\hat{\mathbf{C}}_3$, whose pdf is characterized in Lemma 8.

Remark 6 At this point, it is well-known that the performance degradation due to channel estimation in the form of the secondary throughput is inherent to the US. Specifically, the time allocation and the uncertain interference are responsible of this degradation. The controlled power, determined in Lemma 7, characterized as a function of estimation time allow us to regulate the uncertain interference. As discussed previously in Remark 5, the low estimation time enables a severe control in power, thereby decreasing the secondary throughput. On the other hand, less time allocated for channel estimation increases the secondary throughput. This phenomenon can be captured by observing the variation of the secondary throughput along the estimation time such that the constraints depicted in (3.17) and (3.18) are fulfilled. Subsequently, Problem 5 captures this relationship between the estimation time and the secondary throughput, defined as an estimation-throughput tradeoff. More importantly, this tradeoff is utilized to determine a suitable estimation time at which maximum throughput at the SR is achieved.

Problem 5 The achievable expected secondary throughput subject to the outage constraint on the uncertain interference and the transmit power constraint at the ST, is defined as

$$\begin{aligned} R_s(\tilde{\tau}_{\text{est}}) &= \max_{\tau_{\text{est}}} R_s(\tau_{\text{est}}), \\ &\text{s.t. (3.17), (3.18),} \end{aligned} \quad (3.27)$$

where $R_s(\tilde{\tau}_{\text{est}})$ corresponds to achievable secondary throughput at $\tilde{\tau}_{\text{est}}$.

Solution: The constrained optimization problem is solved by substituting $P_{\text{Tx,ST,cont}}$ from Lemma 6, determined by applying the outage and the transmit power constraints defined in (3.17) and (3.18), in (3.26). The pdf of $\hat{\mathbf{C}}_3$,

determined in (3.25), is used to evaluate the expectation on the secondary throughput. Following this, an expression of the expected secondary throughput as a function of τ_{est}^5 is determined as

$$R_s(\tau_{\text{est}}) = \frac{T - \tau_{\text{est}}}{T} \int_0^{\infty} x f_{\hat{C}_3}(x) dx. \quad (3.28)$$

Solving numerically the expression in (3.28) yields $\tilde{\tau}_{\text{est}}$ and $R_s(\tilde{\tau}_{\text{est}})$.

Corollary 3 Problem 5 considers the optimization of the expected secondary throughput for the proposed framework that employ power control and considers the effect of the imperfect channel knowledge. In accordance to Corollary 2, these USs correspond to the those USs that operate in the interference-limited regime $\gamma_{p,3}^* \geq \gamma_{p,3}$. Besides, it is interesting to compare its performance with those USs that employ channel estimation and satisfy the outage constraint on the uncertain interference, however, employ no power control, i.e., operate at $P_{\text{Tx,ST}}$. With regard to Corollary 2, these systems correspond to the ones operating on the curve $\gamma_{p,3}^* = \gamma_{p,3}$. For the latter approach, the secondary throughput is obtained by substituting $P_{\text{Tx,ST,cont}}$ with $P_{\text{Tx,ST}}$ in (3.26), where τ_{est} in (3.26) is determined using Corollary 2. Such a comparison allows us to quantify the performance gain, procured by the US when power control is employed at the ST.

3.4.2 Random Channel

Here, the objective is to investigate the performance of the proposed approach, where the interacting channels encounter quasi-static block fading. Specifically, the performance of the US is analyzed over multiple frames, where every alternating transmission according to the frame structure, presented in Figure 3.2, observes a different realization of the channel. In this regard, the channel gains $h_{p,3}$, $h_{p,2}$ and h_s are characterized according to Nakagami- m fading model. Analog to the previous chapter, the power gains $|h_{p,3}|^2$, $|h_{p,2}|^2$ and $|h_s|^2$ follow a Gamma distribution [38], whose corresponding cdfs are defined as

$$F_{|h_{p,3}|^2}(x) = 1 - \Gamma\left(m_{p,3}, \frac{m_{p,3}x}{|h_{p,3}|^2}\right), \quad (3.29)$$

⁵Please note that the model parameters $a_{p,2}$ and $b_{p,2}$, defined in (3.15), used for characterizing the pdf of \hat{C}_3 in (3.25) are functions of τ_{est} .

$$F_{|h_{p,2}|^2}(x) = 1 - \Gamma\left(m_{p,2}, \frac{m_{p,2}x}{|\bar{h}_{p,2}|^2}\right), \quad (3.30)$$

$$F_{|h_s|^2}(x) = 1 - \Gamma\left(m_s, \frac{m_s x}{|\bar{h}_s|^2}\right), \quad (3.31)$$

where $m_{p,3}$, $m_{p,2}$ and m_s represent the m parameter, whereas $|\bar{h}_{p,3}|^2$, $|\bar{h}_{p,2}|^2$ and $|\bar{h}_s|^2$ are the expected values for channels $|h_{p,3}|^2$, $|h_{p,2}|^2$ and $|h_s|^2$, respectively.

Perfect Channel Knowledge

The performance analysis subject to channel fading has been considered by Ghasemi *et al.* [44, 92], where the authors in [44, 92] evaluated the expected data rate while constraining the interference at the PR. The influence of the channel fading (however, without channel estimation) has been quantified in terms of the expected data rate and the outage constraint on the uncertain interference⁶

$$\max_{P_{\text{Tx,ST,cont}}} \mathbb{E}_{|h_{p,2}|^2, |h_s|^2} [C_3], \quad (3.32)$$

$$\text{s.t. } \mathbb{P}(P_{\text{Rx,PR}} = |h_{p,3}|^2 P_{\text{Tx,ST,cont}} \geq \theta_1) \leq \rho_{\text{cont}}, \quad (3.33)$$

where $\mathbb{E}_{|h_{p,2}|^2, |h_s|^2} [\cdot]$ corresponds to an expectation with respect to $|h_{p,2}|^2$ and $|h_s|^2$, which are entailed in C_3 , cf. (3.5).

Despite the knowledge of the fading model, similar to the ideal model depicted for the deterministic channel (refer to Section 3.3.3), the characterization in (3.32) and (3.33) assumes the perfect knowledge of the realizations of the power gains ($|h_{p,3}|^2$, $|h_{p,2}|^2$, $|h_s|^2$) for the corresponding channels. In view of this, subsequently, the proposed framework is further extended to investigate the effect of the random channel (channel fading) on the performance of the US.

Imperfect Channel Knowledge

Here, the estimation of the interacting channels in context to the channel fading is considered. First, the expression of the outage constraint on the uncertain

⁶The uncertainty is interference power received at the PR is due to channel fading.

interference is determined as

$$\mathbb{E}_{|h_{p,3}|^2} \left[\underbrace{\mathbb{P} \left(\left(\frac{\hat{P}_{\text{Rx,ST},h_{p,3}} - \sigma_w^2}{P_{\text{Tx,PR}}} \right) P_{\text{Tx,ST,cont}} \geq \theta_I \right)}_{\text{Channel Estimation}} \right] \leq \rho_{\text{cont}}, \quad (3.34)$$

where $\hat{P}_{\text{Rx,ST},h_{p,3}}$ depends on the underlying value of $|h_{p,3}|^2$, which is a random variable. In contrast to the constraint in (3.33), (3.34) captures the variations due to the channel estimation ($\mathbb{P}(\cdot)$ determined in terms of $\hat{P}_{\text{Rx,ST},h_{p,3}}$) and the channel fading ($\mathbb{E}_{|h_{p,3}|^2}[\cdot]$). Based on (3.34) and transmit power constraint defined in (3.18), the expression of the controlled power ($P_{\text{Tx,ST,cont}}$) for the case with the random channel is derived, subsequently.

Lemma 9 Subject to the outage constraint on the uncertain interference and the transmit power constraint at the ST, the controlled power at the ST under Nakagami- m fading is given by

$$P_{\text{Tx,ST,cont}} = \begin{cases} \int_0^\infty \Gamma \left(\frac{\tau_{\text{est}} f_s (1 + x P_{\text{Tx,PR}} / \sigma_w^2)^2}{2 + 4x P_{\text{Tx,PR}} / \sigma_w^2}, \frac{\tau_{\text{est}} f_s (1 + x P_{\text{Tx,PR}} / \sigma_w^2)}{\sigma_w^2 (2 + 4x P_{\text{Tx,PR}} / \sigma_w^2)} \right) \left(\frac{\theta_I P_{\text{Tx,PR}}}{P_{\text{Tx,ST,cont}}} + \sigma_w^2 \right) dF_{|h_{p,3}|^2} = \rho_{\text{cont}}, & \text{for } P_{\text{Tx,ST,cont}} < P_{\text{Tx,ST}} \\ P_{\text{Tx,ST}}, & \text{for } P_{\text{Tx,ST,cont}} \geq P_{\text{Tx,ST}} \end{cases}, \quad (3.35)$$

where $F_{|h_{p,3}|^2}(\cdot)$ is defined in (3.29).

Solution: Since it is complicated to obtain a closed form expression of the integral in (3.35), therefore, the controlled power is evaluated numerically.

Similar to the analysis performed in Corollary 2 for the deterministic channel, the performance bound ($\gamma_{p,3}^*$) in terms of τ_{est} for the random channel is evaluated. To this end, $\gamma_{p,3}^*$ is determined by substituting $P_{\text{Tx,ST,cont}}$ with $P_{\text{Tx,ST}}$ in the expression (3.35)

$$\int_0^\infty \Gamma \left(\frac{\tau_{\text{est}} f_s (1 + x P_{\text{Tx,PR}} / \sigma_w^2)^2}{2 + 4x P_{\text{Tx,PR}} / \sigma_w^2}, \frac{\tau_{\text{est}} f_s (1 + x P_{\text{Tx,PR}} / \sigma_w^2)}{\sigma_w^2 (2 + 4x P_{\text{Tx,PR}} / \sigma_w^2)} \left(\frac{\theta_I P_{\text{Tx,PR}}}{P_{\text{Tx,ST}}} + \sigma_w^2 \right) \right)$$

3 Underlay System

$$dF_{|h_{p,3}|^2} \leq \rho_{\text{cont}}. \quad (3.36)$$

In order to obtain $\gamma_{p,3}^*$, the integral on the left side in (3.36) is represented as a function of $|h_{p,3}|^2$ and τ_{est} . Since no closed form expression of this function is obtained, it is represented as

$$g(|h_{p,3}|^2, \tau_{\text{est}} f_s) \leq \rho_{\text{cont}}.$$

Substituting $|h_{p,3}|^2 = \frac{\gamma_{p,3}^* \sigma_w^2}{P_{\text{Tx,PR}}}$ and replacing with equality, $\gamma_{p,3}^*$ for the random channel is determined as

$$g\left(\frac{\gamma_{p,3}^* \sigma_w^2}{P_{\text{Tx,PR}}}, \tau_{\text{est}} f_s\right) = \rho_{\text{cont}}.$$

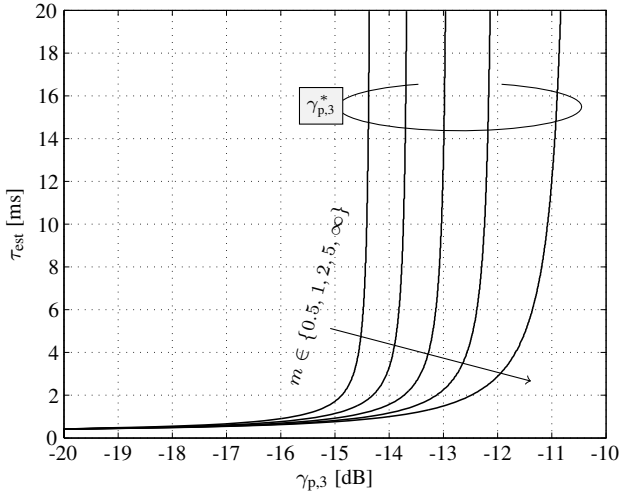


Figure 3.5: An extension of the interference-limited and the power-limited regimes for the US to the random channel. The performance bound ($\gamma_{p,3}^*$) is depicted in terms of estimation time (τ_{est}). The different curves demonstrate the severity in fading.

Remark 7 Figure 3.5 analyzes the variation of $\gamma_{p,3}^*$ with τ_{est} for different $m \in \{0.5, 1, 2, 5, \infty\}$, where $m = \infty$ represents a deterministic channel. It is observed that $\gamma_{p,3}^*$ tends towards a lower value as the channel fading becomes

severe. Hence, this extension of the interference-limited regime enables the US to operate at a lower $\gamma_{p,3}$. Following the analysis from Remark 5, this also reflects that the power control becomes proactive as the severity in the fading increases. This signifies that controlled power employed for regulating the uncertainty interference is mainly dominated by the variations due to the channel fading, specially for the scenarios that observe severe fading. In addition, it is noticed that the deterministic channel is more sensitive to the estimation time as compared to the random channel.

After determining the controlled power in Lemma 9, the throughput at the SR is determined as

$$R_s(\tau_{\text{est}}) = \mathbb{E}_{\hat{C}_3, |h_{p,2}|^2, |h_s|^2} \left[\frac{T - \tau_{\text{est}} \hat{C}_3}{T} \hat{C}_3 \right], \quad (3.37)$$

where $\mathbb{E}_{\hat{C}_3, |h_{p,2}|^2, |h_s|^2} [\cdot]$ corresponds to an expectation over \hat{C}_3 , $|h_{p,2}|^2$ and $|h_s|^2$, whose cdfs are characterized in Lemma 8, (3.30) and (3.31), respectively. It is worth noticing that \hat{C}_3 captures the variations due to channel estimation $|\hat{h}_s|^2$ and $\hat{P}_{\text{Rx,ST}, h_{p,3}}$, refer to (3.23), however, due to channel fading, the underlying values of the channels $|h_{p,2}|^2$ and $|h_s|^2$ are random. In this context, an expectation with respect to $|h_{p,2}|^2$ and $|h_s|^2$, as depicted in (3.37), is performed.

Lastly, similar to the deterministic channel, the estimation-throughput tradeoff corresponding to the random behaviour of the channels is characterized.

Problem 6 The achievable expected secondary throughput subject to the outage constraint on the uncertain interference and the transmit power constraint at the ST under Nakagami- m fading, is defined as

$$R_s(\tilde{\tau}_{\text{est}}) = \max_{\tau_{\text{est}}} R_s(\tau_{\text{est}}), \quad (3.38)$$

s.t. (3.34), (3.18),

where $R_s(\tilde{\tau}_{\text{est}})$ corresponds to achievable secondary throughput at $\tilde{\tau}_{\text{est}}$.

Corollary 4 Here, the approach depicted in Corollary 3 is extended to investigate the performance of those USs that employ channel estimation, operate with no power control, satisfy the outage constraint and are subjected to Nakagami- m fading. The expected secondary throughput for this particular approach is obtained by replacing $P_{\text{Tx,ST,cont}}$ in the expression in (3.37) with $P_{\text{Tx,ST}}$, where τ_{est} is determined using (3.36).

Table 3.1: Parameters for Numerical Analysis

Parameter	Value
f_s	1 MHz
$ h_{p,3} ^2$ (or $ \bar{h}_{p,3} ^2$)	-100 dB
$ h_{p,2} ^2$ (or $ \bar{h}_{p,2} ^2$)	-100 dB
$ h_s ^2$ (or $ \bar{h}_s ^2$)	-80 dB
θ_1	-110 dBm
T	100 ms
ρ_{cont}	0.10
$P_{\text{Tx,ST}}$	0 dBm
σ_w^2	-100 dBm
$\gamma_{p,3}$	0 dB
$P_{\text{Tx,PR}}$	0 dBm
$P_{\text{Tx,PT}}$	0 dBm
N_s	10
m	{1,5}

3.5 Numerical Analysis

In this section, the performance of the US based on the proposed estimation model is evaluated. To accomplish this: (i) simulations are performed to validate the expressions obtained, (ii) the performance loss incurred due to the channel estimation is analyzed. In addition, the ideal model is considered to benchmark and evaluate the performance loss. Unless stated explicitly, the parameters given in Table 3.1 are considered for the analysis.

3.5.1 Deterministic Channel

First, the performance of the proposed framework in context to the deterministic channel is evaluated. Figure 3.6 considers the variation of $P_{\text{Tx,ST,cont}}$ (de-

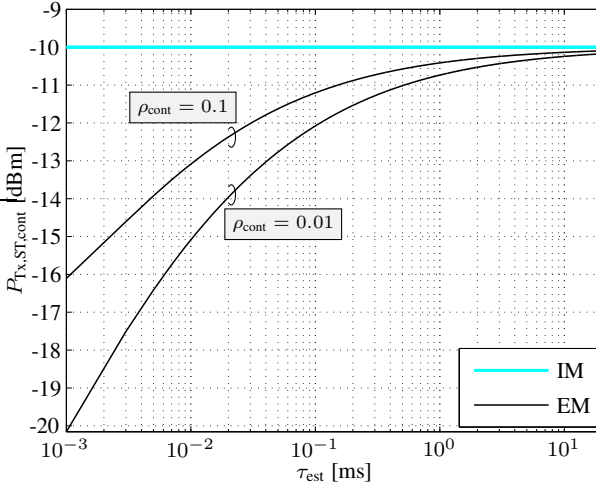


Figure 3.6: Control power versus estimation time with $\gamma_{p,3} = 0$ dB, $\rho_{\text{cont}} \in \{0.01, 0.1\}$ and $P_{\text{Tx,ST}} = 0$ dBm.

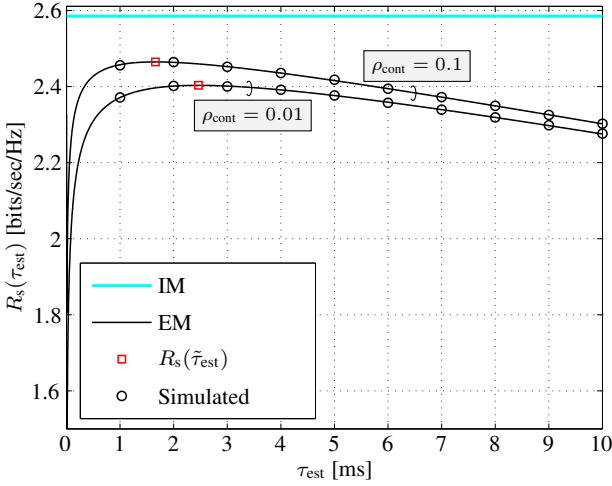


Figure 3.7: Estimation-throughput tradeoff with $\gamma_{p,3} = 0$ dB, $\rho_{\text{cont}} \in \{0.01, 0.1\}$ and $P_{\text{Tx,ST}} = 0$ dBm.

fined in Corollary 2) versus τ_{est} corresponding to the Ideal Model (IM) and the proposed Estimation Model (EM). Since the IM considers perfect channel knowledge, its controlled power remains invariant to the estimation time. In addition, it is noticed that the ST controls its transmit power ($P_{\text{Tx,ST,cont}}$) more severely for low values, consequently affecting the link budget for the access channel. Figure 3.7 analyzes the performance of the US in terms of the estimation-throughput tradeoff, refer to Problem 5. It can be depicted that the estimation-throughput tradeoff yields a suitable estimation time $\tilde{\tau}_{\text{est}}$ that results in an achievable secondary throughput $R_s(\tilde{\tau}_{\text{est}})$. Hereafter, theoretical expressions are considered for the performance analysis with respect to the deterministic channel. In addition, the US operates at the suitable estimation time.

To procure further insights, it is necessary to consider the variation of $R_s(\tilde{\tau}_{\text{est}})$ with $\gamma_{\text{p},3}$ for different choices of the interference from the PT to noise ratio at the SR over the secondary interference channel (regulated using $|h_{\text{p},2}|^2 \in \{-90, -100\}$ dBm), as depicted in Figure 3.8. The power-limited and the interference-limited regimes, classified in Corollary 3, are mapped onto the achievable secondary throughput, refer to Figure 3.8a. Due to the limited transmit power at the ST, $R_s(\tilde{\tau}_{\text{est}})$ gets saturated below a certain $\gamma_{\text{p},3}$, thereby limiting the performance of the US. It is worthy to note that this saturation is due to the existence of the performance bound, which restricts the operation of the US inside the power-limited regime.

Upon increasing $P_{\text{Tx,ST}}$ from -10 dB to 0 dB, the point where saturation is achieved, shifts to a lower $\gamma_{\text{p},3}$. This is due to the fact that higher $P_{\text{Tx,ST}}$ extends the interference-limited regime to a lower $\gamma_{\text{p},3}$. In other words, because of low $\gamma_{\text{p},3}$, the secondary system exploits the benefit of operating at a higher controlled power. Particularly for $P_{\text{Tx,ST}} = -10$ dBm, a severe performance loss indicated by the margin between the IM and the EM is witnessed by the US for $\gamma_{\text{p},3} \leq -2$ dB. This signifies that the consideration of the maximum transmit power of the ST is essential while designing the system. Besides this, Figure 3.8 depicts the performance of the USs with no power control, proposed in Corollary 3. As indicated in Figure 3.3, beyond a certain $\gamma_{\text{p},3} = \gamma_{\text{p},3}^*$, the US with no power control delivers zero secondary throughput. In order to avoid such situations, the US must employ power control in order to achieve non-zero secondary throughput.

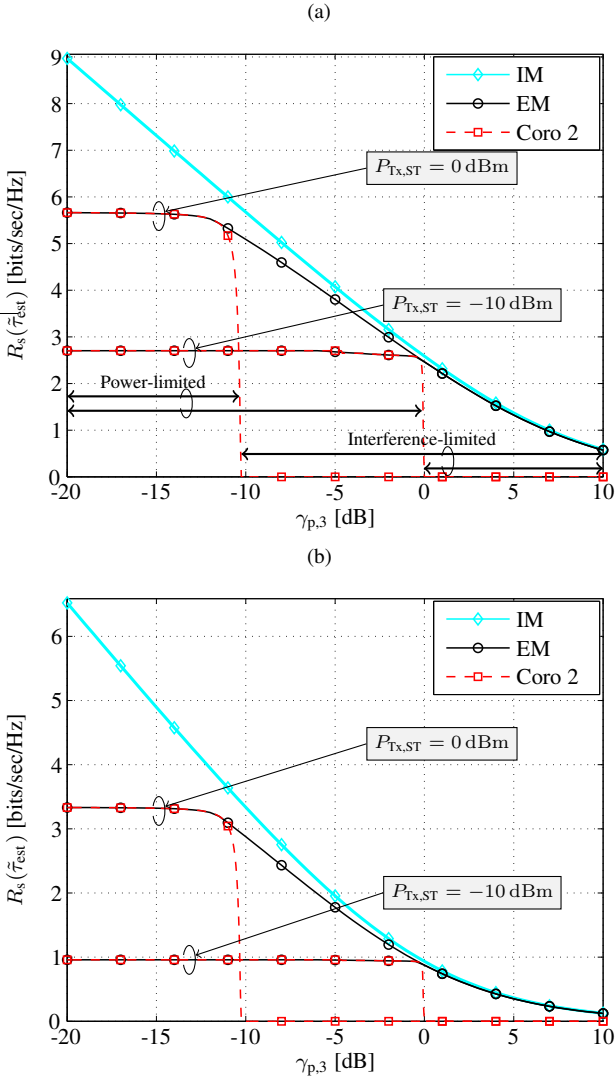


Figure 3.8: $R_s(\tilde{\tau}_{\text{est}})$ versus $\gamma_{p,3}$ with $\rho_{\text{cont}} = 0.1$ and $P_{T_x,ST} \in \{-10, 0\}$ dBm for (a) $|h_{p,2}|^2 = -100$ dBm and (b) $|h_{p,2}|^2 = -90$ dBm, which translate to an interference power (from the PT) to noise ratio of (a) 0 dB and (b) 10 dB, respectively, at the SR.

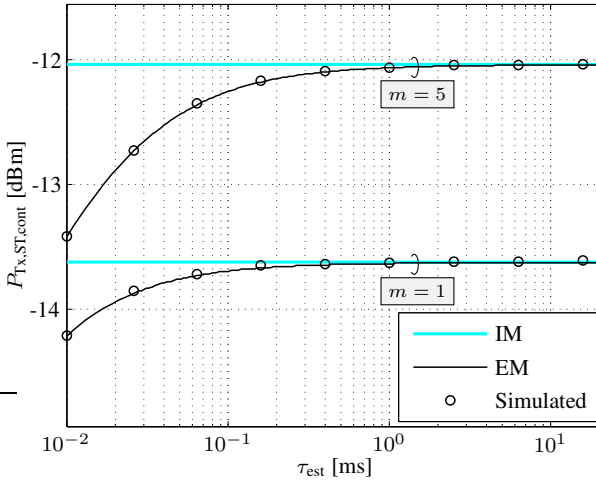


Figure 3.9: Control power versus estimation time with $\gamma_{p,3} = 0$ dB, $\rho_{\text{cont}} = 0.1$ and $P_{\text{Tx,ST}} = 0$ dBm with Nakagami- m fading.

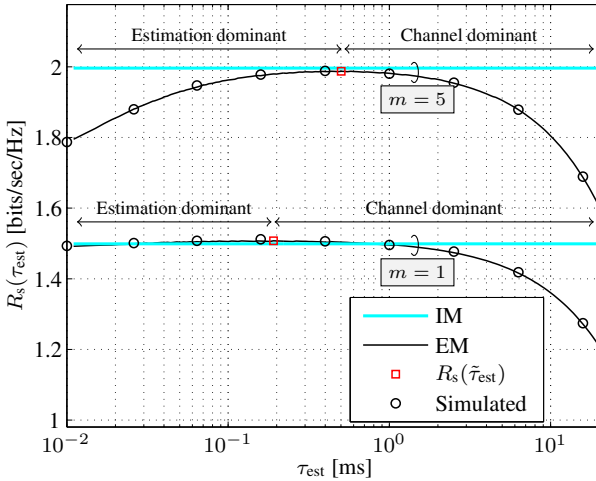


Figure 3.10: Estimation-throughput tradeoff with $\gamma_{p,3} = 0$ dB, $\rho_{\text{cont}} = 0.1$ and $P_{\text{Tx,ST}} = 0$ dBm with Nakagami- m fading. The plot classifies the estimation time into the estimation-dominant and the channel-dominant regime

3.5.2 Random Channel

Here, the performance of the proposed framework is further evaluated for those scenarios, where the interacting channels are under the influence of Nakagami- m fading. For simplification of the analysis, it is assumed that m is same for all the involved channels. In addition, the performance is investigated under following fading scenarios: (i) severe fading $m = 1$, which corresponds to Rayleigh fading and (ii) mild fading $m = 5$.

First, the variation of $P_{\text{Tx,ST,cont}}$ along the estimation time is analyzed. It is observed that the mild fading scenario ($m = 5$) is more sensitive to the estimation time, see Figure 3.9. In reference to the analysis for the deterministic channel considered in Figure 3.6, the controlled power, determined using the EM, converges to one depicted from the IM at a smaller τ_{est} . This is due to the fact that power control is applied to regulate the variations due to both channel estimation and channel fading. However, beyond a certain estimation time, these variations are largely dominated by the channel fading, which are invariant to the increase in the estimation time. Complementing the observations carried out in Figure 3.5, it is concluded that the severe fading scenarios are less sensitive to the estimation time and are subjected to a severe power control.

Besides, the influence of the channel fading on the performance of the US in terms of the estimation-throughput is captured, as depicted in Problem 6. In this regard, the estimation-throughput tradeoff corresponding to the fading scenarios is illustrated in Figure 3.10. It is depicted that for a suitable choice of the estimation time, the performance of the proposed framework – that captures the imperfect channel knowledge – is comparable to the ideal conditions in terms of the achievable secondary throughput. Since the US is subjected to the variations from the channel estimation and the channel fading, the estimation time is classified into an estimation-dominant regime and a channel-dominant regime. These regimes signify that the estimation time can only reduce the imperfections (incurred in the US) due to the channel estimation, however, beyond a certain estimation time ($\tilde{\tau}_{\text{est}}$), the time resources allocated for channel estimation slightly contribute to the performance improvement (in terms of the controlled power, which finally affects the secondary throughput) and mainly result in the performance degradation (due to the factor $\frac{T-\tau_{\text{est}}}{T}$ in (3.37)) in the secondary throughput.

Upon determining the achievable secondary throughput using the estimation-throughput tradeoff, it is worthy to consider the variation of $R_s(\tilde{\tau}_{\text{est}})$ along the received signal to noise ratio at the ST for different choices of the power gain

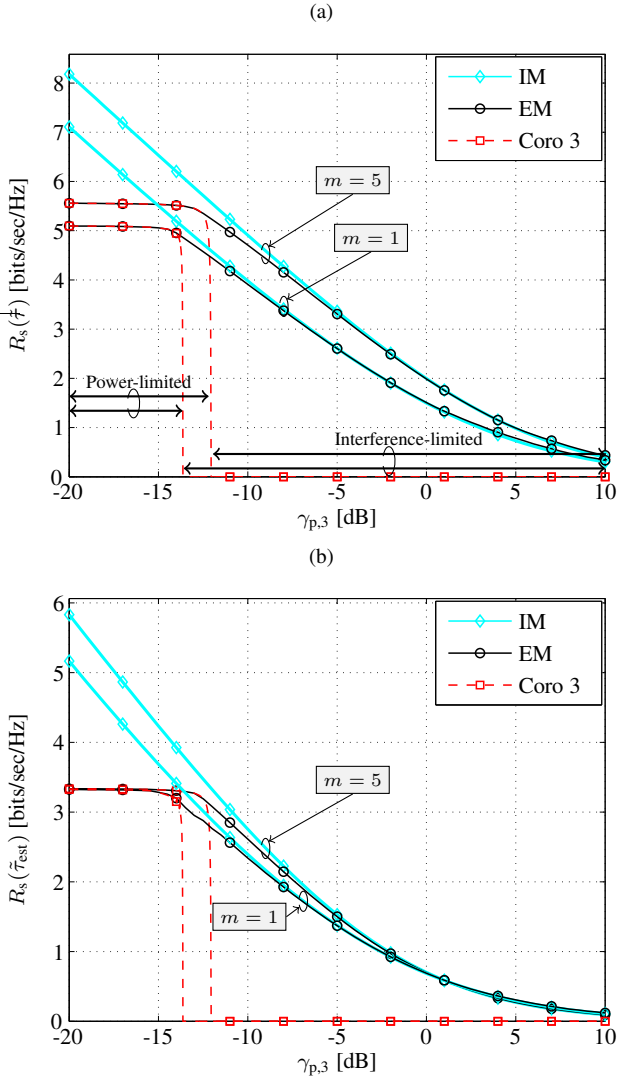


Figure 3.11: $R_s(\tilde{\tau}_{\text{est}})$ versus $\gamma_{p,3}$ for Nakagmi- m fading with $\rho_{\text{cont}} = 0.1$ and $P_{\text{Tx,ST}} = 0$ dBm for $|h_{p,2}|^2 =$ (a) -100 dBm and (b) -90 dBm, which correspond to an interference power (from the PT) to noise ratio of (a) 0 dB and (b) 10 dB at the SR.

over the secondary interference channel. These choices correspond to different values of the interference (from the PT) to noise ratio at the SR, depicted in Figure 3.11. It is observed that for a large range ($\gamma_{p,3} \geq -10$ dB), the achievable secondary throughput determined by the EM closely follows the secondary throughput depicted by the IM. This concludes that the optimum performance for the random channel – depicted by the reduced margin between the IM and the EM – can be reached only if the US chooses to operate at a suitable estimation time, depicted by the proposed framework.

In addition, Figure 3.11 considers the performance of the US with no power control, refer to Corollary 4. Following the discussion in Remark 7, where it was noticed that the performance bound ($\gamma_{p,3}^*$) shifts to a lower $\gamma_{p,3}$, thus enabling the ST to carry out a rigorous power control. This reveals the fact that the power control becomes proactive when the US is subjected to severe fading conditions, refer to Figure 3.5. This effect is finally translated to the secondary throughput, where $m = 1$ approaches the region with no throughput at a lower $\gamma_{p,3}$ as compared to $m = 5$, consider Figure 3.11a.

3.6 Summary

In this chapter, the performance of US has been studied from a deployment perspective by laying emphasis on the fact that the knowledge of the interacting channels is pivotal for the implementation of the underlay principle over the hardware. In this view, a novel approach that incorporates estimation of the involved channels at the secondary system has been proposed. Considering the time resources utilized for the channel estimation and the uncertainty due its imperfect knowledge, it has been shown that the channel estimation has a detrimental effect on the performance, leading to its degradation. To tackle the uncertain interference, an outage constraint that precisely regulates the uncertain interference at the PR has been employed.

Besides, it has been observed that the operation of the power control at the ST is limited by the maximum transmit power. This limitation, complementing with the channel estimation has been studied in terms of the interference-limited and the power-limited regimes to determine the performance bounds of the US. Finally, from the perspective of a system designer, an estimation-throughput tradeoff has been established that allows us to determine the achievable secondary throughput for the US. In consideration to the channel fading, it has

been observed that the performance degradation is highly prone to the scenarios that are subject to mild channel fading.

3.7 Solutions

3.7.1 Solution to Lemma 8

Solution: For simplification, it is essential to deal $\frac{|\hat{h}_s|^2 P_{\text{Tx,ST,cont}}}{\hat{P}_{\text{Rx,SR}}}$ as individual terms $|\hat{h}_s|^2 P_{\text{Tx,ST,cont}}$ and $\hat{P}_{\text{Rx,SR}}$, and determine the pdfs $f_{|\hat{h}_s|^2 P_{\text{Tx,ST,cont}}}(\cdot)$ and $f_{\hat{P}_{\text{Rx,SR}}}(\cdot)$ separately.

Using (3.10) in Lemma 5, the pdf of $|\hat{h}_s|^2 P_{\text{Tx,ST,cont}}$ is determined as

$$f_{|\hat{h}_s|^2 P_{\text{Tx,ST,cont}}}(x) = \frac{1}{\Gamma(a_s)(b_s P_{\text{Tx,ST,cont}})^{a_s}} x^{a_s-1} \exp\left(-\frac{x}{b_s P_{\text{Tx,ST,cont}}}\right), \quad (3.39)$$

where a_s and b_s are defined in (3.11).

Similarly, using Lemma 6, the pdf of $\hat{P}_{\text{Rx,SR}}$ is characterized as

$$f_{\hat{P}_{\text{Rx,SR}}}(x) = \frac{1}{\Gamma(a_{p,2})(b_{p,2})^{a_{p,2}}} x^{a_{p,2}-1} \exp\left(-\frac{x}{b_{p,2}}\right), \quad (3.40)$$

where $a_{p,2}$ and $b_{p,2}$ are defined in (3.15).

Using (3.39) and (3.40), Mellin transform [79] is applied to determine the pdf of $\frac{|\hat{h}_s|^2 P_{\text{Tx,ST,cont}}}{\hat{P}_{\text{Rx,SR}}}$ as

$$f_{\frac{|\hat{h}_s|^2 P_{\text{Tx,ST,cont}}}{\hat{P}_{\text{Rx,SR}}}}(x) = \frac{(x)^{a_s-1} \Gamma(a_s + a_{p,2})}{\Gamma(a_s) \Gamma(a_{p,2}) (b_s P_{\text{Tx,ST,cont}})^{a_s} b_{p,2}^{a_{p,2}}} \left(\frac{1}{b_{p,2}} + \frac{x-1}{b_s P_{\text{Tx,ST,cont}}} \right). \quad (3.41)$$

Finally, substituting the expression $\frac{|\hat{h}_s|^2 P_{\text{Tx,ST,cont}}}{\hat{P}_{\text{Rx,SR}}}$ in \hat{C}_3 yields (3.25).

Chapter 4

Hybrid System

This chapter¹ studies the performance of hybrid cognitive radio systems. A HS combines the benefits of the interweave and the underlay systems by employing a spectrum sensing and a power control mechanism at the ST. From the previous chapters, it can be easily comprehended that the US can employ several techniques such as power control, interference alignment, beamforming that allow CR systems to mitigate the interference at the primary systems. More particularly, the US tends to operate below a certain level defined as the IT. It is worth noticing that the IS aims at interference avoidance, according to which spectrum sensing is employed to detect the presence or absence of PU signals, using different techniques such as energy-based detection, matched filter-based detection, cyclostationary based-detection, etc. However, the IS does not account for the severity of the interference power received at the PR, which in certain cases lies within the tolerance limits defined by the primary systems and in other cases can lead to outage at the PR, resulting in serious performance degradation of the primary system. In contrast to the IS, the detection incapability of US forbids them to transmit with full power, specially during the periods when the primary system remains inactive. By addressing these issues, one can significantly enhance the spectral efficiency of the CR systems. In this context, a joint solution that precisely utilizes the interference

¹That primarily features the performance analysis conducted in [K6].

tolerance capability of the US and the agility of IS to detect spectrum holes, represented as the HS, has been recently considered as a CR system.

Like the previous two chapters, it is examined that the existing baseline models considered for performance analysis of the HS assume perfect knowledge of the involved channels at the ST. However, analog to the interweave and the underlay scenarios investigated in Chapter 2 and Chapter 3, such situations hardly exist in practical deployments. Motivated by this fact, a novel approach that incorporates channel estimation at the secondary system is proposed. In this regard, the performance characterization of the HS under realistic scenarios is significantly enhanced. In order to overcome the impact of imperfect channel knowledge that mainly consists of the uncertain interference at the primary system, outage constraints on the detection probability at the ST and on the interference power received at the PR are proposed. The proposed analysis reveals that the baseline model overestimates the performance of the HS in terms of achievable secondary throughput. In this chapter, corresponding to the HS, an estimation-sensing-throughput tradeoff is established to determine suitable estimation and sensing durations. In this way, the proposed tradeoff allows us to effectively capture the influence of imperfect channel knowledge, and subsequently determine the achievable secondary throughput.

4.1 Related Work

In recent past, an extensive investigation [36, 41, 45–48, 93, 94] has been carried out to determine the performance of a HS. Kang *et al.* [36] established a frame structure for HS, whereby the ST first senses a PU channel in order to decide its operation mode (interweave or underlay) based on the detection result. Further, to decide upon a suitable operation mode, appropriate strategies that maximize the secondary system's throughput have been investigated by [45, 46, 93, 94]. Besides this, Jiang *et al.* [47] employed a double detection threshold, which enables dynamic switching between full and partial access modes. Whereas Filippou *et al.* [48] analyzed the throughput performance of the HS when a MIMO antenna is employed at the secondary system. Lastly, a sensing-throughput tradeoff to characterize the performance of the HS has been investigated by Sharma *et al.* [41].

The fact is, most of the existing models [36, 41, 45–48, 93, 94], used for the performance analysis, assume perfect knowledge of the involved channels at the ST. This assumption is however not viable for practical implementations,

thereby rendering the performance analysis carried out using these models inaccurate. In this context, the performance analysis of the HS that incorporates channel estimation is an interesting research problem. Motivated by this fact, this chapter establishes a fundamental framework that considers the estimation of the involved channels and analyzes the impact of channel estimation on performance of those CR systems that employ hybrid technique for accessing the licensed spectrum.

4.2 Contributions

More specifically, this chapter provides the following contributions:

4.2.1 Analytical Framework

A novel analytical framework for the HS that constitutes the estimation of interacting channels, namely: (i) sensing channel, (ii) interference channels and (iii) access channel is established. Clearly, due to incorporation of channel estimation, the variations induced in the performance parameters (which include the interference received at the PR and the throughput at the SR) can lead to violation of the existing constraints. As a result, with the inclusion of channel estimation, the primary system observes an uncertainty in the interference. In order to combat this uncertain interference, outage constraints on the detection probability at the ST and on the interference power received at the PR are employed. Consequently, the performance of the HS in terms of the achievable secondary throughput is analyzed.

4.2.2 Estimation-Sensing-Throughput Tradeoff

The performance of the proposed framework that incorporates channel estimation is analyzed by considering a fundamental tradeoff between estimation time, sensing time and achievable throughput. This tradeoff is exploited to determine suitable estimation and sensing durations that achieve a maximum performance for the HS in terms of the secondary throughput. Again, the performance degradation in the HS is determined by comparing the proposed framework to those scenarios that consider perfect channel knowledge.

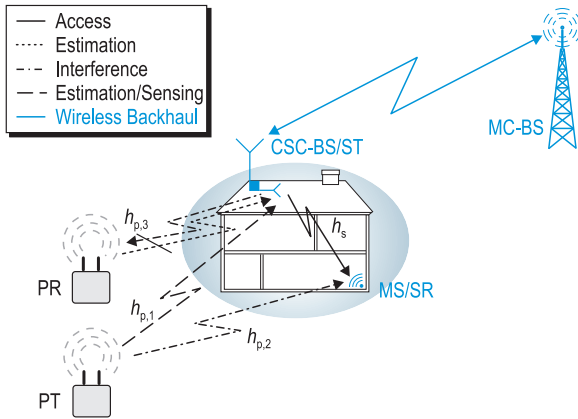


Figure 4.1: A cognitive small cell scenario demonstrating: (i) the hybrid paradigm, (ii) the associated network elements, which constitute Cognitive Small Cell-Base Station/Secondary Transmitter (CSC-BS/ST), Mobile Station/Secondary Receiver (MS/SR), Macro Cell-Base Station (MC-BS) and Primary Transmitter (PT), (iii) the interacting channels: sensing ($h_{p,1}$), interference ($h_{p,2}$, $h_{p,3}$) and access (h_s) channels.

4.3 System Model

4.3.1 Hybrid Scenario and Medium Access

The CSC deployment is transformed into a hybrid scenario, by which the CSC-BS and the MS represent the ST and the SR, respectively. The spectrum sensing and the power control mechanisms are employed at the CSC-BS. As an extension to the existing models depicted in [36, 41], a slotted medium access for the HS, where the time axis is segmented into frames of length T is considered. Following this frame structure, the ST employs periodic sensing, where each frame consists of a sensing time interval τ_{sen} followed by data transmission ($T - \tau_{\text{sen}}$). Depending on the outcome of the sensing, the data transmission takes place with or without power control.

4.3.2 Signal Model

As illustrated in Chapter 2 the primary and the secondary systems employ OFDM to carry out their transmissions. As a result, OFDM signals transmitted by the primary system are modelled as zero mean Gaussian signals by the secondary system.

Subject to the underlying hypothesis, illustrating the presence \mathcal{H}_1 and the absence \mathcal{H}_0 of the primary signal, the discrete and complex received signal at the ST is given by

$$y_{\text{ST}}[n] = \begin{cases} h_{\text{p},1} \cdot x_{\text{PT}}[n] + w_{\text{ST}}[n] & : \mathcal{H}_1 \\ w_{\text{ST}}[n] & : \mathcal{H}_0 \end{cases}, \quad (4.1)$$

where $x_{\text{PT}}[n]$ corresponds to a discrete and complex sample transmitted by the PT, $|h_{\text{p},1}|^2$ represents the power gain of the sensing channel for a given frame and $w_{\text{ST}}[n]$ is circularly symmetric AWGN at the ST. In accordance to the Gaussian signal model, the mean and variance for the signal and the noise are determined as: $\mathbb{E}[x_{\text{PT}}[n]] = 0$, $\mathbb{E}[w_{\text{ST}}[n]] = 0$, $\mathbb{E}[|x_{\text{PT}}[n]|^2] = P_{\text{Tx,PT}} = \sigma_s^2$ and $\mathbb{E}[|w_{\text{ST}}[n]|^2] = \sigma_w^2$.

Following the conventional frame structure, the ST performs periodic sensing for a duration of τ_{sen} . The test statistics $\mathbf{T}(\mathbf{y})$ at the ST – evaluated in (2.3), cf. Chapter 2 – represents a random variable, whereby the characterization of the cdf depends on the underlying hypothesis. With regard to the Gaussian signal model, $\mathbf{T}(\mathbf{y})$ follows a central chi-squared (χ^2) distribution for both hypotheses \mathcal{H}_0 and \mathcal{H}_1 [73]. In this regard, the detection probability and false alarm probability are characterized in (2.4) and (2.5), respectively, cf. Chapter 2.

Similar to (4.1), the discrete and complex received signal at the SR conditioned on the sensing outcome is given by

$$y_{\text{SR}}[n] = \begin{cases} h_s \cdot x_{\text{ST}}[n] + h_{\text{p},2} \cdot x_{\text{PT}}[n] + w_{\text{SR}}[n] & : 1 - \text{P}_d \\ h_s \cdot x_{\text{ST}}[n] + w_{\text{SR}}[n] & : 1 - \text{P}_{\text{fa}} \\ h_s \cdot x_{\text{ST,cont}}[n] + h_{\text{p},2} \cdot x_{\text{PT}}[n] + w_{\text{SR}}[n] & : \text{P}_d \\ h_s \cdot x_{\text{ST,cont}}[n] + w_{\text{SR}}[n] & : \text{P}_{\text{fa}} \end{cases}, \quad (4.2)$$

where $x_{\text{ST}}[n]$ and $x_{\text{ST,cont}}[n]$ present the discrete and complex samples with full transmit power $P_{\text{Tx,ST}}$ and controlled transmit power $P_{\text{Tx,ST,cont}}$, respectively. $w_{\text{SR}}[n]$ is circularly symmetric AWGN at the SR, with variance $\mathcal{CN}(0, \sigma_w^2)$.

Additionally, $|h_s|^2$ and $|h_{p,2}|^2$ represent the power gains for the access and the interference channels, cf. Figure 4.1.

Besides that, an interference signal from the ST is encountered at the PR across the channel $h_{p,3}$. This situation clearly happens only when the PT is transmitting, i.e., $(1 - P_d, P_d)$, cf. (4.2). In this regard, the received signal at the PR is given by

$$y_{\text{PR}}[n] = \begin{cases} h_{p,3} \cdot x_{\text{ST,cont}}[n] + w_{\text{PR}}[n] & : P_d \\ h_{p,3} \cdot x_{\text{ST}}[n] + w_{\text{PR}}[n] & : 1 - P_d \end{cases}, \quad (4.3)$$

where $w_{\text{PR}}[n]$ is circularly symmetric AWGN at the PR, with $\mathcal{CN}(0, \sigma_w^2)$.

4.3.3 Problem Description

To employ a power control mechanism, the ST is required to control its transmit power in such a way that the interference power received at the PR is below a certain interference threshold (θ_1). In reference to the HS, constraints on interference power received (corresponding to P_d and $1 - P_d$) at the PR are defined as

$$\mathbb{P}(\mathcal{H}_1) \cdot P_d \cdot |h_{p,3}|^2 P_{\text{Tx,ST,cont}} \leq \theta_1 \quad (4.4)$$

and

$$\mathbb{P}(\mathcal{H}_1) \cdot (1 - P_d) \cdot |h_{p,3}|^2 P_{\text{Tx,ST}} \leq \theta_1, \quad (4.5)$$

where $\mathbb{P}(\mathcal{H}_1) (= 1 - \mathbb{P}(\mathcal{H}_0))$ represents the occurrence probability of the hypothesis \mathcal{H}_1 . According to [41], (4.5) is usually handled by the regulatory bodies. In this regard, using (4.4) and the knowledge of θ_1 , the controlled power is computed as $\frac{\theta_1}{\mathbb{P}(\mathcal{H}_1) \cdot P_d \cdot |h_{p,3}|^2}$.

Next, the throughput received at the SR, corresponding to the cases illustrated in (4.2), is characterized. Subject to the sensing outcome $1 - P_{\text{fa}}, 1 - P_d, P_{\text{fa}}, P_d$, the corresponding throughputs at the SR are defined as

$$R_0(\tau_{\text{sen}}) = \frac{T - \tau_{\text{sen}}}{T} \cdot \overbrace{\log_2 \left(1 + |h_s|^2 \frac{P_{\text{Tx,ST}}}{\sigma_w^2} \right)}^{C_0} \cdot (1 - P_{\text{fa}}) \cdot \mathbb{P}(\mathcal{H}_0), \quad (4.6)$$

$$R_1(\tau_{\text{sen}}) = \frac{T - \tau_{\text{sen}}}{T} \cdot \overbrace{\log_2 \left(1 + \frac{|h_s|^2 P_{\text{Tx,ST}}}{|h_{p,2}|^2 P_{\text{Tx,PT}} + \sigma_w^2} \right)}^{C_1} \cdot (1 - P_d) \cdot \mathbb{P}(\mathcal{H}_1), \quad (4.7)$$

$$R_2(\tau_{\text{sen}}) = \frac{T - \tau_{\text{sen}}}{T} \cdot \overbrace{\log_2 \left(1 + |h_s|^2 \frac{P_{\text{Tx,ST,cont}}}{\sigma_w^2} \right)}^{C_2} \cdot P_{\text{fa}} \cdot \mathbb{P}(\mathcal{H}_0), \quad (4.8)$$

$$R_3(\tau_{\text{sen}}) = \frac{T - \tau_{\text{sen}}}{T} \cdot \overbrace{\log_2 \left(1 + \frac{|h_s|^2 P_{\text{Tx,ST,cont}}}{|h_{p,2}|^2 P_{\text{Tx,PT}} + \sigma_w^2} \right)}^{C_3} \cdot P_d \cdot \mathbb{P}(\mathcal{H}_1), \quad (4.9)$$

where C_0, C_1, C_2 and C_3 represent the data rates.

In order to highlight the relationship between the detector's performance (sensing time) and the secondary throughput, which characterize the performance of the HS, Sharma *et al.* [41] established a sensing-throughput tradeoff subject to a target detection probability (\bar{P}_d) and the interference constraint, defined in (4.4). This tradeoff is represented as

$$R_s(\tilde{\tau}_{\text{sen}}) = \max_{\tau_{\text{sen}}} R_s(\tau_{\text{sen}}) \quad (4.10)$$

$$\begin{aligned} &= R_0(\tau_{\text{sen}}) + R_1(\tau_{\text{sen}}) + R_2(\tau_{\text{sen}}) + R_3(\tau_{\text{sen}}) \\ &\text{s.t. } P_d \geq \bar{P}_d, \\ &\text{s.t. (4.4).} \end{aligned} \quad (4.11)$$

As a consequence, the tradeoff depicted in (4.10) determines a suitable sensing time $\tilde{\tau}_{\text{sen}}$ that achieves the maximum secondary throughput. However, the system model depicted above has the following fundamental issues:

- Without the knowledge of the received power (sensing channel, $h_{p,1}$), the characterization of P_d is not possible, consider Chapter 2, (2.4). This leaves the constraint defined in (4.11) inappropriate.
- Without the knowledge of the interference channel towards the PR ($h_{p,3}$), the power control mechanism cannot be employed at the ST.
- Along with the above mentioned channels, the knowledge of the access (h_s) and interference channel ($h_{p,2}$) is required at the ST for characterizing the throughput at the SR.

With these issues, it is not reasonable to consider the performance analysis depicted by the ideal model (described as the baseline model) for hardware

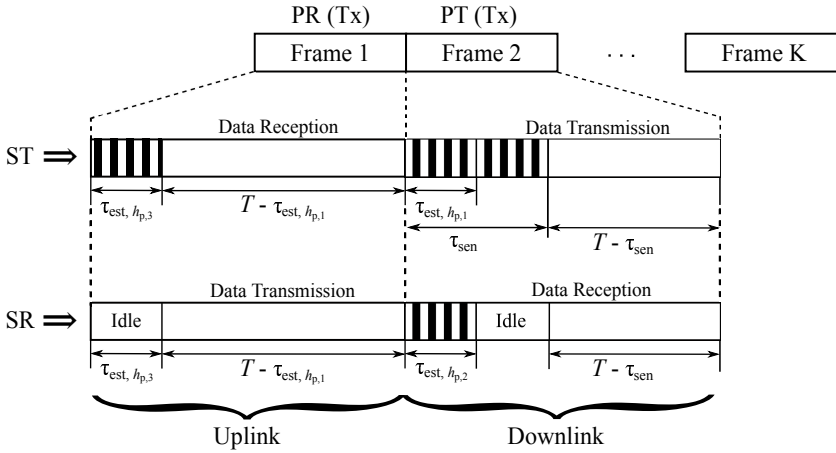


Figure 4.2: Frame structure of HSs illustrating the time allocation for channel estimation, sensing and data transmission from the perspective of a ST and a SR.

implementation. In order to address these issues, an analytical framework that includes the estimation of these channels, and characterizes the performance of the HS, is proposed in this chapter.

4.4 Proposed Approach

4.4.1 Frame Structure

In order to incorporate the estimation of the involved channels, a novel frame structure is proposed in Figure 4.2, according to which $\tau_{\text{est}, h_{p,1}}$ and $\tau_{\text{est}, h_{p,2}}$ are utilized for estimating $h_{p,1}$ and $h_{p,2}$ by the ST and the SR², respectively. Besides that, $\tau_{\text{est}, h_{p,3}}$ is used for estimating $h_{p,3}$. Also, the ST considers the estimation based on the pilot symbols transmitted by the SR.

Apart from this, it is possible that the time interval between two control-based transmissions is large as compared to T . Under such conditions, the frame

²In order to accomplish this, it is assumed that both the ST and the SR align themselves to the control-based transmission from the PT.

structure followed by the secondary system can be adapted from the one proposed in Figure 4.2 in such a way that channel estimation is restricted to particular frames and the remaining frames follow the conventional structure, i.e., sensing followed by data transmission. Hence, the proposed frame structure presents a general framework, and can be adapted to different control-based configurations followed by various primary systems. For scenarios, where the PT and the PR represent a single entity, i.e., interchangeably act as transmitter and receiver, the first two slots $\tau_{\text{est}, h_{p,1}}$ and $\tau_{\text{est}, h_{p,3}}$ of the ST can be combined into one, cf. Figure 4.2.

4.4.2 Channel Estimation

Here, the estimation of the interacting channels is revisited. In this chapter, a similar approach for the channel estimation to the one described in Chapter 2 and Chapter 3, according to which it is logical to employ a received power-based estimation for the sensing and the interference channels, and a pilot-based estimation for the access channel. In addition, with regard to the Gaussian signal model, the characterization of the channel estimation is in accordance to the one considered in Chapter 2. With the purpose of maintaining the continuity of the analysis, the channel estimation concerning the involved channel is briefly summarized below.

Estimation of Sensing Channel ($h_{p,1}$)

The ST estimates the sensing channel by estimating the power received from the PT during $\tau_{\text{est}, h_{p,1}}$. With $\tau_{\text{est}, h_{p,1}} f_s$ samples used for estimation, the estimated received power

$$\hat{P}_{\text{Rx,ST},h_{p,1}} = \sum_{n=1}^{\tau_{\text{est}, h_{p,1}} f_s} |h_{p,1} \cdot x_{\text{PT}}[n] + w_{\text{ST}}[n]|^2 \quad (4.12)$$

follows a χ^2 distribution. The cdf of $\hat{P}_{\text{Rx,ST},h_{p,1}}$ is characterized as

$$F_{\hat{P}_{\text{Rx,ST},h_{p,1}}}(x) = 1 - \Gamma\left(\frac{\tau_{\text{est}, h_{p,1}} f_s}{2}, \frac{\tau_{\text{est}, h_{p,1}} f_s x}{2P_{\text{Rx,ST},h_{p,1}}}\right). \quad (4.13)$$

In order to improve the detector's performance, the samples $f_s \tau_{\text{est}, h_{p,1}}$ considered for the estimation can also be utilized for the sensing $f_s \tau_{\text{sen}}$ as illustrated

in Figure 4.2. In this sense, hereafter, the characterization of the detector incurs the estimation time interval $\tau_{\text{est}, h_{p,1}}$.

Estimation of Access Channel (h_s)

The pilot signal received from the SR undergoes matched filtering and demodulation at the ST, hence, a pilot-based estimation at the ST is employed to acquire the knowledge of the access channel. As a result, \hat{h}_s conditioned on h_s follows a circularly symmetric Gaussian distribution $\hat{h}_s|h_s \sim \mathcal{CN}\left(h_s, \frac{\sigma_w^2}{N_s}\right)$.

Consequently, the estimated power gain $|\hat{h}_s|^2$ follows a non-central chi-squared $\mathcal{X}'^2(\lambda_s, 2)$ distribution with 2 degrees of freedom and non-centrality parameter $\lambda_s = \frac{N_s|h_s|^2}{\sigma_w^2}$. Following Approximation 1 from Chapter 2, the cdf of $|\hat{h}_s|^2$ is characterized as

$$F_{|\hat{h}_s|^2}(x) \approx 1 - \Gamma\left(a_s, \frac{x}{b_s}\right), \quad (4.14)$$

$$\text{where } a_s = \frac{(2 + \lambda_s)^2}{4 + 4\lambda_s} \text{ and } b_s = \frac{\sigma_w^2(4 + 4\lambda_s)}{(2 + \lambda_s)}. \quad (4.15)$$

Estimation of Interference Channel ($h_{p,2}$)

Besides the access channel, the knowledge of the interference channel to the SR from the PT is required for determining the secondary throughput. It is worthy to note that the expression $|h_{p,2}|^2 P_{\text{Tx},\text{PT}} + \sigma_w^2$ in R_1 and R_3 , cf. (4.7) and (4.9), which corresponds to the interference and the noise power, represents $P_{\text{Rx},\text{SR}}$. Hence, by estimating $\hat{P}_{\text{Rx},\text{SR}}$, it is possible to jointly characterize the interference and the noise power, and consequently characterize R_1 and R_3 . In this view, the SR estimates the received power by listening to the control-based transmissions from the PT, cf. Figure 4.2. Similar to the sensing channel, the cdf of the estimated interference power $\hat{P}_{\text{Rx},\text{SR}}$ at the ST is characterized as

$$F_{\hat{P}_{\text{Rx},\text{SR}}}(x) = 1 - \Gamma\left(\frac{\tau_{\text{est}, h_{p,2}} f_s}{2}, \frac{\tau_{\text{est}, h_{p,2}} f_s x}{2P_{\text{Rx},\text{SR}}}\right). \quad (4.16)$$

Estimation of Interference Channel ($h_{p,3}$)

Lastly, the estimation of the interference channel between the ST and the PR is essential for employing power control at the ST. Like the sensing channel, the ST estimates $|h_{p,3}|^2$ by listening to the control-transmission from the PR. The cdf of the received power estimated from $\tau_{\text{est}}, h_{p,3} f_s$ samples is given by

$$F_{\hat{P}_{\text{Rx,ST},h_{p,3}}}^{-1}(x) = 1 - \Gamma\left(\frac{\tau_{\text{est}}, h_{p,3} f_s}{2}, \frac{\tau_{\text{est}}, h_{p,3} f_s x}{2P_{\text{Rx,ST},h_{p,3}}}\right). \quad (4.17)$$

4.4.3 Characterization of Performance Parameters

It is clear that the estimation of the involved channels translates to the variations in the performance parameters, which include detection probability \hat{P}_d at the ST, power received $\hat{P}_{\text{Rx,PR}}$ at the PR and secondary throughput \hat{R}_s at the SR. In particular, the variation, due to the estimation of \hat{P}_d and $\hat{P}_{\text{Rx,PR}}$, leads to the uncertain interference at the primary system, thus seriously degrading the performance of the HS. Such an aspect concerning the uncertain interference has been left aside in the outage constraints (please consider, (4.4) and (4.5)), depicted by the ideal model. This renders the existing constraints defined by the ideal model inaccurate.

Motivated by this fact, the uncertain interference is captured by proposing new outage constraints ρ_d and ρ_{cont} on estimated detection probability (\hat{P}_d) and estimated power received at PR ($\hat{P}_{\text{Rx,PR}}$), respectively, as PU constraints for the HS. These constraints are defined as

$$\mathbb{P}(\hat{P}_d \leq \bar{P}_d) \leq \rho_d, \quad (4.18)$$

$$\mathbb{P}(\hat{P}_{\text{Rx,PR}} \geq \theta_1) \leq \rho_{\text{cont}}. \quad (4.19)$$

In contrast to the ideal model, which captures the interference received individually for the corresponding sensing outcomes: P_d and $1 - P_d$, refer to (4.4) and (4.5), the proposed framework considers an outage over the two constraints jointly (by combining the corresponding sensing outcomes P_d and $1 - P_d$) in terms of the aggregate interference power received at the PR. In this regard,

(4.19) is expanded as

$$\mathbb{E}_{\hat{P}_d} \left[\mathbb{P} \left(\mathcal{H}_1 \cdot \overbrace{\left(\frac{\hat{P}_{\text{Rx,ST},h_{p,3}} - \sigma_w^2}{\sigma_s^2} \right)}^{|h_{p,3}|^2} \times ((1 - \hat{P}_d)P_{\text{Tx,ST}} + \hat{P}_d P_{\text{Tx,ST,cont}}) \geq \theta_I \right) \right] \leq \rho_{\text{cont}}, \quad (4.20)$$

where $\mathbb{E}_{\hat{P}_d} [\cdot]$ and $\mathbb{P}(\cdot)$ (that represents the cdf of $\hat{P}_{\text{Rx,PR}}$) capture the variations due to \hat{P}_d and $\hat{P}_{\text{Rx,PR}}$, respectively.

To proceed further, the cdf of \hat{P}_d , $\hat{P}_{\text{Rx,PR}}$ and \hat{R}_s are characterized. This is done by transforming the cdfs of the estimated parameters, characterized previously in (4.13), (4.14), (4.16) and (4.17). To begin, the cdf of the \hat{P}_d is evaluated to characterize the constraint on the detection probability defined in (4.18).

Lemma 10 The cdf of P_d is characterized as (refer to Section 2.7.3 in Chapter 2 for the solution)

$$F_{\hat{P}_d}(x) = 1 - \Gamma \left(\frac{\tau_{\text{est}, h_{p,1}} f_s}{2}, \frac{\tau_{\text{est}, h_{p,1}} f_s \tau_{\text{sen}} f_s \mu}{4P_{\text{Rx,ST},h_{p,1}} \Gamma^{-1} \left(\frac{\tau_{\text{sen}}}{2}, x \right)} \right). \quad (4.21)$$

Along with $F_{\hat{P}_d}(\cdot)$, defined in (4.21), the cdf of the $\hat{P}_{\text{Rx,PR}}$ is necessary to characterize the outage constraint defined in (4.19).

Lemma 11 The cdf of $\hat{P}_{\text{Rx,PR}}$ is characterized as

$$F_{\hat{P}_{\text{Rx,PR}}}(x) = \int_0^1 \Gamma \left(\frac{\tau_{\text{est}, h_{p,3}} f_s}{2}, \left(\frac{x \sigma_s^2}{h_{p,1} \cdot ((1 - P_d)P_{\text{Tx,ST}} + P_d P_{\text{Tx,ST,cont}})} + \sigma_w^2 \right) \times \frac{\tau_{\text{est}, h_{p,3}} f_s}{2P_{\text{Rx,ST},h_{p,3}}} \right) dF_{\hat{P}_d}. \quad (4.22)$$

Besides that, since the variations in \hat{P}_d , $\hat{P}_{\text{Rx,ST},h_{p,1}}$, $|\hat{h}_s|^2$ and $\hat{P}_{\text{Rx,ST},h_{p,3}}$ translate to the variations in \hat{R}_s , these variations are captured in terms of the expected secondary throughput. More specifically, the variations in $\hat{P}_{\text{Rx,ST},h_{p,1}}$, $|\hat{h}_s|^2$ and

$\hat{P}_{\text{Rx,ST},b_{p,3}}$ result in variations in the data rates C_0 , C_1 , C_2 and C_3 , characterized in (4.6), (4.7), (4.8) and (4.9), respectively. In this view, the pdfs for \hat{C}_0 , \hat{C}_1 , \hat{C}_2 and \hat{C}_3 are characterized in the following Lemmas.

Lemma 12 The pdf of \hat{C}_0 is defined as (refer to (2.25) in Chapter 2)

$$f_{\hat{C}_0}(x) = 2^x \ln 2 \frac{(2^x - 1)^{a_{p,0}-1} \exp\left(-\frac{2^x - 1}{b_{p,0}}\right)}{\Gamma(a_{p,0})b_{p,0}^{a_{p,0}}}, \quad (4.23)$$

$$\text{where } a_{p,0} = a_s \text{ and } b_{p,0} = \frac{P_{\text{Tx,ST}}}{\sigma_w^2} b_s, \quad (4.24)$$

whereas a_s and b_s are defined in (4.15).

Lemma 13 The pdf of \hat{C}_1 is defined as (refer to 2.27 in Chapter 2)

$$f_{\hat{C}_1}(x) = 2^x \ln 2 \frac{(2^x - 1)^{a_{p,0}-1} \Gamma(a_{p,0} + a_{p,1})}{\Gamma(a_{p,0})\Gamma(a_{p,1})b_{p,0}^{a_{p,0}}b_{p,1}^{a_{p,1}}} \left(\frac{1}{b_{p,1}} + \frac{2^x - 1}{b_{p,0}} \right), \quad (4.25)$$

$$\text{where } a_{p,1} = \frac{\tau_{\text{est}} f_s}{2} \text{ and } b_{p,1} = \frac{2P_{\text{Rx,SR}}}{\sigma_w^2 \tau_{\text{est}} f_s}, \quad (4.26)$$

and $a_{p,0}$, $b_{p,0}$ are defined in (4.24).

Following the characterization of the pdfs for \hat{C}_0 and \hat{C}_1 , the pdfs for \hat{C}_2 and \hat{C}_3 can be obtained by substituting the controlled transmit power ($P_{\text{Tx,ST,cont}}$) for full transmit power ($P_{\text{Tx,ST}}$) in (4.23) and (4.25).

Lemma 14 The pdf of \hat{C}_2 is defined as

$$f_{\hat{C}_2}(x) = 2^x \ln 2 \frac{(2^x - 1)^{a_{p,2}-1} \exp\left(-\frac{2^x - 1}{b_{p,2}}\right)}{\Gamma(a_{p,2})b_{p,2}^{a_{p,2}}}, \quad (4.27)$$

$$\text{where } a_{p,2} = a_s \text{ and } b_{p,2} = \frac{P_{\text{Tx,ST,cont}}}{\sigma_w^2} b_s, \quad (4.28)$$

whereas a_s and b_s are defined in (4.15).

Lemma 15 The pdf of \hat{C}_3 is defined as

$$f_{\hat{C}_3}(x) = 2^x \ln 2 \frac{(2^x - 1)^{a_{p,2}-1} \Gamma(a_{p,2} + a_{p,1})}{\Gamma(a_{p,2}) \Gamma(a_{p,1}) b_{p,2}^{a_{p,2}} b_{p,1}^{a_{p,1}}} \left(\frac{1}{b_{p,1}} + \frac{2^x - 1}{b_{p,2}} \right), \quad (4.29)$$

where the parameters $a_{p,1}$, $b_{p,1}$ and $a_{p,2}$, $b_{p,2}$ are defined in (4.26) and (4.28), respectively.

As a result, the expected secondary throughput is given by

$$\begin{aligned} \mathbb{E}_\Omega [R_s(\tau_{\text{sen}})] = & \frac{T - \tau_{\text{est}, h_{p,3}} - \tau_{\text{sen}}}{T} \left[(1 - P_{\text{fa}}) \cdot \mathbb{P}(\mathcal{H}_0) \cdot \mathbb{E}_{\hat{C}_0} [\hat{C}_0] + \right. \\ & (1 - \mathbb{E}_{\hat{P}_d} [\hat{P}_d]) \cdot \mathbb{P}(\mathcal{H}_1) \cdot \mathbb{E}_{\hat{C}_1} [\hat{C}_1] + P_{\text{fa}} \cdot \mathbb{P}(\mathcal{H}_0) \cdot \mathbb{E}_{\hat{C}_2} [\hat{C}_2] + \\ & \left. \mathbb{E}_{\hat{P}_d} [\hat{P}_d] \cdot \mathbb{P}(\mathcal{H}_1) \cdot \mathbb{E}_{\hat{C}_3} [\hat{C}_3] \right], \quad (4.30) \end{aligned}$$

where $\mathbb{E}_\Omega [\cdot]$ denotes the expectation over Ω , where $\Omega \in \{\hat{P}_d, \hat{C}_0, \hat{C}_1, \hat{C}_2, \hat{C}_3\}$. The random variables \hat{P}_d and \hat{C}_1, \hat{C}_3 are functions of independent random variables $\hat{P}_{\text{Rx,ST}}$ and, $|\hat{h}_s|^2$ and $\hat{P}_{\text{Rx,SR}}$, respectively. In this context, the independence property is applied to carry out the expectation on \hat{P}_d , \hat{C}_1 and \hat{C}_3 in (4.30), separately.

4.4.4 Estimation-Sensing-Throughput Tradeoff

Herein, with regard to the proposed framework (estimation model) for the HS, a fundamental relation between estimation time (regulating the variations in the detection probability and interference power received at the PR according to the PU constraint), sensing time (characterizing the detector's performance) and secondary throughput is established. This relationship is characterized as an estimation-sensing-throughput tradeoff. Based on this tradeoff, suitable estimation and suitable sensing time intervals are determined, resulting in an optimum performance for the HS in terms of the achievable secondary throughput.

Problem 7 The achievable expected secondary throughput subject to an outage constraint on detection probability at the ST and an outage constraint on

the interference power at the PR, is given by

$$R_s(\tilde{\tau}_{\text{est}}, h_{p,1}, \tilde{\tau}_{\text{est}}, h_{p,2}, \tilde{\tau}_{\text{est}}, h_{p,3}, \tilde{\tau}_{\text{sen}}) = \max_{\tau_{\text{est}}, h_{p,1}, \tau_{\text{est}}, h_{p,2}, \tau_{\text{est}}, h_{p,3}, \tau_{\text{sen}}, P_{\text{Tx,ST,cont}}} \mathbb{E}_{\Omega} [R_s(\tau_{\text{sen}})] \quad (4.31)$$

s.t. (4.18), (4.20).

Solution: In order to solve the constrained optimization problem, the following assumptions are considered: (i) for the simplicity of the analysis, the estimation times $(\tau_{\text{est}}, h_{p,1}, \tau_{\text{est}}, h_{p,2}, \tau_{\text{est}}, h_{p,3})$ are optimized jointly, i.e., $\tau_{\text{est}}, h_{p,1} = \tau_{\text{est}}, h_{p,2} = \tau_{\text{est}}, h_{p,3}$, (ii) it is assumed that the primary system attains sufficient protection when high detection probability is achieved by the ST. In this sense, it is reasonable to consider first the constraint on the detection probability with desired \bar{P}_d and ρ_d , cf. (4.18).

These assumptions are used to obtain an expression of μ (refer to (2.52) in Chapter 2)

$$\mu \geq \frac{4P_{\text{Rx,ST},h_{p,1}} \Gamma^{-1} \left(1 - \rho_d, \frac{\tau_{\text{est}}, h_{p,1} f_s}{2} \right) \Gamma^{-1} \left(\bar{P}_d, \frac{\tau_{\text{sen}} f_s}{2} \right)}{\tau_{\text{est}}, h_{p,1} \tau_{\text{sen}} (f_s)^2}. \quad (4.32)$$

Next, using the constraint (4.20), the controlled transmit power at the SR is determined as

$$\mathbb{E}_{\hat{P}_d} \left[F_{\hat{P}_{\text{Rx,PR}}}(\hat{P}_d, \theta_I) \right] \geq \rho_{\text{cont}}. \quad (4.33)$$

Solving numerically (4.33) yields $P_{\text{Tx,ST,cont}}$ for the HS. Finally, by substituting μ and $P_{\text{Tx,ST,cont}}$ (computed in (4.33) and (4.32)), and using the pdfs of \hat{P}_d , \hat{C}_0 , \hat{C}_1 , \hat{C}_2 and \hat{C}_3 (determined in Lemma 10, Lemma 12, Lemma 13, Lemma 14 and Lemma 15), an expression of R_s as a function of $\tau_{\text{est}}, h_{p,1}$, $\tau_{\text{est}}, h_{p,2}$, $\tau_{\text{est}}, h_{p,3}$ and τ_{sen} is determined, cf. (4.30). Solving numerically, R_s delivers $\tilde{\tau}_{\text{est}}, h_{p,1}$, $\tilde{\tau}_{\text{est}}, h_{p,2}$, $\tilde{\tau}_{\text{est}}, h_{p,3}$ and $\tilde{\tau}_{\text{sen}}$ that achieves the maximum expected secondary throughput.

4.5 Numerical Analysis

In this section, the performance of the proposed approach is evaluated. In this view, simulations are performed: (i) to validate the expressions obtained in the previous section, (ii) to analyze the performance loss incurred due to

Table 4.1: Parameters for Numerical Analysis

Parameter	Value
f_s	1 MHz
T	100 ms
$\tau_{\text{est}, h_{p,1}}$	1 ms
$\tau_{\text{est}, h_{p,2}}$	1 ms
$\tau_{\text{est}, h_{p,3}}$	1 ms
$ h_{p,1} ^2$	-120 dB
$ h_{p,2} ^2$	-120 dB
$ h_{p,3} ^2$	-100 dB
$ h_s ^2$	-80 dB
θ_1	-110 dBm
$P_{\text{Tx,PT}} = P_{\text{Tx,PR}}$	0 dBm
$P_{\text{Tx,ST}}$	-10 dBm
ρ_{cont}	0.1
ρ_d	0.1
σ_w^2	100 dBm
N_s	10

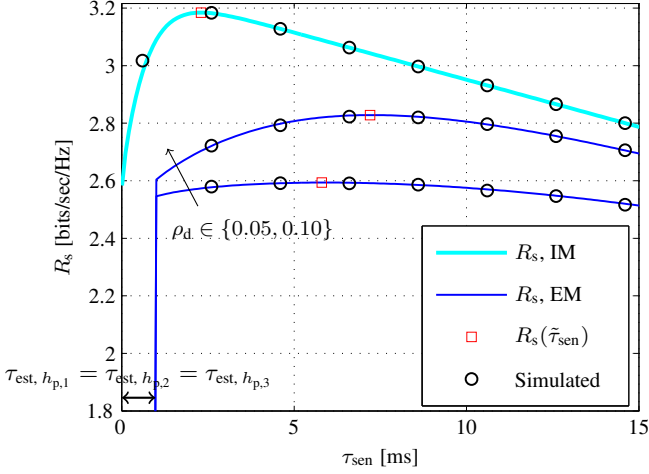


Figure 4.3: Sensing-throughput tradeoff for the Ideal Model (IM) and Estimation Model (EM) for $\tau_{\text{est}, h_{p,1}} = \tau_{\text{est}, h_{p,2}} = \tau_{\text{est}, h_{p,3}} = 1$ ms.

the time allocation for the estimation and the imperfect channel knowledge. In order to illustrate the performance degradation, the ideal model is considered to benchmark the performance of the proposed approach. Unless stated explicitly, the choice of parameters given in Table 4.1 is considered for analysis.

First the performance of the HS is analyzed in terms of a sensing-throughput tradeoff corresponding to the Ideal Model (IM) and Estimation Model (EM) by fixing $\tau_{\text{est}, h_{p,1}} = \tau_{\text{est}, h_{p,2}} = \tau_{\text{est}, h_{p,3}} = 1$ ms, cf. Figure 4.3. With the inclusion of channel estimation in the frame structure, the ST procures no throughput at the SR for the interval $\tau_{\text{est}, h_{p,1}}$. As indicated by the margin between the IM and the EM, a certain performance degradation is witnessed by the EM due to the incorporation of channel estimation. Moreover, the sensing-throughput tradeoff yields a suitable sensing time $\tilde{\tau}_{\text{sen}}$ that achieves the maximum performance in terms of the secondary throughput $R_s(\tilde{\tau}_{\text{sen}})$. Hereafter, the theoretical expressions are considered for the analysis. In addition, the proposed EM operates at the suitable sensing time.

Following the previous discussions, it is well-known that the combination of interweave and underlay systems is intended to enhance the performance of the HS. Hence, it is worthy to acquire insights on the performance gain in terms of the achievable secondary throughput due to the association of the underlay and

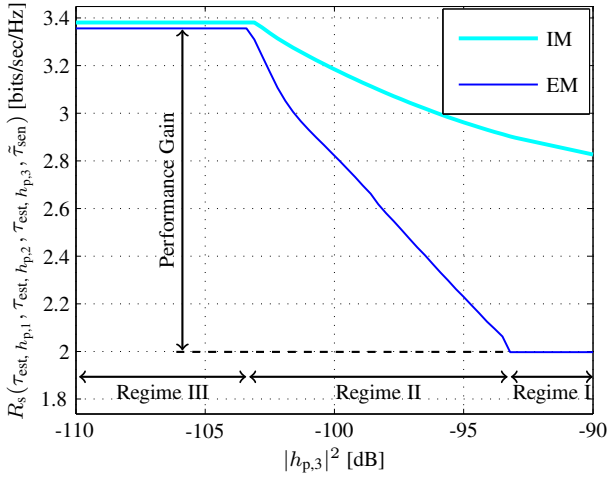


Figure 4.4: Achievable secondary throughput versus interference channel gain $|h_{p,3}|^2$, where the system is operating at $\tilde{\tau}_{\text{sen}}$ and the estimation time is fixed to $\tau_{\text{est}, h_{p,1}} = \tau_{\text{est}, h_{p,2}} = \tau_{\text{est}, h_{p,3}} = 1$ ms.

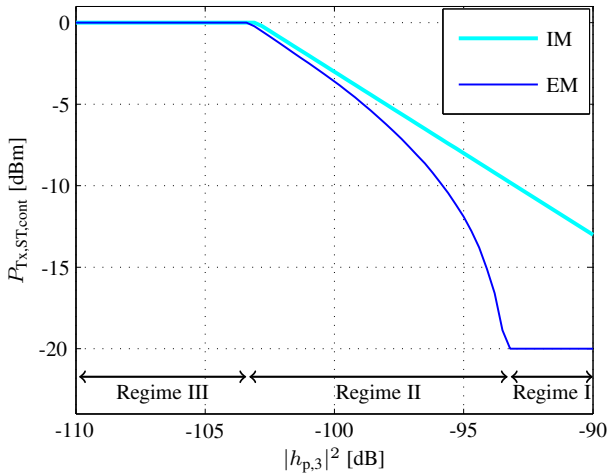


Figure 4.5: Optimum power control versus path loss $|h_{p,3}|^2$, where the system is operating at $\tilde{\tau}_{\text{sen}}$ and the estimation time is fixed to $\tau_{\text{est}, h_{p,1}} = \tau_{\text{est}, h_{p,2}} = \tau_{\text{est}, h_{p,3}} = 1$ ms.

the interweave techniques in the HS. In this regard, it is essential to observe the variation of the achievable secondary throughput corresponding to the interference channel from the ST to the PR, cf. Figure 4.1. Before proceeding with the analysis, it is essential to understand that the performance of the underlay system decreases with the increase in the channel gain $|h_{p,3}|^2$. To simplify the analysis, the channel gain $|h_{p,3}|^2 \in [-110, -90]$ dBm is categorized in three different regimes: (i) Regime I, (ii) Regime II and (iii) Regime III, cf. Figure 4.4.

Under Regime I, large channel gain $|h_{p,3}|^2 > -93$ dB results in a severe power control, causing the controlled power to fall below a certain level $P_{\text{Tx,ST,cont}} \leq -20$ dBm, please consider Figure 4.5. For the considered value of the channel gain $|h_s|^2 = -80$ dB over the access channel, such a low power transmission do not translate into an effective performance gain to the HS. As a result, no benefits are attained from the underlay system while operating in this regime. Conversely, the HS procures secondary throughput mainly by finding spectrum holes in the PU traffic, thereby operating as an IS. In contrast to that, the Regime II (-103 dB $< |h_{p,3}|^2 < -93$ dB) witnesses a significant performance gain as HS procures benefits from the US and the IS.

Moreover, below a certain channel gain $|h_{p,3}|^2 < -103$ dB (Regime III), it is observed that no performance gain is attained. This is due to the fact that the ST is limited by the maximum transmit power, i.e., beyond -103 dB, $P_{\text{Tx,ST,cont}}$ operates at $P_{\text{Tx,ST}}$, as illustrated in Figure 4.5. From this discussion, it can be concluded that the interference tolerance capability of the US and the detection capability of the IS incorporated by the HS can be transformed into significant performance gain only in situations where the channel gain between the ST and the PR falls within a certain range, for instance $|h_{p,3}|^2 \in [-103, -93]$ dBm for the considered case.

Besides maximizing the secondary throughput over the sensing time, it is interesting to observe the variation of the achievable throughput with the estimation time. As proposed in Problem 7, $\tau_{\text{est}, h_{p,1}} = \tau_{\text{est}, h_{p,2}} = \tau_{\text{est}, h_{p,3}}$ is considered for the analysis. Corresponding to the estimation model, Figure 4.6 reveals the estimation-sensing-throughput tradeoff. The existence of such a performance tradeoff in the system can be explained as follows, the variations due to the estimation of $|h_{p,1}|^2$ and $|h_{p,3}|^2$ causes variations in \hat{P}_d and $\hat{P}_{\text{Rx,PR}}$, captured using the outage constraints. As a result, a small increase in $\tau_{\text{est}, h_{p,1}}$ ($= \tau_{\text{est}, h_{p,2}} = \tau_{\text{est}, h_{p,3}}$) reduces the uncertain interference, allowing an increase in the controlled power at the ST, thus increasing the secondary throughput. However, upon increasing the estimation time beyond $\tilde{\tau}_{\text{est}, h_{p,1}}$

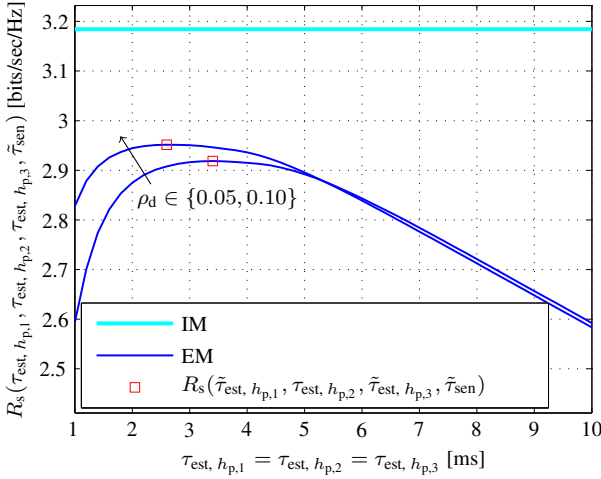


Figure 4.6: Achievable secondary throughput versus the estimation time $\tau_{\text{est}, h_{p,1}} = \tau_{\text{est}, h_{p,2}} = \tau_{\text{est}, h_{p,3}}$ operating at the suitable sensing time $\tilde{\tau}_{\text{sen}}$.

($= \tilde{\tau}_{\text{est}, h_{p,2}} = \tilde{\tau}_{\text{est}, h_{p,3}}$) slightly contributes to the performance improvement and largely consumes the time resources, leading to the performance degradation.

Moreover, it is noticed that performance degradation of the secondary system evaluated in terms of $R_s(\tau_{\text{est}, h_{p,1}} = \tau_{\text{est}, h_{p,2}} = \tau_{\text{est}, h_{p,3}}, \tilde{\tau}_{\text{sen}})$ becomes more sensitive to the estimation time $\tilde{\tau}_{\text{est}, h_{p,1}}$ ($= \tilde{\tau}_{\text{est}, h_{p,2}} = \tilde{\tau}_{\text{est}, h_{p,3}}$) as ρ_d decreases. From this analysis, it can be concluded that a suitable choice of estimation time becomes significant, specially for HSs, which are subjected to the aggressive policies imposed by the primary systems or the regulatory bodies.

To procure further insights, the variation of the detector's performance with the estimation time is analyzed. For the EM, it is observed that, for all values of the estimation time, expected detection probability stays strictly above \bar{P}_d , cf. Figure 4.7. This indicates that the proposed approach yields a reasonable performance of the detector incorporated in the HS. It is further noticed that the expected detection probability degrades slightly for low values of the estimation time. This is due to the fact that low values of $\tau_{\text{est}, h_{p,1}}$ shifts the probability mass of \hat{P}_d towards lower values, thus attaining a small value of its expectation.

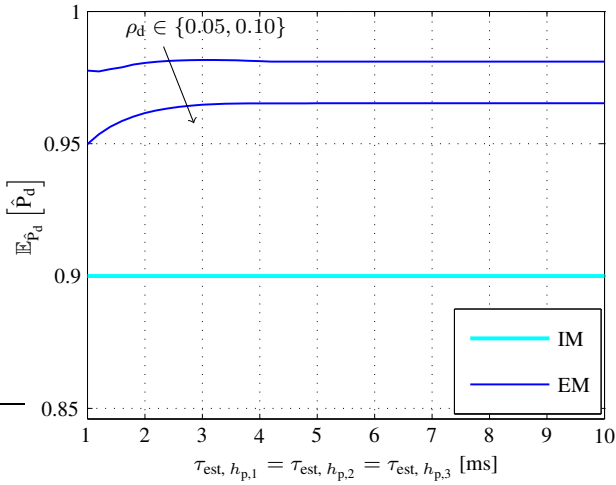


Figure 4.7: Expected detection probability versus $\tau_{\text{est}, h_{p,1}} = \tau_{\text{est}, h_{p,2}} = \tau_{\text{est}, h_{p,3}}$ operating at the suitable sensing time $\tilde{\tau}_{\text{sen}}$.

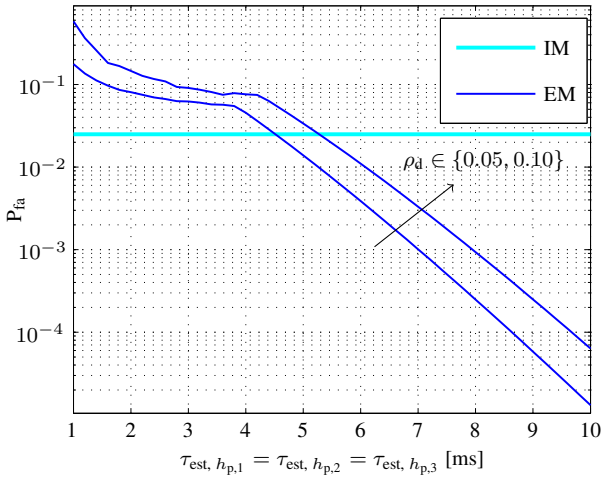


Figure 4.8: False alarm probability versus $\tau_{\text{est}, h_{p,1}} = \tau_{\text{est}, h_{p,2}} = \tau_{\text{est}, h_{p,3}}$ operating at the suitable sensing time $\tilde{\tau}_{\text{sen}}$.

Finally, the variation of P_{fa} along the estimation time is illustrated in Figure 4.8. From the HS's perspective, it is worthy to note that low P_{fa} is beneficial only if the HS procures its large contribution of the performance while operating in interweave mode, refer to (4.30). From Figure 4.8, it is noticed that the P_{fa} improves with estimation time, particularly $\tau_{est, h_{p,1}}$. It is important to note that the detector's performance is similar to one depicted by the ISs in Chapter 2, according to which the estimation time and the sensing time jointly control the variations due to the channel estimation and the performance of the detector. Beyond $\tilde{\tau}_{est, h_{p,1}}, \tilde{\tau}_{sen}$, the time resources contribute only to improve the detector's performance, therefore lead to the performance degradation. Because of the presence of the outage constraint on \hat{P}_d , an improvement in the detector's performance is observed by considering a reduction in P_{fa} , cf. Figure 4.8

4.6 Summary

In this chapter, the performance of cognitive radio as a hybrid system that exploits the benefits of both underlay and interweave paradigms from a deployment perspective is investigated. It has been argued that the lack of channels' knowledge renders the existing models unsuitable for the performance characterization. In this view, an analytical framework that incorporates channel estimation, and subsequently quantifies the performance of HSs in relation to imperfect channel knowledge has been established. More importantly, a fundamental tradeoff among the estimation time, sensing time and the secondary throughput is proposed that captures the effect of the channel estimation in terms of the time resources allocated for the channel estimation and the uncertain interference due to the imperfect knowledge of the involved channels. In this context, this tradeoff jointly characterizes the performance of the primary and the secondary systems.

In addition, while comparing the ideal scenario (those models that constitute the perfect channel knowledge) and the proposed model that employs channel estimation, it is clearly illustrated that the performance degradation due to the incorporation of the channel estimation can be effectively controlled by choosing to operate at the suitable estimation time and the suitable sensing time. In reference to the performed analysis, it is further depicted that the performance benefits procured by the HS, due to the association of the interweave and underlay systems, are largely influenced by the channel gain over the link ST-PR, which depicts the level of the interference received at the PR.

Chapter 5

Validation and Demonstration

Previous chapters (Chapter 2, Chapter 3 and Chapter 4) focused on characterizing the performance of different CR systems jointly in terms of the interference power received by the PR and the throughput at the SR by taking the estimation of the involved channels into account. In addition, it has been motivated that the low complexity and the versatility towards unknown primary user signals requirements, facilitating hardware deployment, can be satisfied only if conventional channel estimation techniques (such as pilot-based channel estimation) are substituted with non-conventional channel estimation techniques (such as received power-based estimation, proposed in the thesis) for acquiring the channels' knowledge, particularly for the channels between the primary and the secondary systems, corresponding to different systems. However, the aforementioned analysis in the previous chapters has been limited to the theoretical expressions.

With regard to the analytical expressions that are necessary for the performance analysis, it is essential as-well-as challenging to depict the hardware realizability of CR systems. Motivated by this fact, this chapter, which is based on [K7, K8], reconciles the theory established in the previous chapters and the hardware feasibility of the CSC. As a result, to a great extent, this chapter complements the performance analysis by deploying the CR techniques on a hardware. By doing this, the applicability of the assumptions considered while

deriving the analytical expressions can be examined. Moreover, these investigations facilitate the evolution of the proposed analytical framework. Without any specific argumentation, an US is considered for the deployment.

In this regard, this chapter provides the following contributions:

- Empirical validation: The performance of the USs in accordance to the received power-based estimation employed for the channel between the PR and the ST is validated by means of a hardware deployment. The variations (induced due to incorporation of channel estimation) in the system parameters are validated by comparing their probability density functions, obtained from the measurements, to those computed analytically. Moreover, the joint performance of the underlay system is validated in terms of an estimation-throughput tradeoff, proposed in Chapter 3.
- Demonstrator: Upon validating the theoretical expressions, a hardware demonstrator following the guidelines of an US is deployed. In this context, the applicability of the proposed framework in realistic scenarios is justified. Further, a graphical user interface is designed to procure insights on the operation of the demonstrator.

5.1 System Model

5.1.1 Model Simplifications

In contrast to the framework presented in Chapter 3, the following simplifications and modifications are considered for the hardware implementation.

- The channel estimation (received power-based) is only deployed for the link between the PR and the ST, which is associated with the interference received at the PR. In order to simplify the deployment, the interference from the PTs at the SR is neglected. Although the knowledge of the interference from the PTs is essential for characterizing the secondary throughput, the knowledge of the interference at the PR is critical for the imposition of the PU constraints. In addition, perfect knowledge of the

access channel between the ST and the SR that employs the pilot-based channel estimation is considered¹.

- The measurements taken to perform the validation, and the demonstration for the proposed deployment scenario consider the deterministic behaviour of the interference channel.
- As an alternative to the outage constraint, proposed in Chapter 3 for regulating the uncertain interference at the PR, a confidence probability constraint is employed for capturing the variations due to channel estimation around the interference temperature.
- Lastly, in contrast to the OFDM signal considered in Chapter 3, in this chapter all transmit signals (which include pilot and data signals) at the primary and the secondary systems are modeled as a constant power signal.

In accordance to these simplifications, the system model for the US depicted in Chapter 3 is slightly modified.

5.1.2 Underlay Scenario and Medium Access

In accordance with Chapter 3, the channels between the PR and the ST and between the ST and SR are designated as the interference and the access channels with channel gains $h_{p,3}$ and h_s , respectively. A power control mechanism is employed at the ST to ensure that interference received at the PR is below a certain level. In order to exercise power control mechanism, it is necessary to acquire the knowledge of the channel between the ST and the PR. As proposed in Chapter 3, the ST can retrieve this information by listening to a pilot or beacon signal transmitted by the PR.

A slotted medium access is implemented at the ST with a frame duration of T . The knowledge of the interference channel is acquired by employing channel reciprocity over the link PR-ST. In order to incorporate channel estimation in context to the power control mechanism, the frame interval is divided in two phases, namely estimation and data transmission, refer to Figure 5.1. During the estimation phase τ_{est} (also referred as estimation time), the ST measures

¹In contrast to the received power-based estimation, the employment of pilot-based channel estimation has an negligible effect on the performance degradation in terms of the time allocated within the frame structure and the amount of variations induced. In this context, perfect channel estimation for access channel presents a reasonable assumption.

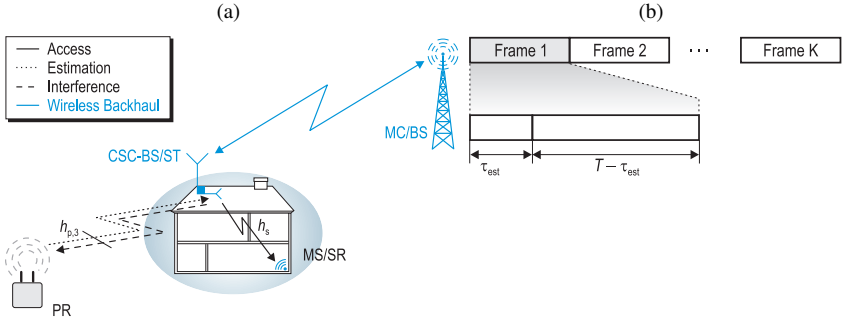


Figure 5.1: With regard to Chapter 3, a simplified illustration of (a) the CSC scenario demonstrating an underlay paradigm. (b) Frame structure from the perspective of the ST that presents a time duration (τ_{est}) allocated for the estimation of the interference channel.

the received power of the signal (a pilot signal with known transmit power, refer to Section 3.3.5 in Chapter 3 for a detailed discussion) transmitted by the PR. Based on this received power, the ST implicitly acquires the knowledge of $|h_{\text{p},3}|^2$, using which it controls its transmit power for the secondary link while satisfying a constraint on the interference received by the PR. During the data transmission phase $T - \tau_{\text{est}}$, the ST transmits data with the controlled power to the SR.

5.1.3 Signal Model

The discrete and complex signal received at the ST is given by

$$y_{\text{ST}}[n] = h_{\text{p},3} \cdot x_{\text{PR}}[n] + w_{\text{ST}}[n], \quad (5.1)$$

where $x_{\text{PR}}[n]$ corresponds to a discrete and complex constant power signal transmitted by the PR, $|h_{\text{p},3}|^2$ represents the power gain for the channel PR-ST and $w_{\text{ST}}[n]$ is circularly symmetric AWGN at the ST. $P_{\text{Tx,PR}}$ corresponds to the transmit power at the PR and $w_{\text{ST}}[n]$ is a Gaussian random variable with $\mathbb{E}[w_{\text{ST}}[n]] = 0$ and $\mathbb{E}[|w_{\text{ST}}[n]|^2] = \sigma_w^2$.

By listening to the transmissions from the PR, the estimated received power at

the ST, computed using $\tau_{\text{est}}f_s$ samples, is given as

$$\hat{P}_{\text{Rx,ST},h_{p,3}} = \frac{1}{\tau_{\text{est}}f_s} \sum_{n=1}^{\tau_{\text{est}}f_s} |h_{p,3} \cdot x_{\text{PR}}[n] + w_{\text{ST}}[n]|^2, \quad (5.2)$$

where f_s denotes the sampling frequency.

After implementing the power control at the ST, during the data transmission, the received signal at the PR is given by

$$y_{\text{PR}}[n] = h_{p,3} \cdot x_{\text{ST,cont}}[n] + w_{\text{PR}}[n], \quad (5.3)$$

and, on the other side, the received signal at the SR follows

$$y_{\text{SR}}[n] = h_s \cdot x_{\text{ST,cont}}[n] + w_{\text{SR}}[n], \quad (5.4)$$

where $x_{\text{ST,cont}}[n]$ presents the signal with controlled power ($P_{\text{Tx,ST,cont}}$) at the ST.

During the data transmission phase, the controlled power at the ST is determined as

$$\hat{P}_{\text{Tx,ST,cont}} = \frac{1}{(T - \tau_{\text{est}})f_s} \sum_{n=1}^{(T - \tau_{\text{est}})f_s} |x_{\text{ST,cont}}[n]|^2 \quad (5.5)$$

Further, $|h_{p,3}|^2$ and $|h_s|^2$ represent the power gains for the channels ST-PR and ST-SR, respectively, cf. Figure 5.1.

During the data transmission phase, the received powers at the PR and the SR are evaluated as

$$\hat{P}_{\text{Rx,PR}} = \frac{1}{(T - \tau_{\text{est}})f_s} \sum_{n=1}^{(T - \tau_{\text{est}})f_s} |y_{\text{PR}}[n]|^2 \quad (5.6)$$

and

$$\hat{P}_{\text{Rx,SR}} = |h_s|^2 \hat{P}_{\text{Tx,ST,cont}}, \quad (5.7)$$

respectively. Likewise (5.1), $w_{\text{PR}}[n]$ and $w_{\text{SR}}[n]$ represent circularly symmetric AWGN at the PR and the ST with zero mean and variance $\mathbb{E} [|w_{\text{PR}}[n]|^2] = \mathbb{E} [|w_{\text{SR}}[n]|^2] = \sigma_w^2$, respectively.

After utilizing τ_{est} for channel estimation, the throughput at the SR over the access channel² is given by

$$\hat{R}_s = \frac{T - \tau_{\text{est}}}{T} \log_2 \left(1 + \frac{|h_s|^2 \hat{P}_{\text{Tx,ST,cont}}}{\sigma_w^2} \right). \quad (5.8)$$

5.2 Theoretical Analysis

In order establish a close relationship between the analytical framework and the hardware implementation, the sequence of events depicted by the underlay scenario in Figure 5.1 are summarized as follows:

1. The ST estimates the power received $\hat{P}_{\text{Rx,ST},h_{p,3}}$ (i.e., employs received power-based estimation) by listening to the pilot signal transmitted by the PR over the interference channel. In the context of the hardware implementation, an unmodulated sinusoidal signal is sent as a pilot or beacon signal.

Please note that a sinusoidal signal is mathematically equivalent to the constant power signal sent by the PR, resembling a continuous phase modulated signal (for instance, a minimum shift keying signal) or a discrete phase modulated signal (for instance, a phase shift keying signal), which represents a perfectly downsampled signal. For the latter case, perfect implies an appropriate selection of the sampling point so that no inter symbol interference is procured by the system (in other words, Nyquist criterion is satisfied). In correspondence to the signal model that assumes i.i.d. samples, such a requirement is essential for the evaluation of the received power (energy detection or received power-based estimation), which is necessary for validating the theoretical expressions, derived in the thesis.

2. With the knowledge of $P_{\text{Tx,PR}}$ and the estimate $\hat{P}_{\text{Rx,ST},h_{p,3}}$, the ST indirectly acquires the knowledge of $|h_{p,3}|^2$. Upon acquiring this knowledge, a power control is employed at the ST. Using $\hat{P}_{\text{Rx,ST},h_{p,3}}$, $\hat{P}_{\text{Tx,ST,cont}}$ is determined as

$$\hat{P}_{\text{Tx,ST,cont}} = \frac{\theta_1 K}{\hat{P}_{\text{Rx,ST},h_{p,3}}}, \quad (5.9)$$

²Please note, it is assumed that the access channel is perfectly known at the ST and SR procures no interference from the PT.

where K represents a scaling factor. The scaling factor is required at the ST to hold $\mathbb{E} \left[\hat{P}_{\text{Rx,PR}} \right]$ at θ_1 . It is defined as

$$K = \frac{1}{\mathbb{E}_{\hat{P}_{\text{Rx,ST},h_{p,3}}} \left[\frac{|h_{p,3}|^2}{\hat{P}_{\text{Rx,ST},h_{p,3}}} \right]}, \quad (5.10)$$

where $\mathbb{E}_{\hat{P}_{\text{Rx,ST},h_{p,3}}} [\cdot]$ represents the expectation over $\hat{P}_{\text{Rx,ST},h_{p,3}}$.

3. The ST transmits data to the SR at $\hat{P}_{\text{Tx,ST,cont}}$. The estimated power (represented as $\hat{P}_{\text{Rx,ST},h_{p,3}}$) over the interference channel induces variations in the controlled power (represented as $\hat{P}_{\text{Tx,ST,cont}}$). With regard to the relation between the controlled power at the ST and the received power at the PR, represented as

$$P_{\text{Rx,PR}} = |h_{p,3}|^2 P_{\text{Tx,ST,cont}}, \quad (5.11)$$

the variations in $\hat{P}_{\text{Tx,ST,cont}}$ translate to the variations in $P_{\text{Rx,PR}}$ (represented as $\hat{P}_{\text{Rx,PR}}$) around θ_1 , resulting in uncertain interference at the PR. Unless captured, these variations may severely degrade the performance of the US. Besides this, due to the relationship between the controlled power and the secondary throughput, defined in (5.8), the variations are further translated to the secondary throughput.

4. These variations in the system parameters ($\hat{P}_{\text{Rx,ST},h_{p,3}}$, $\hat{P}_{\text{Tx,ST,cont}}$, $\hat{P}_{\text{Rx,PR}}$ and \hat{R}_s) are characterized in terms of their pdfs. In particular, the pdf of $\hat{P}_{\text{Rx,PR}}$ is utilized to employ an interference constraint (also referred as confidence probability constraint) in terms of confidence probability P_c at the ST so that the uncertain interference at the PR can be regulated effectively. In addition, by utilizing the pdf of \hat{R}_s , the performance of the access channel is determined in terms of the expected secondary throughput.
5. Finally, subject to the confidence probability constraint, the performance of the US is jointly characterized in terms of a tradeoff between the estimation time and the secondary throughput.

5.2.1 Characterization of the System Parameters

In order to capture the variations induced due to channel estimation, the pdfs of the aforementioned system parameters ($\hat{P}_{\text{Rx,ST},h_{p,3}}$, $\hat{P}_{\text{Tx,ST,cont}}$, $\hat{P}_{\text{Rx,PR}}$, \hat{R}_s) are

5 Validation and Demonstration

characterized, subsequently.

In accordance to the employed signal model, $P_{\text{Rx,ST},h_{p,3}}$ is modeled as a non-central chi-squared distribution \mathcal{X}'^2 , whose pdf is characterized as [95]

$$f_{\hat{P}_{\text{Rx,ST},h_{p,3}}}(x) = \frac{\tau_{\text{est}}f_s}{2\sigma_w^2} \left(\frac{\tau_{\text{est}}f_s x}{\lambda} \right)^{\frac{\tau_{\text{est}}f_s - 2}{4}} \exp\left(-\frac{\tau_{\text{est}}f_s x + \lambda}{2\sigma_w^2}\right) \times \quad (5.12)$$

$$I_{\frac{\tau_{\text{est}}f_s}{2} - 1} \left(\frac{\sqrt{\tau_{\text{est}}f_s x \lambda}}{\sigma_w^2} \right),$$

where $\tau_{\text{est}}f_s$ is the degree of freedom and also the number of complex samples used for the estimation. σ_w^2 is the noise variance of the in-phase and the quadrature-phase components of the received pilot signal ($y_{\text{ST}}[n]$, refer to 5.1), and $I_{\frac{\tau_{\text{est}}f_s}{2} - 1}(\cdot)$ is the modified Bessel function of the first kind of order $\frac{\tau_{\text{est}}f_s}{2} - 1$ [96]. Furthermore, the non-centrality parameter is defined as

$$\lambda = \sum_{n=1}^{\tau_{\text{est}}f_s} \mathbb{E}[|y_{\text{ST}}[n]|^2] = \tau_{\text{est}}f_s \times A^2. \quad (5.13)$$

The evaluation of λ in (5.13) can be explained as follows: a sinusoidal signal that represents a pilot signal consists of a constant amplitude, which is down-converted by an I/Q demodulator at the ST. In this regard, the complex samples $y_{\text{ST}}[n]$ have a constant envelope of value A .

Corresponding to (5.9), $\hat{P}_{\text{Tx,ST,cont}}$ follows an inverse non-central chi-squared distribution. The pdf for $\hat{P}_{\text{Tx,ST,cont}}$ is given by

$$f_{\hat{P}_{\text{Tx,ST,cont}}}(x) = \frac{\tau_{\text{est}}f_s K \theta_1}{2\sigma_w^2 x^2} e^{-\frac{\tau f_s}{2\sigma_w^2} \left(\frac{K \theta_1}{x} + |h_{p,3}|^2 P_{\text{Tx,PR}} \right)} \left(\frac{K \theta_1}{x |h_{p,3}|^2 P_{\text{Tx,PR}}} \right)^{\frac{\tau_{\text{est}}f_s}{4} - \frac{1}{2}} \times \quad (5.14)$$

$$I_{\frac{\tau_{\text{est}}f_s}{2} - 1} \left(\frac{\tau_{\text{est}}f_s}{\sigma_w^2} \sqrt{\frac{K \theta_1 |h_{p,3}|^2 P_{\text{Tx,PR}}}{x}} \right).$$

Following the relation in (5.11) and substituting $f_{\hat{P}_{\text{Tx,ST,cont}}}(x)$, defined in (5.14), the pdf of $\hat{P}_{\text{Rx,PR}}$ is determined as

$$f_{\hat{P}_{\text{Rx,PR}}}(x) = \frac{|h_{p,3}|^2 \tau_{\text{est}}f_s K \theta_1}{2\sigma_w^2 x^2} e^{-\frac{\tau_{\text{est}}f_s |h_{p,3}|^2}{2\sigma_w^2} \left(\frac{K \theta_1}{x} + P_{\text{Tx,PR}} \right)} \left(\frac{K \theta_1}{x P_{\text{Tx,PR}}} \right)^{\frac{\tau_{\text{est}}f_s}{4} - \frac{1}{2}} \times \quad (5.15)$$

$$I_{\frac{\tau_{\text{est}} f_s}{2} - 1} \left(\frac{\tau_{\text{est}} f_s |h_{p,3}|^2}{\sigma_w^2} \sqrt{\frac{K \theta_1 P_{\text{Tx,PR}}}{x}} \right).$$

Consequently, the cdf of $\hat{P}_{\text{Rx,PR}}$ is given by

$$F_{\hat{P}_{\text{Rx,PR}}}(x) = Q_{\frac{\tau_{\text{est}} f_s}{2}} \left(\sqrt{\frac{\tau_{\text{est}} f_s P_{\text{Tx,PR}} |h_{p,3}|^2}{\sigma_w^2}}, \sqrt{\frac{\tau_{\text{est}} f_s |h_{p,3}|^2 \theta_1 K}{\sigma_w^2 x}} \right), \quad (5.16)$$

where $Q_{\frac{\tau_{\text{est}} f_s}{2}}(\cdot)$ is the Marcum Q-function [96].

Next, the pdf of the secondary throughput \hat{R}_s is determined as

$$\begin{aligned} f_{\hat{R}_s}(x) &= \frac{T}{T - \tau_{\text{est}}} \frac{\tau_{\text{est}} f_s K \theta_1 |h_s|^2 \ln 2}{2\sigma_w^4} \left(\frac{p(x) + 1}{[p(x)]^2} \right) \times \\ &\exp \left(-\frac{\tau_{\text{est}} f_s}{2\sigma_w^2} \left(\frac{K \theta_1 \alpha_s}{p(x) \sigma_w^2} + |h_{p,3}|^2 P_{\text{Tx,PR}} \right) \right) \times \\ &\left(\frac{K \theta_1 |h_s|^2}{p(x) |h_{p,3}|^2} P_{\text{Tx,PR}} \sigma_w^2 \right)^{\frac{\tau_{\text{est}} f_s}{4} - \frac{1}{2}} \times \\ &I_{\frac{\tau_{\text{est}} f_s}{2} - 1} \left(\frac{\tau_{\text{est}} f_s}{\sigma_p^2} \sqrt{\frac{K \theta_1 |h_{p,3}|^2 P_{\text{Tx,PR}} |h_s|^2}{p(x) \sigma_w^2}} \right), \end{aligned} \quad (5.18)$$

where $p(x) = 2^{\frac{T x}{T - \tau_{\text{est}}}} - 1$.

5.2.2 Estimation-Throughput Tradeoff

In accordance with estimation theory, it is clear that small τ_{est} results in large variations for the $\hat{P}_{\text{Rx,PR}}$, and subsequently results in the deviation of $\hat{P}_{\text{Rx,PR}}$ from the interference threshold (θ_1). If not considered, these variations lead to uncertain interference, which may affect the performance of the US. To capture these variations, an interference constraint defined in terms of a confidence probability P_c and a certain accuracy³ β is proposed. In order to restrict the uncertain interference due to channel estimation, it is important to restrain P_c above a certain desired level \bar{P}_c for a fixed value of β .

³In order to scale the confidence interval relative to θ_1 .

In this regard, the interference constraint on confidence probability (or confidence probability constraint) is defined as

$$P_c = F_{\hat{P}_{\text{Rx,PR}}}((1 + \beta)\theta_1) - F_{\hat{P}_{\text{Rx,PR}}}((1 - \beta)\theta_1) \geq \bar{P}_c, \quad (5.19)$$

where $((1 + \beta)\theta_1)$ and $((1 - \beta)\theta_1)$ represent the confidence interval around θ_1 . According to (5.19), the confidence probability can be computed by inserting confidence interval in $F_{\hat{P}_{\text{Rx,PR}}}(x)$, defined in (5.16).

It is worthy to note that P_c depends on τ_{est} through $F_{\hat{P}_{\text{Rx,PR}}}(x)$. Besides this, $\mathbb{E}_{\hat{R}_s}[\hat{R}_s]$ is also related to the estimation time. Hence, from the design perspective, it is essential to exploit this relationship between the estimation and the secondary throughput⁴, characterized as estimation-throughput tradeoff, is given by

$$R_s(\tilde{\tau}_{\text{est}}) = \max_{\tau_{\text{est}}} \mathbb{E}_{\hat{R}_s} \left[\hat{R}_s(\tau_{\text{est}}) \right] \quad (5.20)$$

s.t. (5.19).

According to this tradeoff, there exists a suitable estimation time $\tilde{\tau}_{\text{est}}$ that satisfies the confidence probability constraint and yields the achievable secondary throughput.

5.3 Hardware Validation

This section performs the validation of the theoretical expressions, derived in the previous section. The measurements necessary for the validation are carried out by means of an SDR platform. The experimental setup for acquiring the measurements is presented, subsequently.

5.3.1 Experimental Setup

Figure 5.2 presents the experimental setup, deployed for performing the validation of the theoretical analysis, carried out in Section 5.2. With the employment

⁴It is worth considering that the estimation-throughput tradeoff determined in Chapter 3 and the one presented in this chapter brings out the same relationship. However, here its quantification is slightly different in contrast to the one determined in Chapter 3.

of the transmit and the receive antennas the interference signal received⁵ at the ST can influence the measurements, resulting in the deviation of the empirical results from their analytical counterpart. To avoid this issue, the interference channel is implemented by means of a coaxial cable. In addition, attenuators are used to realize different values of $\gamma_{p,3}$. The use of the coaxial cable is limited to the validation process. For the deployment of the demonstrator later in Section 5.4, the coaxial cable is replaced with antennas.

The CSC-BS or the ST is emulated using a Universal Software Radio Peripheral (USRP) B210, an SDR platform from Ettus Research [97] and a host computer, which is connected to the USRP by means of a USB cable, refer to Figure 5.2. The host computer performs the following tasks: (i) it enables the access to the USRP by controlling certain RF parameters such as center frequency and sampling frequency, and (ii) it allows the baseband processing over the complex samples. The PR, which transmits the pilot signal, is realized using a Rhode & Schwarz 200A vector signal generator. Like the ST, for the implementation of the demonstrator later in Section 5.4, the signal generator emulating the PR is replaced with an USRP and a host computer. The signal generator is used instead of a USRP for excluding any kind of discrepancy in the transmit signal that may degrade the validation process. Finally, to complement the validation process, the measurement data is analyzed offline using MATLAB.

Since the USRP employs a homodyne receiver⁶, spurious effects such as DC offset, flicker noise ($1/f$) and I/Q imbalance arising from the analog front-end can affect the accuracy of the analytical expressions, thereby influencing the validation process. These spurious effects, particularly the DC offset and the flicker noise, become significant at low signal to noise ratio. In order to retrieve the complex samples close to the one obtained while characterizing the system model that do not take such spurious effects into account, the following signal processing (referred as pre-processing) is proposed at the host computer, please consider Figure 5.3:

- The received signal is oversampled with sampling frequency of 200 kHz. In order to filter out the spurious effects, the local oscillator is tuned at

⁵The experiments were performed over the ISM bands with center frequency fixed at 2.45 GHz, the interference signal from the operational wireless LAN was observed within the band of interest (in-band) or as an out-of-band emissions from the neighbouring channels.

⁶A homodyne receiver implements a direct downconversion of the bandpass to the baseband signal.

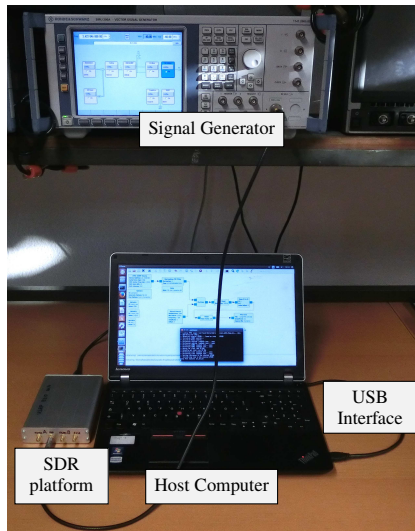
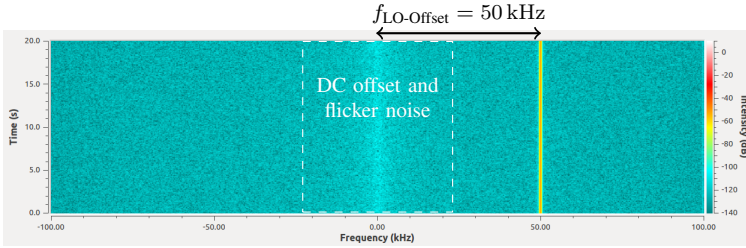


Figure 5.2: An illustration of the measurement setup required for the calibration and the validation process.

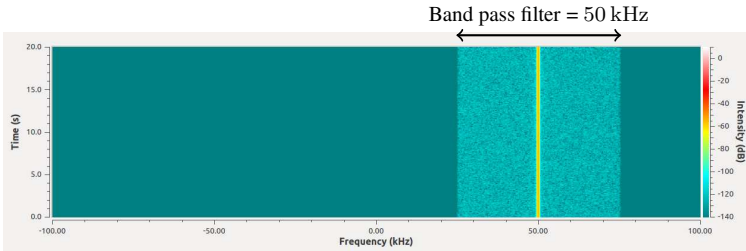
a certain offset frequency defined as $f_{\text{LO-Offset}} = 50 \text{ kHz}$, refer to Figure 5.3a.

- Subsequently, a bandpass filter with bandwidth = 50 kHz, corresponding to a oversampling factor = 4, is employed to obtain the desired bandpass signal at the $f_{\text{LO-Offset}}$. This filters out the DC offset and the flicker noise present at low frequencies, cf. Figure 5.3b.
- In order to obtain the lowpass equivalent of the desired signal, a digital downconversion (i.e., multiplying with a complex sinusoid with frequency $f_{\text{LO-Offset}} = 50 \text{ kHz}$) of the bandpass filtered signal is performed, cf. Figure 5.3c.
- It is worth noticing that the proposed framework considers i.i.d. samples while characterizing the pdfs of the corresponding systems parameters. In this regard, a decimation filter (with decimation factor = 4) over the downconverted signal is applied, cf. Figure 5.3d, to reduce the correlation between the samples, arising due to oversampling.

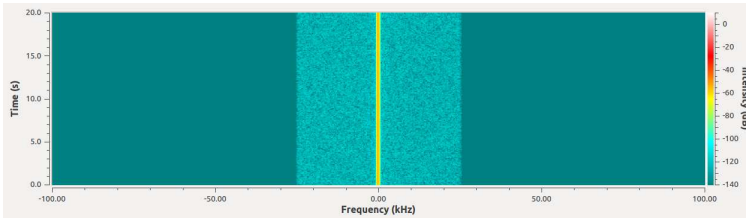
(a) Signal with oversampling, where the local oscillator is tuned at $f_{LO-Offset} = 50$ kHz



(b) Signal after bandpass filtering, filter bandwidth = 50 kHz



(c) Signal after digital downconversion



(d) Signal after decimation

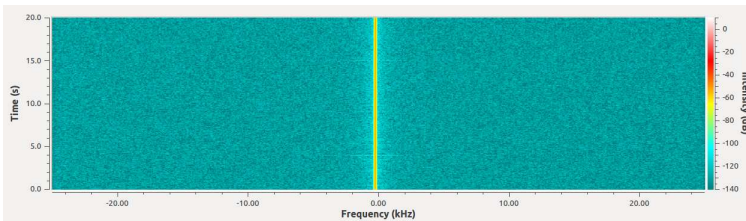


Figure 5.3: An illustration of the signal processing steps carried out at the host computer to preclude the spurious effects such as the DC offset and the flicker noise on the signal received at the ST.

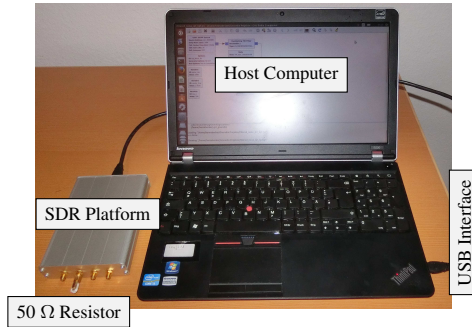


Figure 5.4: A measurement setup for acquiring the noise power.

5.3.2 Determining Noise Power

Besides these spurious effects, it is challenging to accurately determine the noise power (σ_w^2), which is an important parameter for characterizing the pdfs. In this regard, σ_w^2 is determined using the variance of the envelope of $y_{ST}[n]$ – *on the fly*. This is done because the value of the noise power evaluated during the calibration (that involves no signal transmission, refer to Figure 5.4) differed from the one determined while performing the measurements for different values of signal to noise ratio ($\gamma_{p,3}$) received at the ST over the interference channel. It is noticed that the latter approach, presented later in Section 5.3.3), provided a closer fit to the analytical expressions.

5.3.3 Validation of System Parameters

Since the stochastic model is the basis of the proposed analysis, it is reasonable to first validate the pdfs of the system parameters ($\hat{P}_{RX,ST,h_{p,3}}$, $\hat{P}_{TX,ST,cont}$, $\hat{P}_{RX,PR}$, and \hat{R}_S), derived in Section 5.2. To this end, measurements are performed in accordance to the setup illustrated in Figure 5.2. The measurement data is plotted in terms of histogram and scaled to determine the relative frequency ($f_{hist}(x)$, a discrete function) over a certain set of bins, $x \in \mathcal{X}_{bins}$. Figure 5.5 compares the histograms, obtained from the measurements, and the pdfs, determined using the analytical expressions for a certain set of system parameters, depicted in Table 5.1. The plots justify the validity of the derived theoretical expressions,

Table 5.1: Values of the parameters determined while performing the experiments.

Parameter	Value
$\gamma_{p,3}$	22 dB
N	100
τ_{est}	2 ms
θ_1	-110 dBm
T	100 ms
$ h_s ^2$	1
σ_w^2	-96.74 dBm

which include the pdfs of the system parameters. As a result, these pdfs are eligible for capturing the performance of the CR systems over the hardware.

The experiments were repeated for different values of $\gamma_{p,3}$. It was observed that for a considerable range of $\gamma_{p,3} \in (4, 30)$ dB, the theoretical expressions depicted a significant accuracy to the experimental data, refer to Table 5.2. The accuracy is quantified in terms of a relative error (ϵ), defined as

$$\epsilon = \frac{1}{|\mathcal{X}_{\text{bins}}|} \times \sum_{x \in \mathcal{X}_{\text{bins}}} \frac{f_{\hat{P}_{\text{Rx},ST,h_{p,3}}}(x) - f_{\text{hist}}(x)}{f_{\text{hist}}(x)}, \quad (5.21)$$

$|\mathcal{X}_{\text{bins}}|$ represents the cardinality of $\mathcal{X}_{\text{bins}}$, which excludes the bins with $f_{\text{hist}}(x) = 0$. The different values of $\gamma_{p,3}$ correspond to the different channel conditions. Hence, this observation concludes that the proposed framework is robust to the fluctuations in the channel gain.

5.3.4 Validation of Estimation-Throughput Tradeoff

Following the validation of the pdfs that captures the variations in the system parameters, it is interesting to validate the performance of the CR system in terms of the estimation-throughput tradeoff, characterized in (5.20). Thus, the feasibility of the optimization problem that respects the interference constraint

5 Validation and Demonstration

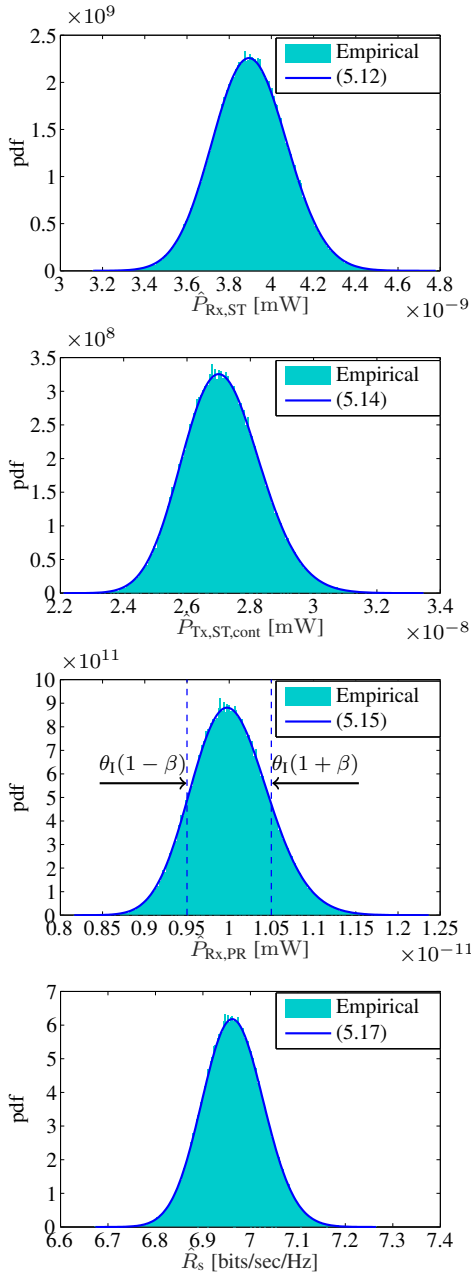


Figure 5.5: Validating the theoretical expressions of the pdf and the experimental results with a certain choice of the system parameters depicted in Table 5.1.

Table 5.2: ϵ for different values of $\gamma_{p,3}$

$\gamma_{p,3}/[\text{dB}]$	ϵ
4.08	0.0568
9.10	0.0601
14.11	0.0522
19.12	0.0437
24.09	0.0506
29.09	0.0634
34.03	0.1179
39.38	0.0800
45.08	0.1695

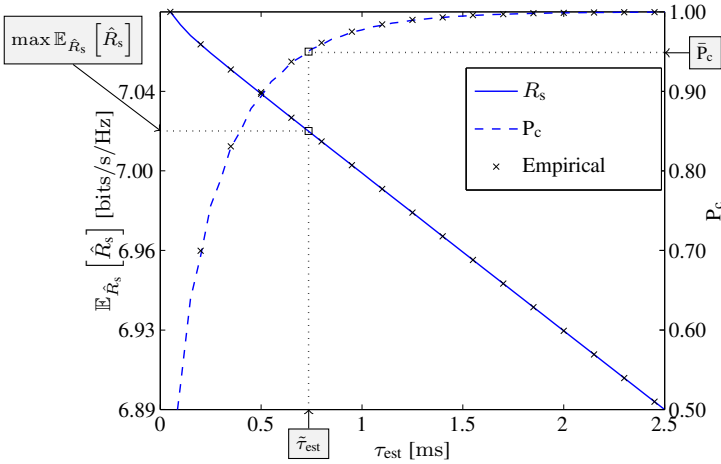


Figure 5.6: Validating the estimation-throughput tradeoff for the choice of parameters depicted in Table 5.1. The figure illustrates the suitable estimation time $\tilde{\tau}_{\text{est}}$ at which the confidence probability is satisfied, see the projection of \square on the curve P_c , at the same time achieves the maximum expected secondary throughput, see the projection of \square on the curve \hat{R}_s .

on P_c is validated. As discussed previously, a large τ_{est} improves the performance of the primary system by reducing the variations in $\hat{P}_{\text{RX,PR}}$, depicted by observing an increase in P_c , cf. Figure 5.6. Conversely, from the perspective of the secondary system, an increase in τ_{est} causes a reduction in the expected secondary throughput.

These variations of the expected throughput and the confidence probability versus the estimation time are presented in Figure 5.6, which illustrates a joint validation of the performance parameters ($\mathbb{E}_{\hat{R}_s} [\hat{R}_s]$ and P_c) for the underlay CR system. Again, the validation is achieved by comparing the measurements of the performance parameters with their analytical expressions for different τ_{est} . In contrast to the analytical framework, presented in Section 5.2, the empirical values of P_c are determined by computing a numerical integration in the region within the confidence interval $(1 \pm \beta)\theta_1$, cf. Figure 5.5.

After performing the validation, following conclusions can be outlined:

- The accuracy of the derived expressions and the feasibility of the received power-based estimation (proposed in this thesis) have been justified by means of a hardware realization.
- Furthermore, in accordance to the validation process, the applicability of the simplifications and solutions, proposed in Section 5.1.1, has been accounted.

This signifies that the proposed framework is capable of illustrating the underlay principle by means of a demonstrator.

5.4 Hardware Demonstration

Although the validation is an important part of the system design, it is restricted to offline verification of the proposed approach. From a deployment perspective, it is interesting to demonstrate the online operation of the underlay paradigm on the hardware. This section provides insights on the involved challenges while deploying the proposed approach in the form of a demonstrator. In the thesis, the operation of CR systems at a suitable estimation time that is associated with the maximum secondary throughput has been analyzed, which represents the optimum performance of a CR system. However, in practice, it is difficult to determine the value of this parameter while the system is

operating – *on the fly*. In this regard, the subsequent section discusses this challenging task, and proposes a heuristic approach of determining the estimation time.

5.4.1 Determining Estimation Time

The analytical expression (5.20) and Figure 5.6 illustrate a dependency of the performance parameters (P_c and $\mathbb{E}_{\hat{R}_s} [\hat{R}_s]$) on the estimation time τ_{est} . This dependency, depicted as the estimation-throughput tradeoff, is utilized to determine the suitable estimation time $\tilde{\tau}_{\text{est}}$ that achieves the maximum secondary throughput. However, $\tilde{\tau}_{\text{est}}$ can be determined for a certain value of $\gamma_{p,3}$, which represents a certain channel gain. In practice, the mobility of the ST or the PR, or the surroundings objects cause variations in the channel gain, which consequently induce variations in $\gamma_{p,3}$. Under this situation, it is challenging to select $\tilde{\tau}_{\text{est}}$ such that the system adheres to the confidence probability constraint and still achieves the maximum secondary throughput for a corresponding range of $\gamma_{p,3}$.

To approach this issue, the variation of $\tilde{\tau}_{\text{est}}$ for a certain range of $\gamma_{p,3}$ and different values of the confidence probability constraint $\bar{P}_c \in \{0.90, 0.95, 0.99\}$ is investigated⁷, cf. Figure 5.7. Thus, the maximum value of the suitable estimation time for a certain range of $\gamma_{p,3}$ and \bar{P}_c is selected as the estimation time for the demonstrator, given by

$$\tau'_{\text{est}} = \max\{\tilde{\tau}_{\text{est}} | \gamma_{p,3} \in (-10, 20) \text{ dB}; P_c = \bar{P}_c\}. \quad (5.22)$$

Since the τ'_{est} is not optimal for all $\gamma_{p,3}$, it is different from $\tilde{\tau}_{\text{est}}$. Hence, a different notation is assigned for its representation. By doing this, it is assured that the confidence probability constraint is satisfied for different realizations of the channel gain, which reside within the interval $\gamma_{p,3} \in (-10, 20)$ dB.

Besides, from Figure 5.7, it is further observed that $\tilde{\tau}_{\text{est}}$ decreases monotonically with $\gamma_{p,3}$. According to Figure 5.7, the descent is slow in beginning and then increases tremendously. This behaviour can be explained as follows: For large values of $\gamma_{p,3}$, $P_{\text{Tx,ST,cont}}$ is low, this reduces the variations of $\hat{P}_{\text{Rx,PR}}$ around θ_1 . As a result, a lower value of $\tilde{\tau}_{\text{est}}$ is sufficient to maintain these variations within the confidence interval. On the other hand, the signal received

⁷Such investigations can be performed during the validation process, which is normally included at the system design.

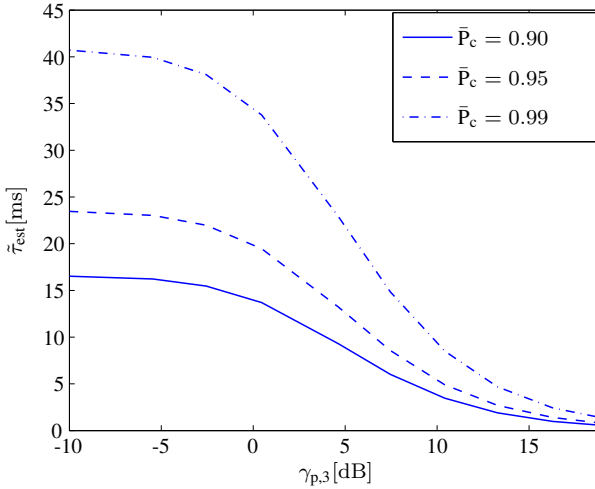


Figure 5.7: The variation of the suitable estimation time ($\tilde{\tau}_{\text{est}}$) versus the received signal to noise ratio at the ST ($\gamma_{p,3}$) for different values of confidence probability constraint $\bar{P}_c \in \{0.90, 0.95, 0.99\}$.

with low $\gamma_{p,3}$, which corresponds to a higher $P_{\text{Tx,ST,cont}}$. However, the limited number of samples available for the estimation and the sensitivity of the deployed hardware make it difficult to distinguish the received signal from the noise. Thus leading to a saturation of $\tilde{\tau}_{\text{est}}$ below a certain $\gamma_{p,3}$. Upon increasing the number of samples for the channel estimation or selecting a hardware with higher sensitivity, the saturation region can be reduced to a lower $\gamma_{p,3}$.

Consequently, the analysis in Figure 5.7 is used for determining the estimation time τ'_{est} for the demonstrator. For a certain value of the confidence probability constraint $\bar{P}_c = 0.95$, the estimation time allocated for the channel estimation is determined to be $\tau'_{\text{est}} = 24$ ms, cf. Figure 5.7. With this, the confidence probability constraint is satisfied for all $\gamma_{p,3} \in (-10, 20)$ dB at the cost of a decreased performance in expected secondary throughput. This happens due to the inefficient utilization of the time resources, particularly, for the situation with high $\gamma_{p,3}$, which results in a low value of the suitable estimation time.

5.4.2 Simplifications and Solutions

In order to successfully deploy the demonstrator, in addition to the simplifications proposed for the hardware validation in Section 5.4.2, following simplifications are accounted in the system model:

1. The controlled power according to the proposed framework can be evaluated using (5.9). However, this requires knowledge of the scaling factor K . According to (5.10), K can be computed by averaging the received power $\hat{P}_{\text{Rx,ST},h_{p,3}}$ after attaining multiple realizations (or measurements), which corresponds to the expected received power. After mounting the antennas at the ST and the PR, it is possible that the channel gain fluctuates over the acquired realizations. These fluctuations make it difficult to carry out the computation of K while the system is operating. Such a random behaviour of the channel is in contrast to the deterministic behaviour of the channel, considered while establishing the system model.

To resolve this issue, the controlled power for the demonstrator is computed based on a single realization of the $\hat{P}_{\text{Rx,ST},h_{p,3}}$. As a result, the estimated channel gain, evaluated from $\hat{P}_{\text{Rx,ST},h_{p,3}}$, is approximated as

$$|\hat{h}_{p,3}|^2 = \frac{\mathbb{E} \hat{P}_{\text{Rx,ST},h_{p,3}} \left[\hat{P}_{\text{Rx,ST},h_{p,3}} \right] - \sigma_w^2}{P_{\text{Tx,PR}}} \approx \frac{\hat{P}_{\text{Rx,ST},h_{p,3}} - \sigma_w^2}{P_{\text{Tx,PR}}}. \quad (5.23)$$

As σ_w^2 is negligible compared to $\hat{P}_{\text{Rx,ST},h_{p,3}}$, (5.23) can be further approximated as

$$|\hat{h}_{p,3}|^2 = \frac{\hat{P}_{\text{Rx,ST},h_{p,3}} - \sigma_w^2}{P_{\text{Tx,PR}}} \approx \frac{\hat{P}_{\text{Rx,ST},h_{p,3}}}{P_{\text{Tx,PR}}}. \quad (5.24)$$

The above simplification, however, increase the variation in the system. In this regard, a certain deviation in the performance, computed using the theoretical expression and the one depicted by the demonstrator, is expected.

2. Furthermore, in order to exercise channel reciprocity, the analytical framework considers that TDD is employed at the primary and secondary systems. In order to realize TDD, a perfect frame synchronization between the PR and the ST is needed, which is difficult to achieve in practice⁸. To simplify this matter, FDD between the PR and the ST is pro-

⁸Even for preliminary analysis, it is cumbersome to deploy two different system and realize TDD.

posed. This simplification is described as follows: The signals are transmitted and received at different frequencies (2.422 GHz and 2.423 GHz) over separate antennas, as illustrated in Figure 5.8. With this technique, the channel reciprocity may be compromised, and a further deviation in the performance can be observed.

Therefore, it is utmost necessary to observe the impact of these simplifications on the performance of the demonstrator, specially, in terms of the violation of the confidence probability constraint. In this regard, the principle operation of the underlay paradigm, described in Section 5.1.2, is mapped onto the hardware and the above mentioned simplifications are applied. The signal flow illustrating the operation of the hardware demonstrator is presented in Figure 5.8. The graphical user interface and the different CR related techniques such as the channel estimation (received power-based estimation), the power control mechanism, the confidence probability constraint are implemented over the software (GNU Radio) at the host computer.

5.4.3 User Interaction and Observations

Figure 5.9 and Figure 5.10 present the graphical user interfaces of the demonstrator, allowing access to the parameters evaluated at the ST (which include, $\hat{P}_{\text{Rx,ST},h_{p,3}}$, $\hat{P}_{\text{Tx,ST,cont}}$, and \hat{R}_s) and the PR (which include, $\hat{P}_{\text{Rx,PR}}$ and P_c), respectively. A hardware calibration of the demonstrator is performed to provide physical significance to the digital values obtained from the USRPs. Because the SR has not been implemented over the hardware, a slider that allows us to modify the gain for the access channel ($|h_s|^2$) is employed, demonstrating the effect of the variations in $|h_s|^2$ on the performance of the system.

As expected, the changes in the value of θ_1 at the ST caused the variations (in the measurements of $\hat{P}_{\text{Rx,PR}}$ at the PR) to shift approximately to the same value. This indicates that the expected received power $\mathbb{E}_{\hat{P}_{\text{Rx,PR}}} [\hat{P}_{\text{Rx,PR}}]$ is fixed to the interference threshold, as proposed in the analytical framework. A snapshot of this phenomenon is presented in Figure 5.9 and Figure 5.10, whereby $\theta_1 = 55$ dBm and $\hat{P}_{\text{Rx,PR}} = -56.17$ dBm is noticed. In addition, due to the modification of the confidence probability constraint⁹, the ST adapts its $P_{\text{Tx,ST,cont}}$ according to the new parameters, defining the confidence probability constraint, cf. Figure 5.9. Moreover, the changes in the $P_{\text{Tx,ST,cont}}$ are further reflected in the expected secondary throughput.

⁹Changing the interference threshold changes the confidence interval.

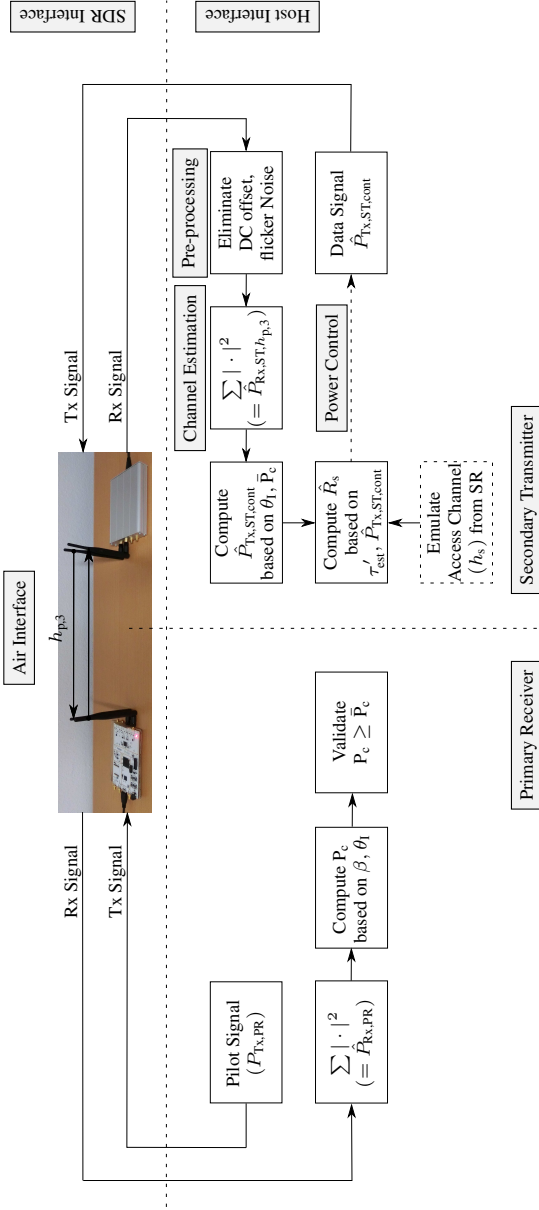


Figure 5.8: Setup and block diagram of the deployed demonstrator.

These observations justify the feasibility of the received power-based estimation, which enables the ST to procure the channel knowledge for the link PR-ST, evaluated by listening to the pilot signal, transmitted by the PR. With the availability of channel knowledge, this further demonstrates the operation of the power control mechanism in accordance to the underlay principle. In particular, the response of the demonstrator to the dynamic conditions can be analyzed by varying the distance – i.e., varying the channel gain – between the PR and the ST. This effect is captured over the graphical user interface by observing the changes in $\hat{P}_{\text{Rx,ST},h_{p,3}}$ and other corresponding parameters that depend on $|h_{p,3}|^2$. It is worthy to note that, as the distance is increased beyond a certain value, the ST operates at its maximum transmit power. The events like these are interesting to understand the response of the demonstrator under adverse situations.

Despite these facts, it is observed that for the given accuracy $\beta = 0.05$, the demonstrator fails to achieve the target value of the confidence probability constraint $P_c = 0.95$. Certainly, this violation is largely caused due to the simplifications undertaken in Section 5.4.2. Also, in contrast to the hardware validation, for the demonstrator, the pilot signal is produced by a USRP, thus offering a worse signal quality than that produced by the signal generator. In order to tackle this violation of the confidence probability constraint, the proposed confidence probability constraint is sustained by increasing the tolerance limit to $\beta = 0.20$. As a result, the confidence probability reaches the target value $P_c = 0.95$, thereby satisfying the confidence probability constraint, refer to Figure 5.10.

To demonstrate a preliminary performance of a CR system, these simplifications are affordable at this stage, however, it is important to relax these simplifications in future. Despite this deviation from the theoretical behaviour, it can be concluded that the USRPs, representing an SDR platform, is a viable choice for demonstrating the analysis proposed in the thesis. In the end, to wrap up the discussions, the key observations while deploying the demonstrator for the US are summarized as follows:

- The deployed demonstrator reveals the necessity of the channel knowledge for the operation of a CR system in a practical situation.
- With the incorporation of channel estimation, the deployed hardware demonstrates the operation of an US that employs a power control mechanism at the ST, which is facilitated by performing received power-based channel estimation at the ST.



Figure 5.9: A snapshot of the performance parameters at the ST displayed by means of the graphical user interface.

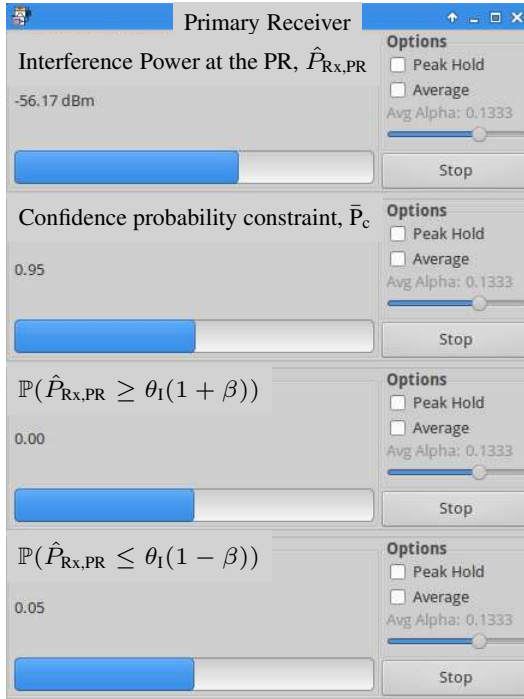


Figure 5.10: A snapshot of the performance parameters at the PR displayed by means of the graphical user interface.

- Subsequently, the demonstrator clearly presents the effect of imperfect channel knowledge, in particular, the uncertain interference at the PR. In addition, it justifies the applicability of the confidence probability constraint at the ST, imposed for regulating the uncertain interference.
- Finally, the demonstrator illustrates the capability of adapting to the changes in the environment, particularly, in terms of the channel between the ST and the PR.

5.5 Summary

In this chapter, the performance of an underlay system in consideration to a hardware implementation has been analyzed. To this end, an analytical framework has been validated by means of hardware measurements. In reference to the deployment process, it has been concluded that the knowledge of the interacting channels plays a crucial role in the hardware realization of the CR systems, the main aspect outlined in the thesis. Following the validation process, it has been justified that the proposed analysis that incorporates the received power-based estimation for the links between the primary and the secondary systems, proposed in the thesis, facilitates the hardware feasibility of a CR system by supporting low complexity and the versatility towards unknown primary user signals. Based on the experimental validation, a hardware demonstrator that depicts the principle functionality of the underlay system has been examined.

More importantly, in this chapter, the major challenges such as

- a certain pre-processing to exclude spurious effects, affecting the hardware validation of the derived expressions,
- a careful selection of the estimation time for a given operation regime, defined in terms of signal to noise ratio received at the ST,
- a proper implementation of the power control and
- a simplified approach to workaround channel reciprocity,

considered while deploying the demonstrator, have been discussed adequately. Consequently, the corresponding solutions and simplifications to overcome these challenges have been proposed.

Conclusion

In a nutshell, it is easy to recognize that an extensive amount of literature has already been involved with cognitive radio¹. Despite its huge popularity and in-depth knowledge acquired on this topic, an autonomous as-well-as exhaustive implementation of such a concept is underdeveloped. One main reason behind this is the fact that the existing models (developed for the performance characterization) have focused more on theoretical analysis and little on the hardware deployment. In this regard, due to the complexity of the underlying problem, these models tend to overlook certain aspects such as noise uncertainty, channel knowledge, signal uncertainty and hardware imperfections (including RF distortions, synchronization and quantizations errors) [59] that are fundamental to a hardware implementation. The lack of such imperfections in the system model renders the performance analysis of the CR system incomplete.

The knowledge of the involved channels residing within a CR system is one of such aspects dealt in this thesis. From a physical layer perspective, it has been identified that the channel knowledge is extremely necessary for the realization of the CR techniques on a hardware, thus allowing a CR system to control the interference accumulated by the primary system. In this thesis, this notion

¹For instance, as on 01.05.16, 17915 search results are retrieved upon typing the keyword cognitive radio in IEEE Xplore, a database for scientific publications available at <http://ieeexplore.ieee.org/Xplore/home.jsp>.

has been extensively justified and resolved through adequate analysis while considering a hardware deployment.

Above all, the inclusion of the channel estimation requires a proper allocation of time resources in the frame structure, and appropriate measures to counter variations due to the estimation error induced in the system. Surely, these factors have a detrimental effect on the performance of a CR system, leading to the performance degradation. These channel estimation related issues have been carefully identified and characterized in this thesis, which ultimately allows us to depict the performance of the CR systems in a fairly realistic scenario. Besides, following the deployment perspective, a received power-based channel estimation technique is proposed for the estimation, particularly, for the channels that exist between the two systems.

Briefly, the analysis performed in the thesis does not only provide answers to specific questions related to imperfect channel knowledge, including

1. How to counter the uncertain interference induced in different CR systems?
2. How to evaluate the performance degradation?
3. How to determine the suitable estimation time and suitable sensing time that yields the maximum throughput achieved?

but also promotes techniques such as

1. implementation of the channel estimation at the secondary system
2. energy-based detection and
3. received power-based channel estimation

that ultimately encourage hardware feasibility of CR systems.

6.1 Summary

This section summarizes the major findings from each chapter.

Chapter 2 outlined the fact that the spectrum sensing mechanism can be accomplished at the ST only if the knowledge of the involved channels (namely, sensing, interference and access channels) is accessible at the ST. Through analysis, it is clearly identified that the channel estimation degrades the performance of

the IS. In this context, an estimation-sensing-throughput tradeoff is established that allows us to regulate this performance degradation, and consequently determine the achievable throughput at the SR.

On the similar basis, Chapter 3 showed that the power control mechanism requires the knowledge of the involved channels (namely, interference – primary and secondary – channels and access channel) at the ST. The estimation-throughput tradeoff, a novel approach to jointly characterize the performance of the US and analyze the performance degradation, is presented. Following the main analysis, it is indicated that the performance degradation of the US can be effectively controlled only if the estimation time is selected appropriately.

The notion of the channel estimation presented in the previous two chapters is extended to the hybrid scenario in Chapter 4, whereby the spectrum sensing and the power control mechanisms are simultaneously enabled at the ST. Through numerical analysis, it is emphasized that a significant performance gain is achievable by combining the IS and the US. Similar to Chapter 2, an estimation-sensing-throughput tradeoff is formulated that allowed us to investigate the variation of the achievable throughput along the estimation and the sensing time.

While the previous three chapters focused on the theoretical analysis, the feasibility – in terms of validation and demonstration – of the proposed analysis is discussed in Chapter 5. In this regard, a software defined radio platform following the guidelines of an US is considered for the hardware implementation.

6.2 Outlook

With regard to the performance analysis and the deployment-centric viewpoint towards CR systems emphasized in the thesis, the following extensions or considerations to the proposed framework could be of great interest for future investigations. For instance, this thesis focused only on a half duplex CR communication, i.e., the CR techniques (which include spectrum sensing and power control) are time-interlaced with the data transmission. Recently, there has been significant advancement concerning the feasibility of in-band full duplex communication, for a detailed discussion over in-band full duplex communication, please consider [8, 98, 99] and the references therein. In this context, the CR communication can be transformed into the in-band full duplex, whereby

the CR techniques and the data transmission occurs simultaneously in time and over the same frequency channel. The design challenges and the corresponding performance tradeoffs related to the in-band full duplex CR communication are precisely dealt within [100, 101].

In addition, the performed analysis considers that the ST and the SR are installed with single antenna. As a matter of fact, state-of-the-art standards are mostly equipped with multiple antennas. With an intention of establishing a preliminary analysis involving channel estimation in context to CR systems, the performance enhancement procured by upgrading the existing spectrum sensing (detector performance) due to the deployment of multiple antennas [102, 103], has been completely neglected in the thesis. Based on a hardware deployment, the authors in [K14] argued that the hardware complexity in context with the CR system escalates with the deployment of multiple antennas, prohibiting the usage of well-known combining techniques such as equal-gain combining and maximum-ratio combining [63]. In this regard, non-conventional techniques, such as square-law selector and square-law combiner (following the principle of energy detection) are able to reduce complexity, thereby promoting the feasibility of multiple antennas.

Given the complexity of the underlying problem, impairments due to the asynchronous (in time domain) access by the secondary system to the licensed spectrum is left aside throughout the thesis. The asynchronous access is due to the unknown (which can be random also) behaviour of PU traffic. In these circumstances, the assumption concerning the synchronous access (i.e., perfect alignment to the primary system's medium access) becomes invalid. As a consequence, this asynchronous access certainly has an impact on the performance of the CR systems. A careful integration of the asynchronous access to the proposed analysis presents a promising research direction. To tackle this problem, the reader is encouraged to consult the references [104, 105].

Also, the performance evaluation, presented in the thesis, considers symmetric fading, i.e., the channel gains are subjected to the same value of m , which represents Nakagami- m parameter, characterizing the severity of channel fading. However, depending on the deployment scenario, the derived expressions can be utilized to realize asymmetric fading [80] by substituting different values of m corresponding to different channels. In this regard, the proposed framework can be extended to study the influence of asymmetric fading on the performance.

Finally, the performance analysis in this thesis has been confined to a single of PT, PR and ST and SR, a classical way of illustrating a node-wide perspective

of a CR system. The effect of the presence of other PTs and other STs in the network on the performance – evaluated using parameters such as spatial interference at the PR and spatial throughput at the SR, illustrating a network-wide perspective – has not been treated in the thesis. The concept of stochastic geometry, widely accepted for modelling the wireless networks, has been recently applied to the perform analysis for the cognitive radio networks. In order to establish an in-depth understanding of this concept, it is advisable to consult the references [26, 106–110], [K12].

As a closing remark, spectrum is a precious component that can enable wireless connectivity to the billions of devices residing inside a 5G network. To meet this escalating demand of more spectrum, cognitive radio, competing with technologies such as the millimeter-wave technology and the visible light communication, represents a viable option. Having said that, there exist certain scenarios, including the one considered in the thesis (refer to Chapter 1), that facilitate the co-existence of these technologies within a 5G system.

Acronyms and Abbreviation

3GPP	3 rd Generation Partnership Project
4G	Fourth-Generation of Wireless Mobile Technology
5G	Fifth-Generation of Wireless Mobile Technology
AC	Average Constraint
AWGN	Additive White Gaussian Noise
BS	Base Station
CR	Cognitive Radio
CSC	Cognitive Small Cell
CSC-BS	Cognitive Small Cell-Base Station
CSIT	Channel State Information at Transmitter
DC	Direct Current
EM	Estimation Model (Proposed Approach)
FDD	Frequency Division Duplexing
HS	Hybrid System
IoT	Internet of Things
IS	Interweave System
IM	Ideal Model
I/Q	In-phase and Quadrature-phase
IT	Interference Threshold
LSA	Licensed Shared Access
LTE	Long-Term Evolution
MC-BS	Macro Cell-Base Station
MS	Mobile Station
OC	Outage Constraint
OFDM	Orthogonal Frequency Division Multiplexing
PR	Primary Receiver
PT	Primary Transmitter

Acronyms and Abbreviation

PU	Primary User
QoS/QoE	Quality of Service/Quality of Experience
RF	Radio Frequency
SC	Small Cell
SDR	Software Define Radio
SNR	Signal to Noise Ratio
SR	Secondary Receiver
ST	Secondary Transmitter
TDD	Time Division Duplexing
US	Underlay System
USB	Universal Serial Bus
UWB	Ultra Wide Band
USRP	Universal Serial Radio Peripheral
UWB	Ultra Wide Band
VLC	Visible Light Communication
WiMAX	Worldwide Interoperability for Microwave Access
cdf	cumulative distribution function
cf.	confer (refer to)
e.g.	exempli gratia (for example)
i.e.	id est (that is)
i.i.d.	independent and identically distributed
mmW	millimeter-Wave
pdf	probability density function
Rx	Receiver
Tx	Transmitter

Notations and Symbols

T	Frame duration
f_s	Sampling frequency
$f_{\text{LO-Offset}}$	Local oscillator offset frequency
τ_{sen}	Sensing time interval
τ_{est}	Estimation time interval
τ'_{est}	Estimation time interval for the demonstrator
R_s	Throughput at SR (secondary throughput)
C_0	Date rate at SR without interference from PT, where no power control is employed at ST
C_1	Date rate at SR without interference from PT, where no power control is employed at ST
C_2	Date rate at SR without interference from PT, where power control is employed at ST
C_3	Date rate at SR with interference from PT, where power control is employed at ST
$h_{p,1}$	Channel coefficient for the link PR-ST
$h_{p,2}$	Channel coefficient for the link PT-SR
$h_{p,3}$	Channel coefficient for the link PR-ST
h_s	Channel coefficient for the link ST-SR
P_d	Detection probability
P_{fa}	False alarm probability
P_c	Confidence probability
\bar{P}_d	Target detection probability
\bar{P}_c	Target confidence probability
μ	Decision threshold
ρ_d	Outage constraint over detection probability at ST
ρ_{cont}	Outage constraint on controlled power at ST

θ_I	Interference temperature at PR
β	Accuracy of the parameter
ϵ	Relative error between the normalized histogram bins and probability density function
$x_{PT}[\cdot]$	Discrete and complex signal transmitted by PT
$x_{PR}[\cdot]$	Discrete and complex signal transmitted by PR
$x_{ST,cont}[\cdot]$	Discrete and complex signal transmitted by ST with controlled power
$x_{ST}[\cdot]$	Discrete and complex signal transmitted by ST with no power control (maximum transmit power)
$y_{ST}[\cdot]$	Discrete and complex signal received at ST
$y_{SR}[\cdot]$	Discrete and complex signal received at SR
$y_{PR}[\cdot]$	Discrete and complex signal received at PR
$w_{PR}[\cdot]$	Circularly symmetric additive white Gaussian noise at PR
$w_{ST}[\cdot]$	Circularly symmetric additive white Gaussian noise at ST
$w_{SR}[\cdot]$	Circularly symmetric additive white Gaussian noise at SR
$P_{R_x,ST,h_{p,1}}$	Power received at ST over the PT-ST over $h_{p,1}$
$P_{R_x,ST,h_{p,3}}$	Power received at ST over the PR-ST over $h_{p,3}$
$P_{R_x,PR}$	Interference power received at PR over the ST-PR link
$P_{R_x,SR}$	Interference power received at SR over the PT-SR link
$P_{T_x,ST,cont}$	Transmit power at ST with power control
$P_{T_x,ST}$	Transmit power at ST with full transmit control
$P_{T_x,PR}$	Transmit power at PR
σ_w^2	Noise power
σ_s^2	Transmit power at PT, when transmit signal is modeled as OFDM
$\gamma_{p,1}$	Signal to noise power received at ST over PT-ST link
$\gamma_{p,2}$	Interference (from PT) to noise ratio for PT-SR link
$\gamma_{p,3}$	Signal to noise power received at ST over PR-ST link
γ_s	Signal to noise power received at SR over ST-SR link
$F_{(\cdot)}$	Cumulative distribution function of random variable (\cdot)
$f_{(\cdot)}$	Probability density function of random variable (\cdot)
$\mathbb{E}_{(\cdot)}$	Expectation with respect to (\cdot)
\mathbb{P}	Probability measure
$\mathbf{T}(\cdot)$	Test statistics
$\tilde{(\cdot)}$	Suitable value of parameter (\cdot) that achieves maximum performance
$\hat{(\cdot)}$	Estimate value of parameter (\cdot)
K	Scaling factor that holds the expected power received at the PR at interference temperature

N_s	Number of pilot symbols used for pilot based estimation at the SR
\mathcal{N}	Gaussian or normal distribution
\mathcal{X}^2	Central chi-squared distribution
\mathcal{X}'^2	Non-central chi-squared distribution
$\lambda_{(\cdot)}$	Non-centrality parameter of a non-central chi-squared distribution
$a_{(\cdot)}, b_{(\cdot)}$	Shape and scale parameters of a Gamma distribution
$I_N(\cdot)$	Modified Bessel function of first kind of order N
$Q_N(\cdot, \cdot)$	Marcum Q-function
$\Gamma(\cdot, \cdot)$	Regularized upper-incomplete Gamma function
$\Gamma^{-1}(\cdot, \cdot)$	Inverse of the regularized upper-incomplete Gamma function
\mathcal{H}_1	Hypothesis illustrating the presence of primary user
\mathcal{H}_0	Hypothesis illustrating the absence of primary user (noise only)

Bibliography

- [1] Cisco, “Cisco Visual Networking Index: Global Mobile Data Traffic Forecast Update, 2013 – 2018,” *White Paper*, Feb. 2014.
- [2] Ericsson, “Ericsson Mobility Report,” Tech. Rep., Nov. 2015. [Online]. Available: <http://www.ericsson.com/res/docs/2015/mobility-report/ericsson-mobility-report-nov-2015.pdf>
- [3] 3GPP, <http://www.3gpp.org/>, [Online; accessed Jun. 1, 2016].
- [4] Qualcomm, “Rising to meet the 1000x mobile challenge,” Tech. Rep., Sep. 2013.
- [5] J. G. Andrews, S. Buzzi, W. Choi, S. V. Hanly, A. Lozano, A. C. K. Soong, and J. C. Zhang, “What Will 5G Be?” *IEEE J. Sel. Areas Commun.*, vol. 32, no. 6, pp. 1065–1082, Jun. 2014.
- [6] E. G. Larsson, O. Edfors, F. Tufvesson, and T. L. Marzetta, “Massive MIMO for next generation wireless systems,” *IEEE Commun. Mag.*, vol. 52, no. 2, pp. 186–195, Feb. 2014.
- [7] H. Halbauer, S. Saur, J. Koppenborg, and C. Hoek, “3D beamforming: Performance improvement for cellular networks,” *Bell Labs Technical Journal*, vol. 18, no. 2, pp. 37–56, Sep. 2013.
- [8] A. Sabharwal, P. Schniter, D. Guo, D. W. Bliss, S. Rangarajan, and R. Wichman, “In-Band Full-Duplex Wireless: Challenges and Opportunities,” *IEEE J. Sel. Areas Commun.*, vol. 32, no. 9, pp. 1637–1652, Sep. 2014.

- [9] J. G. Andrews, H. Claussen, M. Dohler, S. Rangan, and M. C. Reed, "Femtocells: Past, Present, and Future," *IEEE J. Sel. Areas Commun.*, vol. 30, no. 3, pp. 497–508, Apr. 2012.
- [10] X. Gelabert, P. Legg, and C. Qvarfordt, "Small Cell densification requirements in high capacity future cellular networks," in *IEEE International Conference on Communications (ICC) Workshops*, Jun. 2013, pp. 1112–1116.
- [11] T. S. Rappaport, S. Sun, R. Mayzus, H. Zhao, Y. Azar, K. Wang, G. N. Wong, J. K. Schulz, M. Samimi, and F. Gutierrez, "Millimeter Wave Mobile Communications for 5G Cellular: It Will Work!" *IEEE Access*, vol. 1, pp. 335–349, 2013.
- [12] S. Wu, H. Wang, and C. H. Youn, "Visible light communications for 5G wireless networking systems: from fixed to mobile communications," *IEEE Netw.*, vol. 28, no. 6, pp. 41–45, Nov. 2014.
- [13] F. Schaich and T. Wild, "Waveform contenders for 5G – OFDM vs. FBMC vs. UFMC," in *6th International Symposium on Communications, Control and Signal Processing (ISCCSP)*, May 2014, pp. 457–460.
- [14] J. Bazzi, P. Weitkemper, K. Kusume, A. Benjebbour, and Y. Kishiyama, "Design and Performance Tradeoffs of Alternative Multi-Carrier Waveforms for 5G," in *IEEE Global Telecommunication Conference (GLOBECOM) Workshops*, Dec. 2015, pp. 1–6.
- [15] V. Chandrasekhar, J. G. Andrews, and A. Gatherer, "Femtocell Networks: A Survey," *IEEE Commun. Mag.*, vol. 46, no. 9, pp. 59–67, Sep. 2008.
- [16] M. A. McHenry, "NSF Spectrum Occupancy Measurements Project Summary," *Shared Spectrum Company*, 2005.
- [17] M. McHenry, E. Livsics, T. Nguyen, and N. Majumdar, "XG Dynamic Spectrum Access Field Test Results," *IEEE Commun. Mag.*, vol. 45, no. 6, pp. 51–57, Jun. 2007.
- [18] J. Mitola and G. Q. Jr. Maguire, "Cognitive radio: making software radios more personal," *IEEE Personal Commun. Mag.*, vol. 6, no. 4, pp. 13–18, Aug. 1999.
- [19] P. Pawelczak, K. Nolan, L. Doyle, S. W. Oh, and D. Cabric, "Cognitive radio: Ten Years of Experimentation and Development," *IEEE Commun. Mag.*, vol. 49, no. 3, pp. 90–100, Mar. 2011.

- [20] A. Goldsmith, S. A. Jafar, I. Maric, and S. Srinivasa, "Breaking Spectrum Gridlock With Cognitive Radios: An Information Theoretic Perspective," *Proceedings of the IEEE*, vol. 97, no. 5, pp. 894–914, May 2009.
- [21] D. Cabric, S. M. Mishra, and R. W. Brodersen, "Implementation issues in spectrum sensing for cognitive radios," in *Conference Record of the Thirty-Eighth Asilomar Conference on Signals, Systems and Computers*, vol. 1, Nov. 2004, pp. 772–776.
- [22] D. Cabric, A. Tkachenko, and R. W. Brodersen, "Experimental Study of Spectrum Sensing Based on Energy Detection and Network Cooperation," in *Proceedings of the First International Workshop on Technology and Policy for Accessing Spectrum*. ACM, 2006. [Online]. Available: <http://doi.acm.org/10.1145/1234388.1234400>
- [23] K. Kim, Y. Xin, and S. Rangarajan, "Energy Detection Based Spectrum Sensing for Cognitive Radio: An Experimental Study," in *IEEE Global Telecommunications Conference (GLOBECOM)*, Dec. 2010, pp. 1–5.
- [24] M. Bennis, M. Simsek, A. Czylik, W. Saad, S. Valentin, and M. Debbah, "When cellular meets WiFi in wireless small cell networks," *IEEE Commun. Mag.*, vol. 51, no. 6, pp. 44–50, Jun. 2013.
- [25] O. Galinina, A. Pyattaev, S. Andreev, M. Dohler, and Y. Koucheryavy, "5G Multi-RAT LTE-WiFi Ultra-Dense Small Cells: Performance Dynamics, Architecture, and Trends," *IEEE J. Sel. Areas Commun.*, vol. 33, no. 6, pp. 1224–1240, Jun. 2015.
- [26] H. ElSawy, E. Hossain, and M. Haenggi, "Stochastic Geometry for Modeling, Analysis, and Design of Multi-Tier and Cognitive Cellular Wireless Networks: A Survey," *IEEE Commun. Surveys Tuts.*, vol. 15, no. 3, pp. 996–1019, Jun. 2013.
- [27] H. ElSawy, E. Hossain, and D. I. Kim, "HetNets with cognitive small cells: user offloading and distributed channel access techniques," *IEEE Commun. Mag.*, vol. 51, no. 6, pp. 28–36, Jun. 2013.
- [28] M. Wildemeersch, T. Q. S. Quek, C. H. Slump, and A. Rabbachin, "Cognitive Small Cell Networks: Energy Efficiency and Trade-Offs," *IEEE Trans. Commun.*, vol. 61, no. 9, pp. 4016–4029, Sep. 2013.
- [29] M. Haenggi, *Stochastic Geometry for Wireless Networks*. Cambridge University Press, 2013.

- [30] M. Haenggi and R. K. Ganti, "Interference in Large Wireless Networks," *Foundations and Trends in Networking*, vol. 3, no. 2, pp. 127–248, 2008, available at <http://www.nd.edu/~mhaenggi/pubs/now.pdf>.
- [31] ETSI TS 103 113, "Electromagnetic compatibility and Radio spectrum Matters (ERM); System Reference document (SRdoc); Mobile broadband services in the 2300 - 2400 MHz frequency band under Licensed Shared Acces regime," Jul. 2013.
- [32] F. K. Jondral, "Software-defined radio-basic and evolution to cognitive radio," *EURASIP Journal on Wireless Communication and Networking*, vol. 2005, no. 3, pp. 275–283, Aug. 2005.
- [33] M. Paolini, "Meeting the Challenges of High-Capacity Indoor and Outdoor Coverage," *Senza Fili Consulting*, Dec. 2007, available at http://www.senzafiliconsulting.com/downloads/SenzaFili_IndoorCoverageSurvey.pdf.
- [34] Y.-C. Liang, Y. Zeng, E. C. Y. Peh, and A. T. Hoang, "Sensing-Throughput Tradeoff for Cognitive Radio Networks," *IEEE Trans. Wireless Commun.*, vol. 7, no. 4, pp. 1326–1337, Apr. 2008.
- [35] X. Kang, Y. C. Liang, A. Nallanathan, H. K. Garg, and R. Zhang, "Optimal power allocation for fading channels in cognitive radio networks: Ergodic capacity and outage capacity," *IEEE Trans. Wireless Commun.*, vol. 8, no. 2, pp. 940–950, Feb. 2009.
- [36] X. Kang, Y.-C. Liang, H. K. Garg, and L. Zhang, "Sensing-Based Spectrum Sharing in Cognitive Radio Networks," *IEEE Trans. Veh. Technol.*, vol. 58, no. 8, pp. 4649–4654, Oct. 2009.
- [37] M. Simon and M. Alouini, *Digital Communication over Fading Channels*, ser. Wiley Series in Telecommunications and Signal Processing. Wiley, 2005.
- [38] A. Goldsmith, *Wireless Communications*. New York, NY, USA: Cambridge University Press, 2005.
- [39] D. Tse and P. Viswanath, *Fundamentals of Wireless Communication*. Cambridge University Press, 2005.
- [40] M. A. Maddah-Ali and D. Tse, "Completely Stale Transmitter Channel State Information is Still Very Useful," *IEEE Trans. Inf. Theory*, vol. 58, no. 7, pp. 4418–4431, Jul. 2012.

- [41] S. Sharma, S. Chatzinotas, and B. Ottersten, "A hybrid cognitive transceiver architecture: Sensing-throughput tradeoff," in *9th International Conference on Cognitive Radio Oriented Wireless Networks and Communications (CROWNCOM)*, Jun. 2014, pp. 143–149.
- [42] H. Pradhan, S. S. Kalamkar, and A. Banerjee, "Sensing-Throughput Tradeoff in Cognitive Radio With Random Arrivals and Departures of Multiple Primary Users," *IEEE Commun. Lett.*, vol. 19, no. 3, pp. 415–418, Mar. 2015.
- [43] Y. Xing, C. N. Mathur, M. A. Haleem, R. Chandramouli, and K. P. Subbalakshmi, "Dynamic Spectrum Access with QoS and Interference Temperature Constraints," *IEEE Trans. Mobile Comput.*, vol. 6, no. 4, pp. 423–433, Apr. 2007.
- [44] A. Ghasemi and E. S. Sousa, "Fundamental limits of spectrum-sharing in fading environments," *IEEE Trans. Wireless Commun.*, vol. 6, no. 2, pp. 649–658, Feb. 2007.
- [45] H. Song, J. P. Hong, and W. Choi, "On the Optimal Switching Probability for a Hybrid Cognitive Radio System," *IEEE Trans. Wireless Commun.*, vol. 12, no. 4, pp. 1594–1605, Apr. 2013.
- [46] S. Gmira, A. Kobbane, and E. Sabir, "A new optimal hybrid spectrum access in cognitive radio: Overlay-underlay mode," in *International Conference on Wireless Networks and Mobile Communications (WINCOM)*, Oct. 2015, pp. 1–7.
- [47] X. Jiang, K.-K. Wong, Y. Zhang, and D. Edwards, "On Hybrid Overlay-Underlay Dynamic Spectrum Access: Double-Threshold Energy Detection and Markov Model," *IEEE Trans. Veh. Technol.*, vol. 62, no. 8, pp. 4078–4083, Oct. 2013.
- [48] M. C. Filippou, G. A. Ropokis, D. Gesbert, and T. Ratnarajah, "Performance analysis and optimization of hybrid MIMO Cognitive Radio systems," in *IEEE International Conference on Communication (ICC) Workshops*, Jun. 2015, pp. 555–561.
- [49] L. Musavian and S. Aissa, "Fundamental capacity limits of cognitive radio in fading environments with imperfect channel information," *IEEE Trans. Commun.*, vol. 57, no. 11, pp. 3472–3480, Nov. 2009.

- [50] H. A. Suraweera, P. J. Smith, and M. Shafi, “Capacity limits and performance analysis of cognitive radio with imperfect channel knowledge,” *IEEE Trans. Veh. Technol.*, vol. 59, no. 4, pp. 1811–1822, May 2010.
- [51] H. Kim, H. Wang, S. Lim, and D. Hong, “On the Impact of Outdated Channel Information on the Capacity of Secondary User in Spectrum Sharing Environments,” *IEEE Trans. Wireless Commun.*, vol. 11, no. 1, pp. 284–295, Jan. 2012.
- [52] P. Stoica and O. Besson, “Training sequence design for frequency offset and frequency-selective channel estimation,” *IEEE Trans. Commun.*, vol. 51, no. 11, pp. 1910–1917, Nov. 2003.
- [53] W. M. Gifford, M. Z. Win, and M. Chiani, “Diversity with practical channel estimation,” *IEEE Trans. Wireless Commun.*, vol. 4, no. 4, pp. 1935–1947, Jul. 2005.
- [54] W. M. Gifford, M. Z. Win, and M. Chiani, “Antenna subset diversity with non-ideal channel estimation,” *IEEE Trans. Wireless Commun.*, vol. 7, no. 5, pp. 1527–1539, May 2008.
- [55] V. G. Chavali and C. R. C. M. da Silva, “Collaborative Spectrum Sensing Based on a New SNR Estimation and Energy Combining Method,” *IEEE Trans. Veh. Technol.*, vol. 60, no. 8, pp. 4024–4029, Oct. 2011.
- [56] S. K. Sharma, S. Chatzinotas, and B. Ottersten, “SNR Estimation for Multi-dimensional Cognitive Receiver under Correlated Channel/Noise,” *IEEE Trans. Wireless Commun.*, vol. 12, no. 12, pp. 6392–6405, Dec. 2013.
- [57] A. Ghasemi and E. S. Sousa, “Spectrum sensing in cognitive radio networks: requirements, challenges and design trade-offs,” *IEEE Commun. Mag.*, vol. 46, no. 4, pp. 32–39, Apr. 2008.
- [58] T. E. Bogale and L. B. Le, “Massive MIMO and mmWave for 5G Wireless HetNet: Potential Benefits and Challenges,” *IEEE Veh. Technol. Mag.*, vol. 11, no. 1, pp. 64–75, Mar. 2016.
- [59] S. Sharma, T. Bogale, S. Chatzinotas, B. Ottersten, L. Le, and X. Wang, “Cognitive Radio Techniques under Practical Imperfections: A Survey,” *IEEE Commun. Surveys Tuts.*, vol. 17, no. 4, pp. 1858–1884, Fourthquarter 2015.
- [60] E. Axell, G. Leus, E. G. Larsson, and H. V. Poor, “Spectrum Sensing for Cognitive Radio : State-of-the-Art and Recent Advances,” *IEEE Signal Process. Mag.*, vol. 29, no. 3, pp. 101–116, May 2012.

- [61] H. Urkowitz, "Energy detection of unknown deterministic signals," *Proceedings of the IEEE*, vol. 55, no. 4, pp. 523 – 531, Apr. 1967.
- [62] V. I. Kostylev, "Energy detection of a signal with random amplitude," in *IEEE International Conference on Communications (ICC)*, vol. 3, 2002, pp. 1606–1610.
- [63] F. F. Digham, M.-S. Alouini, and M. K. Simon, "On the energy detection of unknown signals over fading channels," in *IEEE International Conference on Communications (ICC)*, vol. 5, May 2003, pp. 3575–3579.
- [64] S. P. Herath, N. Rajatheva, and C. Tellambura, "Unified Approach for Energy Detection of Unknown Deterministic Signal in Cognitive Radio Over Fading Channels," in *IEEE International Conference on Communications (ICC) Workshops*, Jun. 2009, pp. 1–5.
- [65] A. Mariani, A. Giorgetti, and M. Chiani, "Energy detector design for cognitive radio applications," in *International Waveform Diversity and Design Conference (WDD)*, Aug. 2010, pp. 053–057.
- [66] E. Peh and Y.-C. Liang, "Optimization for cooperative sensing in cognitive radio networks," in *IEEE Wireless Communications and Networking Conference (WCNC)*, Apr. 2007, pp. 27–32.
- [67] M. Cardenas-Juarez and M. Ghogho, "Spectrum Sensing and Throughput Trade-off in Cognitive Radio under Outage Constraints over Nakagami Fading," *IEEE Commun. Lett.*, vol. 15, no. 10, pp. 1110–1113, 2011.
- [68] Y. F. Sharkasi, M. Ghogho, and D. McLernon, "Sensing-throughput trade-off for OFDM-based cognitive radio under outage constraints," in *International Symposium on Wireless Communication Systems (ISWCS)*, Aug. 2012, pp. 66–70.
- [69] N. Cao, M. Mao, Y. Chen, and M. Long, "Analysis of collaborative spectrum sensing with binary phase shift keying signal power estimation errors," *IET Science, Measurement and Technology*, vol. 8, no. 6, pp. 350–358, 2014.
- [70] T. Wang, Y. Chen, E. L. Hines, and B. Zhao, "Analysis of effect of primary user traffic on spectrum sensing performance," in *Fourth International Conference on Communications and Networking in China*, Aug. 2009, pp. 1–5.

- [71] L. Tang, Y. Chen, E. Hines, and M.-S. Alouini, "Effect of Primary User Traffic on Sensing-Throughput Tradeoff for Cognitive Radios," *IEEE Trans. Wireless Commun.*, vol. 10, no. 4, pp. 1063–1068, Apr. 2011.
- [72] B. Zhao, Y. Chen, C. He, and L. Jiang, "Performance analysis of spectrum sensing with multiple primary users," *IEEE Trans. Veh. Technol.*, vol. 61, no. 2, pp. 914–918, Feb. 2012.
- [73] S. Kay, *Fundamentals of Statistical Signal Processing: Detection theory*, ser. Prentice Hall Signal Processing Series. Prentice-Hall PTR, 1998.
- [74] R. Tandra and A. Sahai, "SNR Walls for Signal Detection," *IEEE J. Sel. Topics Signal Process.*, vol. 2, no. 1, pp. 4–17, Feb. 2008.
- [75] I. S. Gradshteyn and I. M. Ryzhik, *Table of Integrals, Series, and Products*, 6th ed. San Diego, CA: Academic Press., 2000.
- [76] M. Gans, "The Effect of Gaussian Error in Maximal Ratio Combiners," *IEEE Trans. Commun. Technol.*, vol. 19, no. 4, pp. 492–500, Aug. 1971.
- [77] R. Annavajjala and L. B. Milstein, "Performance analysis of linear diversity-combining schemes on Rayleigh fading channels with binary signaling and Gaussian weighting errors," *IEEE Trans. Wireless Commun.*, vol. 4, no. 5, pp. 2267–2278, Sep. 2005.
- [78] M. Abramowitz and I. A. Stegun, *Handbook of Mathematical Functions with Formulas, Graphs, and Mathematical Tables*, ninth Dover printing, tenth GPO printing ed. New York: Dover, 1964.
- [79] F. W. J. Olver, D. W. Lozier, R. F. Boisvert, and C. W. Clark, Eds., *NIST Handbook of Mathematical Functions*. New York, NY: Cambridge University Press, 2010.
- [80] H. A. Suraweera, J. Gao, P. J. Smith, M. Shafi, and M. Faulkner, "Channel Capacity Limits of Cognitive Radio in Asymmetric Fading Environments," in *IEEE International Conference on Communications (ICC)*, May 2008, pp. 4048–4053.
- [81] L. Musavian and S. Aissa, "Capacity and power allocation for spectrum-sharing communications in fading channels," *IEEE Trans. Wireless Commun.*, vol. 8, no. 1, pp. 148–156, Jan. 2009.
- [82] Z. Rezki and M. S. Alouini, "Ergodic Capacity of Cognitive Radio Under Imperfect Channel-State Information," *IEEE Trans. Veh. Technol.*, vol. 61, no. 5, pp. 2108–2119, Jun. 2012.

- [83] E. Stathakis, M. Skoglund, and L. K. Rasmussen, "On combined beamforming and OSTBC over the cognitive radio Z-channel with partial CSI," in *IEEE International Conference on Communications (ICC)*, Jun. 2012, pp. 2380–2384.
- [84] L. Sboui, Z. Rezki, and M. S. Alouini, "A Unified Framework for the Ergodic Capacity of Spectrum Sharing Cognitive Radio Systems," *IEEE Trans. Wireless Commun.*, vol. 12, no. 2, pp. 877–887, Feb. 2013.
- [85] X. Zhang, J. Xing, Z. Yan, Y. Gao, and W. Wang, "Outage Performance Study of Cognitive Relay Networks with Imperfect Channel Knowledge," *IEEE Commun. Lett.*, vol. 17, no. 1, pp. 27–30, Jan. 2013.
- [86] P. J. Smith, P. A. Dmochowski, H. A. Suraweera, and M. Shafi, "The Effects of Limited Channel Knowledge on Cognitive Radio System Capacity," *IEEE Trans. Veh. Technol.*, vol. 62, no. 2, pp. 927–933, Feb. 2013.
- [87] Y. Li, G. Zhu, S. Lin, K. Guan, L. Liu, and Y. Li, "Power allocation scheme for the underlay cognitive radio user with the imperfect channel state information," in *5th IET International Conference on Wireless, Mobile and Multimedia Networks (ICWMMN 2013)*, Nov. 2013, pp. 320–324.
- [88] P. de Kerret, M. C. Filippou, and D. Gesbert, "Statistically coordinated precoding for the MISO cognitive radio channel," in *48th Asilomar Conference on Signals, Systems and Computers*, Nov. 2014, pp. 1083–1087.
- [89] J. M. Peha, "Approaches to spectrum sharing," *IEEE Commun. Mag.*, vol. 43, no. 2, pp. 10–12, Feb. 2005.
- [90] R. Zhang, "On Peak versus Average Interference Power Constraints for Spectrum Sharing in Cognitive Radio Networks," in *3rd IEEE Symposium on New Frontiers in Dynamic Spectrum Access Networks (DySPAN)*, Oct. 2008, pp. 1–5.
- [91] S. Sesia, I. Toufik, and M. Baker, *LTE - The UMTS Long Term Evolution : From Theory To Practice*. Chichester: Wiley, 2009.
- [92] A. Ghasemi and E. S. Sousa, "Capacity of Fading Channels Under Spectrum-Sharing Constraints," in *IEEE International Conference on Communications (ICC)*, vol. 10, Jun. 2006, pp. 4373–4378.
- [93] J. Oh and W. Choi, "A Hybrid Cognitive Radio System: A Combination of Underlay and Overlay Approaches," in *IEEE 72nd Vehicular Technology Conference Fall (VTC 2010-Fall)*, Sep. 2010, pp. 1–5.

- [94] S. Senthuran, A. Anpalagan, and O. Das, “Throughput Analysis of Opportunistic Access Strategies in Hybrid Underlay–Overlay Cognitive Radio Networks,” *IEEE Trans. Wireless Commun.*, vol. 11, no. 6, pp. 2024–2035, June 2012.
- [95] C. D. Charalambous and N. Menemenlis, “Stochastic models for short-term multipath fading channels: chi-square and Ornstein-Uhlenbeck processes,” in *Proceedings of the 38th IEEE Conference on Decision and Control*, vol. 5, 1999, pp. 4959–4964.
- [96] A. Jeffrey and D. Zwillinger, *Table of Integrals, Series, and Products*. Elsevier Science, 2000.
- [97] Ettus Research, <http://www.ettus.com/>, [Online; accessed Dec. 2, 2015].
- [98] D. Bharadia, E. McMillin, and S. Katti, “Full Duplex Radios,” *SIGCOMM Comput. Commun. Rev.*, vol. 43, no. 4, pp. 375–386, Aug. 2013. [Online]. Available: <http://doi.acm.org/10.1145/2534169.2486033>
- [99] G. Liu, F. R. Yu, H. Ji, V. C. M. Leung, and X. Li, “In-Band Full-Duplex Relaying: A Survey, Research Issues and Challenges,” *IEEE Commun. Surveys Tuts.*, vol. 17, no. 2, pp. 500–524, Secondquarter 2015.
- [100] Y. Liao, L. Song, Z. Han, and Y. Li, “Full duplex cognitive radio: a new design paradigm for enhancing spectrum usage,” *IEEE Commun. Mag.*, vol. 53, no. 5, pp. 138–145, May 2015.
- [101] D. Kim, H. Lee, and D. Hong, “A Survey of In-Band Full-Duplex Transmission: From the Perspective of PHY and MAC Layers,” *IEEE Commun. Surveys Tuts.*, vol. 17, no. 4, pp. 2017–2046, Fourthquarter 2015.
- [102] F. F. Digham, M.-S. Alouini, and M. K. Simon, “On the Energy Detection of Unknown Signals Over Fading Channels,” *IEEE Trans. Commun.*, vol. 55, no. 1, pp. 21–24, Jan 2007.
- [103] A. Taherpour, M. Nasiri-Kenari, and S. Gazor, “Multiple antenna spectrum sensing in cognitive radios,” *IEEE Trans. Wireless Commun.*, vol. 9, no. 2, pp. 814–823, Feb. 2010.
- [104] C. Jiang, N. C. Beaulieu, and C. Jiang, “A novel asynchronous cooperative spectrum sensing scheme,” in *IEEE International Conference on Communications (ICC)*, Jun. 2013, pp. 2606–2611.

- [105] C. Jiang, N. C. Beaulieu, L. Zhang, Y. Ren, M. Peng, and H. H. Chen, "Cognitive radio networks with asynchronous spectrum sensing and access," *IEEE Netw.*, vol. 29, no. 3, pp. 88–95, May 2015.
- [106] A. Ghasemi and E. S. Sousa, "Interference Aggregation in Spectrum-Sensing Cognitive Wireless Networks," *IEEE J. Sel. Areas Commun.*, vol. 2, no. 1, pp. 41–56, Feb. 2008.
- [107] C. Lee and M. Haenggi, "Interference and Outage in Poisson Cognitive Networks," *IEEE Trans. Wireless Commun.*, vol. 11, no. 4, pp. 1392–1401, Apr. 2012.
- [108] S. Kusaladharma and C. Tellambura, "Aggregate Interference Analysis for Underlay Cognitive Radio Networks," *IEEE Wireless Commun. Lett.*, vol. 1, no. 6, pp. 641–644, Dec. 2012.
- [109] S. Kusaladharma and C. Tellambura, "Impact of Beacon Misdetection on Aggregate Interference for Hybrid Underlay-Interweave Networks," *IEEE Commun. Lett.*, vol. 17, no. 11, pp. 2052–2055, Nov. 2013.
- [110] X. Song, C. Yin, D. Liu, and R. Zhang, "Spatial Throughput Characterization in Cognitive Radio Networks with Threshold-Based Opportunistic Spectrum Access," *IEEE J. Sel. Areas Commun.*, vol. 32, no. 11, pp. 2190–2204, 2014.

Related Publications

Note: This thesis contains material from the following publications [K1–K9], ©2013–2017 IEEE. Reprinted, with permission. To maintain the consistency of the thesis, the following publications [K10–K14] are not included in the thesis. Also, the thesis contains material that will appear in publication [K9].

- [K1] A. Kaushik, M. Mueller, and F. K. Jondral, “Cognitive Relay: Detecting Spectrum Holes in a Dynamic Scenario,” in *Tenth International Symposium on Wireless Communication Systems (ISWCS)*, 2013, pp. 1–2.
- [K2] A. Kaushik, S. K. Sharma, S. Chatzinotas, B. Ottersten, and F. K. Jondral, “Sensing-Throughput Tradeoff for Cognitive Radio Systems with Unknown Received Power,” in *10th International Conference on Cognitive Radio Oriented Wireless Networks and Communications (CROWNCOM)*, Apr. 2015, pp. 308–320.
- [K3] A. Kaushik, S. K. Sharma, S. Chatzinotas, B. Ottersten, and F. K. Jondral, “Sensing-Throughput Tradeoff for Interweave Cognitive Radio System: A Deployment-Centric Viewpoint,” *IEEE Trans. Wireless Commun.*, vol. 15, no. 5, pp. 3690–3702, May 2016.
- [K4] A. Kaushik, S. K. Sharma, S. Chatzinotas, B. Ottersten, and F. K. Jondral, “Performance Analysis of Interweave Cognitive Radio Systems with Imperfect Channel Knowledge over Nakagami Fading Channels,” in *IEEE 84th Vehicular Technology Conference (VTC)*, Sep. 2016, pp. 1–5.

- [K5] A. Kaushik, S. K. Sharma, S. Chatzinotas, B. Ottersten, and F. K. Jondral, "On the Performance Analysis of Underlay Cognitive Radio Systems: A Deployment Perspective," *IEEE Trans. on Cogn. Commun. Netw.*, vol. 2, no. 3, pp. 273–287, Sep. 2016.
- [K6] A. Kaushik, S. K. Sharma, S. Chatzinotas, B. Ottersten, and F. K. Jondral, "Performance Analysis of Hybrid Cognitive Radio Systems with Imperfect Channel Knowledge," in *IEEE International Conference on Communications (ICC)*, May 2016, pp. 5289–5295.
- [K7] H. Becker, A. Kaushik, S. K. Sharma, S. Chatzinotas, and F. K. Jondral, "Experimental Study of an Underlay Cognitive Radio System: Model Validation and Demonstration," in *11th International Conference on Cognitive Radio Oriented Wireless Networks and Communications (CROWNCOM)*, May–Jun. 2016, pp. 511–523.
- [K8] A. Kaushik, S. K. Sharma, S. Chatzinotas, B. Ottersten, and F. K. Jondral, "Estimation-Throughput Tradeoff for Underlay Cognitive Radio Systems," in *IEEE International Conference on Communications (ICC)*, Jun. 2015, pp. 7701–7706.
- [K9] A. Kaushik, S. K. Sharma, S. Chatzinotas, B. Ottersten, and F. K. Jondral, "Performance Analysis of Cognitive Radio Systems from a Deployment Perspective," in *Handbook of Cognitive Radio*, W. Zhang, Ed. Springer, 2017.
- [K10] A. Kaushik and F. K. Jondral, "On the Estimation of Channel State Transitions for Cognitive Radio Systems," in *IEEE Wireless Communications Networking Conference (WCNC)*, Apr. 2014, pp. 2061–2066.
- [K11] A. Kaushik, M. R. Raza, and F. K. Jondral, "On the Deployment of Cognitive Relay as Underlay Systems," in *9th International Conference on Cognitive Radio Oriented Wireless Networks and Communications (CROWNCOM)*, Jun. 2014, pp. 329–334.
- [K12] A. Kaushik, R. Tanbourgi, and F. Jondral, "Operating characteristics of underlay cognitive relay networks," in *IEEE 25th Annual International Symposium on Personal, Indoor, and Mobile Radio Communication (PIMRC)*, Sep. 2014, pp. 1206–1210.
- [K13] A. Kaushik, F. Wunsch, A. Sagainov, N. Cuervo, J. Demel, S. Koslowski, H. Jäkel, and F. Jondral, "Spectrum sharing for 5G wireless systems (Spectrum sharing challenge)," in *IEEE International*

Symposium on Dynamic Spectrum Access Networks (DySPAN), Sep. 2015, pp. 1–2.

- [K14] L. Rodes, A. Kaushik, S. K. Sharma, S. Chatzinotas, and F. K. Jondral, “Square-Law Selector and Square-Law Combiner for Cognitive Radio Systems: An Experimental Study,” in *IEEE 84th Vehicular Technology Conference (VTC)*, Sep. 2016, pp. 1–5.

Supervised Theses

Keikavoos Afghahi	<i>Energy Detection for Cognitive Radios</i> , Bachelor Thesis, Karlsruhe Institute of Technology, 2013
Muhammad Rehan Raza	<i>Deployment of Wireless Channel Model for Cognitive Relay</i> , Master Thesis, Karlsruhe Institute of Technology, 2013
Piotr Potocki	<i>Deployment of OFDM based Cognitive Relays</i> , Bachelor Thesis, Karlsruhe Institute of Technology, 2014
Cédric Fischer	<i>Low-Complexity Energy-Detector für Cognitive Relay</i> , Bachelor Thesis, Karlsruhe Institute of Technology, 2014
Hanna Becker	<i>Über den Einsatz von Cognitive Relay als Underlay-System</i> , Master Thesis, Karlsruhe Institute of Technology, 2015
Lucas Rodés Guirao	<i>Deployment of Energy Detector for Cognitive Relay with Multiple Antennas</i> , Bachelor Thesis, Karlsruhe Institute of Technology, 2015
Jiaxin Fan	<i>Deployment of Half-Duplex and Full-Duplex Cognitive Radio Systems</i> , Bachelor Thesis, Karlsruhe Institute of Technology, 2016

Index

- 4G, 1
- 5G, 1, 6

- Approximation, 36
- Asymmetric fading, 152
- Asynchronous access, 152
- AWGN, 27, 125

- Band manager, 66
- Bessel function, 128

- Central limit theorem, 28
- Channel
 - deterministic channel, 23, 36, 79
 - random channel, 23, 43, 85
- Channel estimation, 33–34, 75–78, 107–109
 - eigenvalue-based, 31
 - pilot-based, 15, 31, **33**
 - received power-based, 15, 31, **33**, 34, 126
 - received signal to noise ratio-based, 31
- Channel knowledge
 - imperfect, 46, 86
 - perfect, 44, 86
- Channel reciprocity, 72, 123
- Cognitive radio systems
 - classification, 5
 - imperfect channel knowledge, 12
 - performance analysis, 10
 - performance tradeoffs, *see* Trade-offs
- Cognitive small cell, 6
 - hardware feasibility, 9
 - indoor deployment, 9
 - network compatibility, 9
 - network elements, 7
 - spectrum access, 8
- Combining techniques, 152
- Confidence probability, 130
- Constant power signal, 124
- CR communication
 - half duplex, 151
 - in-band full duplex, 1, 151
- CR techniques, 8, 151
- Cramér-Rao bound, 34
- CSIT, 12

- Data rate, 29, 74, 82, 105
- Demonstrator, 122, 138–147
- Distribution
 - central chi-squared, 33
 - Gamma, 44, 61
 - non-central chi-squared, 34

- FDD, 71

- Gamma function, 28

Index

- GNU Radio, 142
- Graphical user interface, 122, 142
- GSM, 4
- Hardware validation, 122, 130–138
 - estimation-throughput tradeoff, 135
 - system parameters, 134
- Homodyne receiver, 131
- Hybrid system, 99–120
 - definition, 5
 - frame structure, 106
 - involved channels, 102
- Interference constraint
 - average constraint, 25, 41
 - confidence probability constraint, 123
 - outage constraint, 25, 41, 79, 109
- Interference threshold, 65, 74, 104
- Interweave system, 21–63
 - definition, 5
 - frame structure, 32
 - involved channels, 26
- LSA, 8
- LTE, 1, 72, 78
- Marcum Q-function, 129
- MATLAB, 131
- Maximum likelihood estimate, 33
- Mellin transform, 62, 98
- Millimeter-wave technology, 3, 153
- MIMO, 1, 12
- Nakagami- m fading, 25, 43, 85, 152
- Nyquist criterion, 126
- OFDM, 27, 75, 103, 123
- Overlay system
 - definition, 6
- Phase shift keying, 27, 126
- Power control
 - deterministic channel, 79
 - random channel, 87
- Pre-processing, 131
 - Bandpass filtering, 132
 - decimation, 132
 - digital downconversion, 132
 - LO-Offset, 131
- Scaling factor, 127, 141
- SDR, 9, 130, 151
- Secondary throughput, 11, 41, 46, 84, 89, 104, 112, 126
- Small cell densification, 2
- Spectrum extension, 3
- Spectrum sensing, 21
 - detection probability, 28
 - detection techniques, 22
 - energy detection, 22, 27
 - false alarm probability, 28
- Spurious effects
 - DC offset, 131
 - flicker noise, 131
 - I/Q imbalance, 131
- Stochastic geometry, 7, 153
- TDD, 71
- Test statistics, 28
- Tradeoffs
 - estimation-sensing-throughput tradeoff, 25, 41, 101, 112
 - estimation-throughput tradeoff, 70, 84, 89, 122, 129
 - sensing-throughput tradeoff, 23, 29, 105
- Uncertain interference, 13

Underlay system, 65–98
 definition, 5
 frame structure, 72
 involved channels, 71
USB, 131
USRP, 131

Vector signal generator, 131
Visible light communication, 5, 153

WiMAX, 1, 9

Sponsorship

The author would like to thank German Federal Ministry of Education and Research (BMBF) for partially funding his research under the grant 16BU1205 within the project *Cognitive Mobility Radio (CoMoRa)*.

The author would also like to thank Luxembourg National Research Fund (FNR), under the project SEMIGOD, for partly supporting his research visit to Interdisciplinary Centre for Security, Reliability and Trust (SnT), University of Luxembourg, Luxembourg.

Biography

Ankit Kaushik (born on June 7, 1984) received a B. Tech degree in electronics and communication engineering from Guru Gobind Singh Indraprastha University, Delhi, India in 2005. He further received a european M. Sc. degree in information and communication technology from University of Karlsruhe (now Karlsruhe Institute of Technology), Karlsruhe, Germany and Politecnico di Torino, Turin, Italy in 2007. From 2007-2012, he was with Leica Camera AG, Germany, where he worked as a Design Engineer.

Since 2012, Ankit Kaushik has been with the Communications Engineering Lab, Karlsruhe Institute of Technology, as a Research Associate. During the winter semester 2015/2016, he was Visiting Researcher with the Security, Reliability and Trust (SnT), University of Luxembourg, Luxembourg. His research interests include software defined radio, cognitive radio communications and networks. He was a recipient of MERIT Scholarship for his Masters Studies within the Erasmus Mundus Scholarship Program and Subjective Winner of 5G Spectrum Challenge held at 2015 IEEE DySPAN conference.

